Kdp-dependent K^+ homeostasis of the halophilic archaeon *Halobacterium salinarum*

Dissertation

zur Erlangung des Grades eines Doktors
der Naturwissenschaften (Dr. rer. nat.)
des Fachbereiches Biologie/Chemie
an der Universität Osnabrück

von
Henrik Strahl

Osnabrück, Oktober 2007

I	**Summary**	**III**
II	**Abbreviations**	**IV**
1.	**Introduction**	**1**
1.1	Life in hypersaline environments	1
1.2	Osmotic stress in hypersaline environment	2
1.3	*Halobacterium salinarum*	3
1.4	Ion homeostasis in *H. salinarum*	4
1.5	Putative ion homeostasis of *H. salinarum* in reference to the genomic sequence	5
1.6	The KdpFABC complex	7
1.7	Genetics and gene regulation in Archaea	8
1.8	Objectives	9
2.	**Results**	**11**
2.1	**K^+ homeostasis in *H. salinarum***	11
2.1.1	K^+ as a growth-limiting factor for *H. salinarum*	11
2.1.2	Cellular adaptation to K^+ limitation	12
2.2	**Sequence analysis of the halobacterial Kdp system**	14
2.2.1	*kdp* operon organization	14
2.2.2	Phylogenetic relationship of the archaeal Kdp systems	16
2.3	**Kdp-dependent K^+ homeostasis of *H. salinarum***	18
2.3.1	Deletion of *kdpFABCcat3* and *kdpFABC*	18
2.3.2	Expression of the *kdpFABCcat3* operon	20
2.3.3	Induced expression of the *kdpFABCcat3* operon	21
2.3.3.1	Medium K^+ dependent expression of the *kdpFABCcat3* operon	21
2.3.3.2	Medium Na^+ dependent expression of the *kdpFABCcat3* operon	23
2.4	**Regulation of *kdpFABCcat3* expression**	25
2.4.1	Sequence-based analysis of the promoter region	25
2.4.2	Truncation analysis of the *kdp* promoter	26
2.4.3	Regulatory function of *cat3*	29
2.5	**Global transcriptional response in *H. salinarum* to K^+ depletion**	34
2.5.1	DNA microarray analysis	34
2.5.2	Cluster of up-regulated genes	37
2.5.3	DNA replication and replicon copy number	39
2.6	**Search for transcriptional regulators of the *kdp* system**	40
2.6.1	Two-component systems	40
2.6.2	Neighboring genes	41
2.6.3	Genomic library screen	43
2.6.4	The halobacterial *kdpFABCcat3* operon as part of a regulon.	46

3. Discussion **48**

3.1 **K^+ homeostasis in *H. salinarum*** 48

3.2 **Sequence analysis of the halobacterial Kdp system** 49

3.3 **Kdp-dependent K^+ homeostasis in *H. salinarum*** 51

3.4 **Induction of the halobacterial Kdp system** 54

3.5 **Regulation of gene expression of the *kdpFABCcat3* operon** 58

3.6 **Global transcriptional response to K^+ depletion** 63

4. Materials and Methods **65**

4.1 *H. salinarum* media, and cultivation 65
4.2 *H. volcanii* media, and cultivation 66
4.3 Strains, plasmids, and oligonucleotides 67
4.4 Cloning of the *kdpFABCcat3* operon 70
4.5 Construction of plasmids, transformation, and knock-out mutagenesis 70
4.6 Measurements of medium and cell K^+ concentrations and cell volume 72
4.7 Sequence analysis and phylogenetic computation 72
4.8 RNA extraction, RT-PCR, and *real time* RT-PCR 72
4.9 β-galactosidase activity assay 73
4.10 DNA microarrays 74
4.11 Copy number measurements 74

5. References **75**

Acknowledgements **85**

Curriculum Vitae **86**

Affirmation **87**

I. Summary

Halobacteria balance high external osmolality by the accumulation of almost equimolar amounts of KCl. Thus, steady K^+ supply is a vital prerequisite for life of these extreme halophiles. So far, K^+ is supposed to enter the cell only passively by use of potential-driven uniporters. However, the genome of the extreme halophilic archaeon *Halobacterium* sp. NRC-1 comprises one single operon containing the genes *kdpFABC* coding for homologs of the bacterial ATP-driven K^+ uptake system KdpFABC, together with an additional ORF so far annotated as *cat3*. Deletion of the *kdpFABCcat3* genes led to a reduced ability to grow upon K^+ limitation, whereas *real-time* RT-PCR measurements revealed both high induction rates and a transcriptional regulation of the Kdp system dependent on external K^+ concentration and growth phase. Synthesis of the KdpFABC complex is essential for *H. salinarum* to grow under extreme potassium-limiting conditions of down to 20 µM K^+. Moreover, *H. salinarum* was shown to adapt to K^+ limitation by significantly decreasing the intracellular K^+ concentration as well as the cell volume. These results provide the first experimental evidence of ATP-driven K^+ uptake in Archaea.

Computational and truncation analysis as well as site directed mutagenesis of the promoter of the *kdpFABCcat3* operon have revealed putative binding sites for two transcriptional regulators enabling a medium K^+-dependent negative regulation of the *kdpFABCcat3* genes. Although the nature of the primary stimulus leading to induction of the *kdpFABCcat3* operon remains unclear, a transcriptional regulatory system responding to changes in membrane potential is postulated. Cat3 was shown to play an essential role in transcriptional regulation of the *kdpFABCcat3* operon enabling a secondary, most likely K^+-independent regulation of gene expression. A potential ATP- or cellular water activity-dependent secondary regulation of the *kdpFABCcat3* operon by Cat3 is discussed. The negative medium K^+-responsive regulation of gene expression additionally modulated by Cat3 as a universal stress potein homologue together with a growth phase-dependent regulation supports the presence of a rather complex machinery enabling a sofisticated transcriptional response to K^+-depletion.

A DNA-micro array study demonstrated several additional genes to be up- and down-regulated in response to K^+ limitation. A subset of the up-regulated genes was shown to exhibit a singificant clustering regarding chromosomal localization. The reason for this observed clustering, however, remains unclear. The DNA-micro array study together with sequence analysis identified another operon, which potentially sheares a commom transcriptional regulator with the *kdp*-operon, thereby supporting a coordinated expression in a K^+-responsive regulon.

II. Abbreviations

5-FOA	5-fluoro orotic acid
Ap^R	ampicillin resistance
ATCC	American Type Culture Collection
ADP	adenosine-5´-diphosphate
ATP	adenosine-5´-triphosphate
Biotin	vitamin K
BRE	TFB recognition element
CAA	casaminoacids
cDNA	complementary DNA
ct	cycle threshold
FEP	flame emission photometry
INR	transcription initiation region
Mv^R	mevinolin/simvastatin resistance
Nb^R	novobiocin resistance
OD_x	optical density at x nm
ONPG	O-nitrophenyl-ß-D-galactopyranoside
ORF	open reading frame
Ori	origin of replication
PCR	polymerase chain reaction
PEG	polyethylene glycol
pmf	proton motive force
RT-PCR	reverse transcriptase polymerase chain reaction
TBP	TATA-box binding protein
TCA	trichloracetic acid
TFB	transcription factor B
Thiamin	vitamin B1
Usp	universal stress protein

1. Introduction

1.1 Life in hypersaline environments

Two distinct types of environments represent habitates for xerophilic organisms characterised by the ability to grow under conditions of low water activity (a_W): food preserved by dehydration or addition of high levels of sugars, and hypersaline environments where high concentration of salts (usually NaCl) result in low water activity. These environments are mainly inhabitated by microbial life forms. In high-sugar environments, the dominating organisms are xerophilic filamentous fungi and yeasts capable to grow in water activities (a_W) as low as 0.61. The high-salt environments, in contrast, are inhabitated almost exclusively by prokaryotes (extreme halophilic Archaea and Bacteria) capable to grow in saturated brines (a_w 0.75) (Grant, 2004; Oren, 1999). Although many halophilic and halotolerant algae can grow in elevated NaCl concentrations (Grant, 1991), only eukaryotes of the species *Dunaniella salina* are reported to grow in saturated NaCl concentration (Oren, 2005). In addition, these unicellular green algae are the most important primary producer in hypersaline environments and, thereby, play a tremendous role in the ecology of these habitats (Oren, 2005).

Hypersaline lakes and solar salterns are the major and most intensively studied habitates of halophilic organisms. *Thalassohalin*e water bodies have gained their high salinity by evaporation of sea water and, as a result, the composition of salts is defined by the composition of sea water and the successive precipitation of different minerals (typically calcite ($CaCO_3$), gypsum ($CaSO_4*2H_2O$), halite (NaCl), sylvite (KCl), and carnallite ($KCl*MgCl_2*6H_2O$) (Grant, 2004). In contrast, the ion composition of *athalassohaline* water bodies is secondarily influenced by the geology of the area, in which they develop. For instance, the ion composition of the Dead Sea is highly influenced by leaching of Mg^{2+} from geologically older salt deposits (Eugster & Hardie, 1978). In addition, the ion composition of hypersaline water bodies highly influences the pH of the brine. As in marine environments, the pH is mainly influenced by the buffer system defined by the equilibrium between CO_3^{2-}, HCO_3^-, and CO_2. In concentrated brines, the presence of Ca^{2+} leads to the neutralisation of alkaline CO_3^{2-} via precipitation of calcite ($CaCO_3$). Since the Ca^{2+} concentration in sea water is relatively high, the precipitation of calcite during evaporation in *thalassohaline* water bodies is sufficient to stabilise the pH in near neutral range. However, in *athalassohaline* water bodies depleted in Ca^{2+}, the rising concentration of CO_3^{2-} leads to the acidification of

the brine and to the development of "soda lakes" with a pH above 11 (Grant, 2004). As a concequence, both ion composition and pH highly influences the composition of microorganisms inhabitating these environments. In contrast to hypersaline lakes and solar salterns, far less is known about the additional high salt environments such as hypersaline soils, salt marshes, desert plants, sea floor brines, oil field brines and ancient evaporate deposits as well as about the microorganisms inhabitating these environments (Grant, 2004).
Independent of the details of the environment, all organisms living in hypersaline habitats face the same principal challenge. Since biological membranes are permeable to water, cells can not maintain cytoplasmic water activities higher than in the surrounding environment. The presence of higher concentrations of osmotically active compounds in the environment would inevitably lead to a loss of water from the cell and, thus, to dehydration of the cell. To maintain vitality, all living organisms must preserve adequate levels of water in the cytoplasm. Hence, the concentration of osmotically active compounds in the cytoplasm must be at least at the level of the environment. Most organisms maintain a cytoplasmic osmolality even higher than that of the surrounding medium, resulting in the diffusion of water into the cell and, as a concequence, in generation ofturgor. With the postulated exception of halophilic Archaea of the order *Halobacteriales*, all known halophilic organisms maintain a turgor (Walsby, 1971).

1.2 Osmotic stress in hypersaline environment

Two fundamentally different strategies exists among living organisms to cope with the osmotic stress in highly saline environments. Whereas most organisms respond to osmotic stress by accumulation or synthesis of organic compounds (compatible solutes–strategy) (Roesser & Müller, 2001; Yancey, 2005), halophilic Archaea of the order *Halobacteriales* and halophilic Bacteria of the order *Haloanaerobiales* accumulate inorganic salts ("salt-in"-strategy) (Oren, 1999; Roberts, 2005). The use of one of these strategies encounters the cell with different challenges. In cells using the compatible solutes-strategy, a highly efficient uptake or energy-intensive synthesis of compatible solutes must take place. The exclusion of Na^+ from the cytoplasm in an environment with usually high concentrations of Na^+, however, results in a high Na^+ potential ($\Delta\psi_{Na^+}$), which can readily be used to energize secondary uptake of e.g. compatible solutes (Pflüger & Müller, 2004).
In cells using the "salt in"-strategy, no energy-intensive synthesis of compatible solutes is needed, and the ion concentration of the cytoplasm is usually fairly similar to that of the surrounding medium. The composition of salts, however, is completely different. Whereas the

medium is typically dominated by Na^+, K^+ is highly preferred in the cytoplasm and is accumulated to the molar range (Wagner *et al.,* 1978; Oren, 1999). As a consequence, the presence of highly efficient ion transport systems are required, and all biological processes taking place in the cytoplasm must be adapted to function with these environments. The proteome of all organisms using the "salt in"-strategy shows similar unique adaptations to conditions of high cytoplasmic ion concentrations. Typically, proteins of these organisms exhibit a large excess of acidic residues arranged on the surface of the proteins. In addition, the content of hydrophobic residues is lowered and the content of "near" hydrophobic residues like serine and threonine is elevated (Kennedy *et al.*, 2001). This adaptation seems to ensure the active conformation and stability of the proteins in high salt concentrations. In low salt concentrations, however, the high density of acidic residues on the protein surface destabilises the active conformation of the protein by electric repellence. This is most likely the reason why all known organisms adapting to high salinity by using the "salt in"-strategy are obligate halophilic (Lanyi, 1974; Oren *et al*., 1999; Kennedy *et al.,* 2001).

Although in general presented as two distinct strategies, some evidence exist in the literature supporting at least partial parallel use of both strategies. Several halophilic Bacteria and Archaea accumulating compatible solutes in response to osmotic stress, also exhibit elevated cellular ion concentrations (Desmairis *et al*., 1997; Ventosa *et al.,* 1998). In addition, a similar type of adaptation of the proteome as in organisms using the "salt in"–strategy is reported for the halophilic compatible solute-accumulating bacterium *Halomonas elongata* (Gandbhir *et al*., 1995; Oren, 1995). The halophilic archaeon *Halobacterium salinarum* is reported to posses high cellular salt concentrations (Wagner *et al*., 1978; Lanyi *et al*., 1979; see results). However, *H. salinarum* is also able to take up a compatible solute glycin betaine and other trimethylammonium compounds in high concentrations and even shows corresponding chemotaxis towards them (Kokoeva *et al*., 2002). In addition, as it is typical for coupounds used as an osmoprotectant, no metabolism of these compounds was detected (Kokoeva *et al*., 2002). To what extent glycin betaine is used by *Halobacterium* as an osmoprotectant is yet unknown.

1.3 *Halobacterium salinarum*

H. salinarum is an obligate halophilic archaeon highly adapted to envoronments of extremly high salinity. *H. salinarum* species primarily inhabitate thalassohaline salt lakes and solar salterns, thereby exhibiting optimal growth in the presence of NaCl concentrations between 2 M and saturation. *H. salinarum* is an aerob chemorganotroph growing on degradation

products of other organisms. Particulary in solar salterns, the countinuous evaporation results in a cascade of growth of different macro- and microorganisms adapted to different salinities, resulting in an accumulation of organic material. In the late phase of the evaporation process, in which high NaCl concentrations are reached, this accumulated organic material is used by extreme halophilic Archaea and Bacteria, resulting in rather dense populations (Oren, 1999).
Whereas most other characterized extreme halophilic microorganisms are able to metabolize sugars, the main energy source of *H. salinarum* during aerobic growth is amino acids catabolized via the citric acid cycle (Ng *et al.,* 2000). The reduced solubility of oxygen in highly concentrated brines together with high bacterial and achaeal cell densities results in at least partially anaerobic growth conditions. Under these conditions, the organic compounds DMSO and TMAO can be utilized by *H. salinarum* as alternative terminal electron acceptors (Müller & DasSarma, 2005), and fermentation of arginine via the arginine deiminase pathway is used (Ruepp & Soppa, 1996). In addition to chemoorganotrophy, *H. salinarum* can grow phototrophically with light as the sole energy source, thereby utilizing the pmf generated by the light-driven H^+-pump bacterorhodopsin (Kayushin & Skulachev, 1974; Danon & Stoeckenius, 1974). The high synthesis of bacterioopsin upon low oxygen saturation and clustering of bacteriorhodopsin in a paracrystalline purple membrane represent a characteristic feature of this organism.
H. salinarum exhibits a rod-shaped mono- or bipolarly flagellated morphology (Adam & Oesterhelt, 1984) and a sophisticated sensory system enabling the cells to activly find optimal conditions in their envoronment (Nutsch *et al.,* 2005). In addition to flagella-mediated motility, *H. salinarum* features gas vesicles, by which the cells can activly regulate their bouancy and, thereby, adjust their position in a water column (Stoeckenius & Kunau, 1968). By doing so, the cells can accumulate in water depths, which feature optimal growth conditions with respect to oxygen saturation and light intensity (Walsby, 1994).

1.4 Ion homeostasis in *H. salinarum*

Obligate halophilic *Halobacterium* species are well-adapted to conditions of extremely high salt concentrations. Optimal growth of these haloarchaea occurs around 2-4.3 M NaCl. *Halobacterium* species uses, as discussed above, the "salt in"–strategy to maintain the osmotic balance with the hypersaline medium (Oren, 1999; Roberts, 2005). In contrast to the high external Na^+ concentration, K^+ is accumulated inside the cell in equimolar amounts, resulting in osmotic equilibrium with the environment with no significant turgor (Wagner *et al.,* 1978; Lanyi *et al*., 1979; see results). As a consequence, highly efficient uptake of K^+ is of

vital importance for *H. salinarum* to survive in the hypersaline enrironment. The main part of the K^+ gradient is supposed to be generated *via* an uniport system, through which K^+ passively enters the cell along with the membrane potential ($\Delta\psi_m$) (Wagner *et al*., 1978; Lanyi *et al*., 1979). An active transport in combination with the balanced interconversion of ion gradients according to the Nernst equation is obligatory in order to establish and maintain rather steep gradients of in Na^+ and K^+ gradient, which have been shown to also serve also as reservoir in storing energy in the absence of oxidative and photophosphorylation (Wagner *et al.,* 1978; Brown *et al.,* 1983). However, following the Nernst equation, passive K^+ uptake can only occur if the potential of the cation ($\Delta\psi_{K+}$) is equal to or less negative than $\Delta\psi_m$. As soon as $\Delta\psi_{K+}$ is more negative than $\Delta\psi_m$, K^+ transport has to be energized either by symport or antiport with other ions or by the hydrolysis of ATP (Oren, 1999).

Although ATP-dependent K^+ accumulation has previously been reported for *Haloferax volcanii,* an additional member of the family of Halobacteriaceae (Meury and Kohiyama, 1989), this ATP dependency could be attributed to its regulatory effect on the activity of a putative TrkAH homolog most likely serving as a K^+/H^+ symporter (Bakker, 1993; Stumpe *et al*., 1996; Oren, 1999). Thus, no experimental data have yet been reported for a possible primary ATP-driven uptake system supplying the cell with K^+ in the absence of potential-driven facilitated diffusion.

1.5 Putative ion homeostasis in *H. salinarum* in reference to the genomic sequence

The genome of two isolates of *Halobacterium* species have been sequenced; *Halobacterium* NRC-1 (Ng *et al.,* 2000) and *H. salinarum* R1 (Oesterhelt *et al.,* unpublished; www.halolex.mpg.de). The overall difference in the genomic sequence between these two strains is minimal (Oesterhelt, personal correspondence). The genome of both strains is composed of one circular chromosome and several extrachromosomal replicons. Whereas the extrachromosomal replicons encode several essential genes and, thus, can be considered as "minichromosomes" (Ng *et al.,* 2000), the size and number of these "minicromosomes" differs between *Halobacterium* NRC-1 and *H. salinarum* R1. *Halobacterium* NRC-1 is reported to be composed of a main chromosome (approx. 2 Mbp) and the two satellites pNRC100 (approx. 190 Kbp) and pNRC200 (approx. 365 Mbp). The genome of *H. salinarum R1*, in contrast, consists of a homologous main chromosome (approx. 2 Mbp) and four extrachromosomal satellites pHS1 (approx. 150 Kbp), pHS2 (approx. 195), pHS3 (approx. 285 Kbp), and pHS4 (approx. 41 Kbp). This variability in genomic composition together with the presence of a high number of 91 IS elements most likely reflects a highly dynamic

character of the genome adapted to withstand the rather harsh hypersaline and high-solar-radiation environment (Kennedy *et al.,* 2001).

The genome sequences now available provide valuable insights into the composition of putative ion transport systems (Figure 1). Furthermore, it opens the gate for a re-evaluation of rather old experimental data concerning monovalent cation transport processes in *H. salinarum*. Published experimental data regarding transport of Na^+ strongly supports the presence of H^+/Na^+ exchanger activity in *H. salinarum* (Luisi *et al.,* 1980; Kamo *et al.,* 1982; Murakami & Konishi, 1985, and Murakami & Konishi, 1988). The genome of *H. salinarum* encodes three copies of a putative Na^+/H^+ exchanger of the NhaC-type (Ito *et al.,* 1997). Whereas two of the corresponding genes (*nhaC1* and *nhaC2*), are localized on the main chromosome, the third gene (*nhaC3*) is localized on one of the extrachromosal replicons (pHS3 in *H. salinarum* R1 and pNRC200 in *Halobacterium* NRC-1). Thus, the experimental data regarding transport of Na^+ are in good agreement with the presence of putative tranporters encoded in the genome. In case of K^+, however, the genome sequence revealed the presence of a whole battery of different K^+ uptake systems, which was not predicted on the basis of published experimental data. As discussed above, K^+ uptake is postulated to be accomplished via $\Delta\psi_m$–driven facilitated diffusion (Lanyi & Hilliker 1976; Ginzburg & Ginzburg, 1975; Wagner *et al*., 1978; Lanyi *et al*., 1979; Pérez-Fillol & Rodríguez-Valera, 1986). Supporting these data, the genome of *H. salinarum* encodes two putative $\Delta\psi_m$–driven K^+-channels on the main chromosome (*pchA1* and *pchA2*). However, the genomic sequence revealed in addition the presence of four copies of a Trk-type K^+-uptake system. Three of them, namely *trkH1-3*, are located on the main chromosome whereas the fourth homogue *trkH4* in *H. salinarum* R1 is encoded by the extrachromosomal replicon pHS3 absent in *Halobacterium* NRC-1. Although no Trk-like transport activity has been reported for *H. salinarum* so far, the mere presence of the Trk-system in four or three conserved copies strongly indicates the fundamental role of these systems in K^+ homeostasis of *H. salinarum*. Suprisingly, in addition to these K^+ uptake systems, a homolog of the bacterial ATP-driven KdpFABC complex was found, which normally serves as an inducible, high-affinity K^+-uptake system (Bramkamp *et al*., 2007). The corresponding annotated genes (*kdpABC*) are located on one of extrachromosomal replicons (pHS3 in *H. salinarum* R1 and pNRC200 in *Halobacterium* NRC-1).

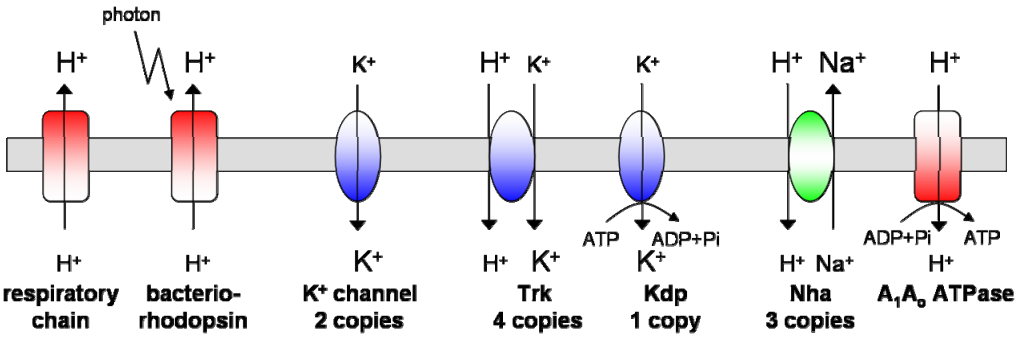

Figure 1: Overview of the monovalent cation transport systems in *H. salinarum*

1.6 The KdpFABC complex

As the first archaeal species, the genome sequence of *Halobacterium* NRC-1 and *H. salinarum* R1 revealed the presence of a putative homolog of the Kdp system, which was until then only reported to exist in Bacteria. Whereas homologs of the bacterial *kdpD* and *kdpE* genes could not be detected within the genome, the *kdp(F)ABC* genes were found to be organized in a putative operon together with an additional gene annotated as *cat3*. The KdpFABC complex has been reported in a variety of bacteria and belongs to the family of P-type ATPases, a group of ATP-driven transporters characterized by the formation of a phosphointermediate during the catalytic cycle and by the inhibition by *ortho*-vanadate (Palmgren & Axelsen, 1998). Among the P-type ATPases, the KdpFABC complex is unique in several ways: (i) It is composed of four subunits, (ii) the catalytic activity (KdpB) and the binding/transport of K^+ (KdpA) are located on different subunits, and (iii) it has a high specificity and selectivity for its substrate (Bramkamp *et al*., 2007). In *E. coli*, KdpC is absolutely necessary for the formation of a functional complex *in vivo* (Gaßel & Altendorf, 2001) and a role in regulation of the catalytic activity of KdpB has been postulated (*Ahnert et al.,* 2006). Deletion mutants of *kdpF* in *E. coli* revealed no altered phenotype, although the purified KdpABC complex lacking KdpF exhibited no ATPase activity. However, the activity of the complex was restored by the addition of purified KdpF, suggesting that KdpF has a stabilizing function on the homodimeric KdpFABC complex at least *in vitro* (Gaßel *et al.,* 1999).

In *E. coli*, expression of the *kdpFABC* operon is strongly induced by K^+ limitation and, to a minor extends, by high osmolality in the medium. Expression is under control of the regulatory proteins KdpD and KdpE, which constitute a typical sensor kinase/response regulator system. The membrane-bound sensor kinase KdpD probably senses changes in the cytoplasm as a result of alterations in K^+ concentration and in turgor, and the response

regulator KdpE in its phosphorylated form acts as a dimeric transcriptional activator for the *kdp* regulon (Jung & Altendorf, 2002; Hamann *et al.,* 2007).

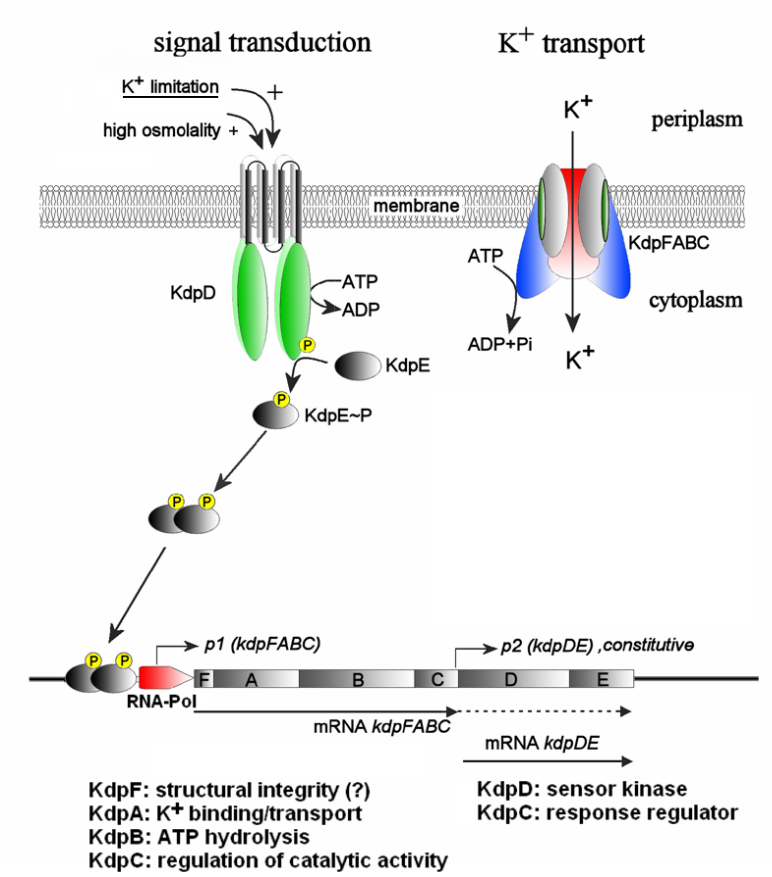

Figure 2: Overview of the Kdp system of *E. coli*.
Left: the signal cascade of the sensor kinase (KdpD) and response regulator (KdpE). Right: the membrane bound K^+-transporting KdpFABC complex. Lower panel: the organisation of the *kdpFABCDE* regulon.

1.7 Genetics and gene regulation in Archaea

Although the genomic constitution based on a circular chromosome (or chromosomes) closely resembles that found in Bacteria, the basic genetic machinery of Achaea including replication, transcription, and translation is highly similar to that found in Eucarya. The presence of DNA condensed to chromatin (Shioda *et al.,* 1989; Takayanagi *et al.,* 1992), multiple origins of replication on a single chromosome (Zhang & Zhang, 2003; Norais *et al.,* 2007), and a replication maschinery homologous to the eucaryal type (Kelman, 2000; Grabowski & Kelman, 2003) indicate the existence of a high functional homology between Archaea and Eukarya regarding these cellullar mechanisms. Although Archaea lack a nuclear membrane and comprise a coupled transcription and translation as in Bacteria, the trancriptional machinery of Archaea closely resembles that of Eucarya (Huet *et al.,* 1983; Bell & Jackson, 2001; Reeve, 2003; Allers & Mevarech, 2005). The RNA polymerase found in Achaea

exhibits significant sequence homology to eucaryal RNA polymerase II, and the trancription initiation complex requires additional transcription factors TBP (TATA-box binding protein) and TFB (trancription factor B), both of which are homologs of the eucaryal counterparts TBP and TFIIB (Bell & Jackson, 2001). Thus, the achaeal promoters with a TATA-box (Reiter *et al*., 1990; Palmer and Daniels, 1995), BRE (TFB responsive element; Qureshi and Jackson, 1998; Soppa, 1999) and INR element (transcription start site; Palmer & Daniels, 1995) feature conserved promoter elements related to eucaryal analogs. The regulation of gene expression by trancriptional regulators, however, seemst to comprise features similar to Eucarya as well as to Bacteria. The emerging genome sequencing projects have revealed the presence of numerous homogs of bacterial transcriptional regulators in Archaea (Aravind & Koonin, 1999) and the function of several of these transcriptional regulators in Archaea has been studied in detail (Cohen-Kupiec *et al.,* 1997; Bell *et al.,* 1999; Bell & Jackson, 2000; Lie *et al.,* 2005). In other systems studied, however, the mechanism of gene regulation and the regulatory proteins more closely resemble systems found in Eukarya (Ouhammouch *et al.,* 2003; Hofacker *et al.,* 2004). Thus, the core transcriptional machinery of Archaea represents a system homologous to the eucaryal RNA polymerase II, however in a simplified form requiring only two additional transcriotion factors (TBP and TFB). In contrast, the regulation of gene expression facilitates transcritional regulators of both eukaryal and bacterial type.

1.8 Objectives of the thesis

The KdpFABC complex has been reported in a variety of Bacteria and belongs to the family of P-type ATPases (Palmgren & Axelsen, 1998). The Kdp system was reported to be widespread within Bacteria but no homogues were so far found to exist in Archaea or Eucarya. The genome sequence of *H. salinarum*, however, revealed the first time genes homologous to this "bacterial" K^+ uptake system within the domain of Archaea. At least in *E. coli*, this high affinity, ATP-dependent, and K^+ translocating KdpFABC complex is induced as a response to K^+ limitation and, in a minor extend, to high osmolality and thereby ensuring an adequate supply of K^+ (Jung and Altendorf, 2002). Although efficient K^+ supply is of vital importance for both organisms, significant differences exist in details. Whereas the uptake of K^+ by the KdpFABC complex is involved in the regulation of turgor in *E. coli* (Jung and Altendorf, 2002), no singificant turgor is reported to exist in *H. salinarum* (Walsby, 1971). In contrast, high cellular K^+ concentrations in the molar range are accumulated, and the

cytoplasm of *H. salinarum* is maintained in an iso-osmotic equilibrium with the surrounding medium (Wagner *et al.,* 1978; Lanyi *et al*., 1979, see results). As a consequence, the so far unknown cellular function of the Kdp system is likely to be different in *H. salinarum* comparedn to *E. coli* or other Bacteria exhibing turgor. Therefore, a major effort of this thesis was the analysis of this putatively novel cellular function of the Kdp system in *H. salinarum* thereby resulting in characterization of the first archaeal Kdp system.

Furthermore, a special attention was paid to the induction of the halobacterial Kdp system and the underlying mechanism of gene regulation. In Bacteria, the expression of the genes encoding the correspoding Kdp(F)ABC complex is regulated by a KdpD/KdpE sensor kinase/response regulator system. Whereas detailed information about the mode of action of KdpD/KdpE is available for several Bacteria (Jung *et al.,* 2000; Jung and Altendorf, 2002; Heermann *et al.,* 2003; Schleussinger *et al.,* 2006; Ballal *et al.,* 2007; Zimmann *et al.,* 2007), the nature of the primary stimulus sensed by KdpD is still a matter of debate. Although homologs of KdpD/KdpE are absent in the genome of *H. salinarum*, the corresponding genes *kdp(F)ABC* are organized in a single operon together with an additional gene *cat3*. The putative gene product of *cat3* exhibits structural homologies to a part of KdpD. Thus, the analysis of the role of this conserved protein in the regulation of both halobacterial and bacterial Kdp systems could help to understand the nature of the stimulus not only in *Halobacterium* but also in Bacteria.

Although the mere presence of a $\Delta\psi_m$ –driven channel-like K^+ transport activity was reported for *H. salinarum* so far (Lanyi & Hilliker 1976; Ginzburg & Ginzburg, 1975; Wagner *et al*., 1978; Lanyi *et al*., 1979; Pérez-Fillol & Rodríguez-Valera, 1986), the genome sequence of two halobacterial strains (*Halobacterium* NRC-1; Ng *et al.,* 2000 and *H. salinarum* R1; Oesterhelt *et al.,* unpublished; www.halolex.mpg.de) with K^+-channels, Trk-type K^+ uptake systems, and a Kdp system revealed the presence of a whole battery of different types of K^+-transport systems. Obviously, the current opinion of K^+ homoeostasis of *H. salinarum* solely mediated via membrane potential-driven K^+ uniporters is only one aspect of a more complex cellular machinery. In applying analyse of the K^+ homeostasis as such, the global trancriptional response to K^+ availability as well as analyse of transcriptional regulation of genes involved in K^+ uptake, this study represents an attempt to elucidate the dicrepancy between existing experimental data about K^+ transport processes in *H. salinarum* and genomic data about the encoded K^+ transport systems.

2. Results

2.1 K^+ homeostasis in *H. salinarum*

2.1.1 K^+ as a growth-limiting factor for *H. salinarum*

In order to elucidate the growth requirements of *H. salinarum* with respect to K^+, *H. salinarum* strain R1 was cultivated in medium containing 25 % total salt with varying concentrations of KCl. Growth was observed to occur over a large range of K^+ concentrations, ranging from 1 mM to 2.5 M (data not shown). *H. salinarum* exhibited identical growth behavior without notable effects on generation time or maximal optical density if cultivated in K^+ concentrations of 5 and 100 mM (Figure 3). In contrast, if *H. salinarum* was cultivated in the presence of initial K^+ concentrations of 3 mM and below, the stationary growth phase was already entered at lower cell densities, arguing for limiting growth conditions due to the lack of K^+. In these cultures, the addition of KCl was sufficient to re-initiate growth, thereby confirming the role of K^+ as a growth-limiting factor.

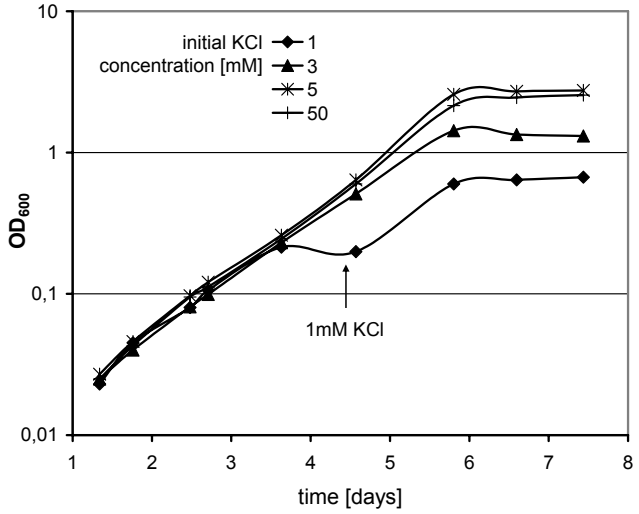

Figure 3: Cultivation of *H. salinarum* R1 with different initial K^+ concentrations.
Growth was monitored as optical density of the culture. Addition of 1 mM KCl to the culture with an initial K^+ concentration of 1 mM is indicated by an arrow.

Since *H. salinarum* is able to accumulate high concentrations of KCl during growth, the K^+ concentration in the medium is highly biased by the transport activity of a growing culture. In

order to define the K^+ concentrations enabling growth of *H. salinarum*, the residual medium K^+ concentration in the stationary growth phase was measured by flame emission photometry (FEP) (Figure 4). In all cultures, uptake of K^+ could be observed by means of a decrease in the medium K^+ concentration. Cultures grown in the presence of growth-limiting K^+ concentrations (3 mM and 1 mM) exhibited an identical residual K^+ concentration of 20 µM in the medium. In case of cultures with a non-limiting initial K^+ concentration of 5 mM and above, the residual K^+ concentration is at higher level, which is in accord with K^+ not being the growth-limiting factor. This supports the notion, that 20 µM K^+ in the medium represents the minimal concentration of K^+ supporting growth of *H. salinarum*, thereby demonstrating the presence and activity of high-affinity K^+ uptake systems.

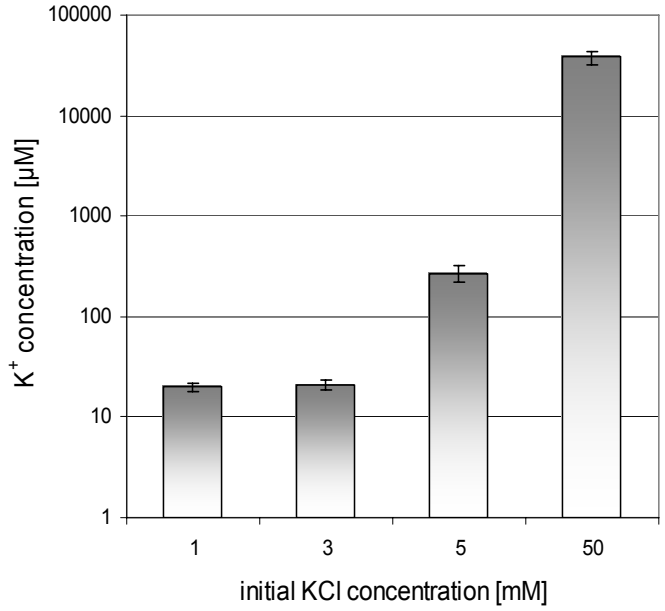

Figure 4: K^+ depletion in the medium caused by growth of *H. salinarum*.
Residual K^+ concentration in the medium as measured by flame emission photometry in triplicate from stationary growth phase cultures of *H. salinarum* R1 grown with different initial K^+ concentrations.

2.1.2 Cellular adaptation to K^+ limitation

The measured subtantial amouts of K^+ taken up by a growing culture of *H. salinarum* readily implicate the presence of high cellular K^+ concentrations. The cellular K^+ is discussed to play the main role in balancing the osmolality of the cytoplasm with the medium (Wagner *et al.,* 1978; Oren, 1999). In order to maintain the isoosmotic equilibrium with the medium, the cellular K^+ concentration needs to be adapted in response to changes in, at least, medium overall osmolality. In addition, the cellular K^+ concentration is reported to be influenced by extracellular factors like for example changes in illumination (Wagner *et al.*, 1978).

Therefore, the effect of limiting K^+ concentrations in the medium on the cellular K^+ concentration was analyzed. Cellular K^+ concentrations were measured for cells grown with initial K^+ concentrations of 100 and 3 mM. Similar to the growth phenotypes described above, the culture grown with 3 mM KCl entered stationary growth phase at an earlier stage due to K^+ limitation (Figure 5).

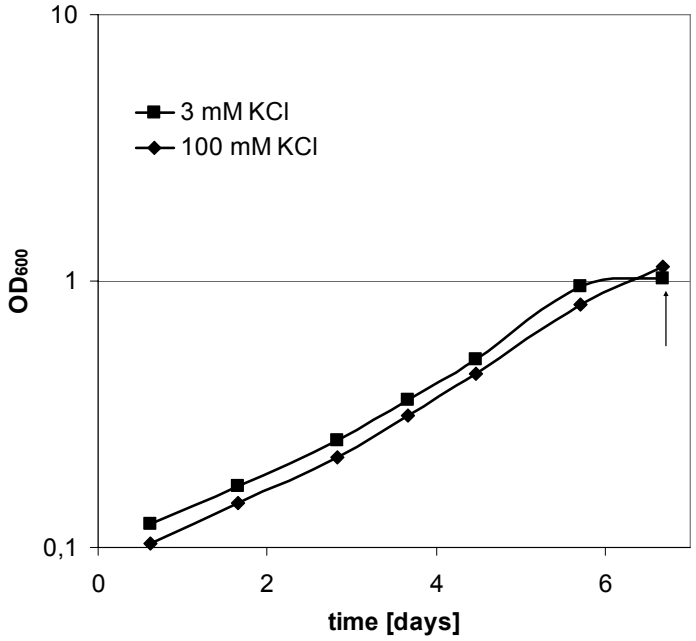

Figure 5: Cultivation of *H. salinarum* R1 in media initially containing 3 mM or 100 mM KCl. Growth was monitored as optical density of the culture. Time point for sample collection is highlighted by an arrow.

Cellular K^+ was analyzed by FEP upon centrifugation and osmotic cell lysis. The cellular K^+ concentration was calculated using the measured cell volume and the cell count of parallel samples. Cultures grown with non-limiting K^+ concentration of 100 mM of KCl exhibited a cellular K^+ concentration of approx. 4 M (Figure 6). In contrast, the culture grown at an initial K^+ concentration of 3 mM showed a significantly reduced K^+ concentration of approx. 2.8 M in the stationary growth phase, corresponding to a reduction in the internal K^+ concentration by about 30 %. Microscopic analysis of corresponding cells revealed that in parallel to the reduction of the cellular K^+ concentration, the mean volume of the cells is reduced by approx 20 %. These results indicate that *H. salinarum* is able to down-regulate the intracellular K^+ concentration in response to a reduced availability of K^+ in the medium, thereby also decreasing the $\Delta\psi_{K+}$ across the membrane. As a result, both the activity of high affinity K^+ uptake systems and a simultaneous reduction of the cellular K^+ concentration allow *H. salinarum* to tolerate very low external K^+ concentrations. However, a decrease in internal K^+

is balanced by a concomitant increase in Na^+ in order to keep the iso-osmotic balance in *H. salinarum*. Thus, the ion composition inside the cell is drastically altered under conditions of extreme K^+ limitation. In addition, the cell volume is reduced under conditions of low medium K^+ concentrations and, as a consequence, a lower net amount of K^+ is needed to maintain the lower cellular K^+ concentration. In parallel, the reduction of the cell volume leads to an increased surface/volume ratio of the cell. As a consequence, proportionally more surface area is present to perform K^+-uptake upon K^+ depletion.

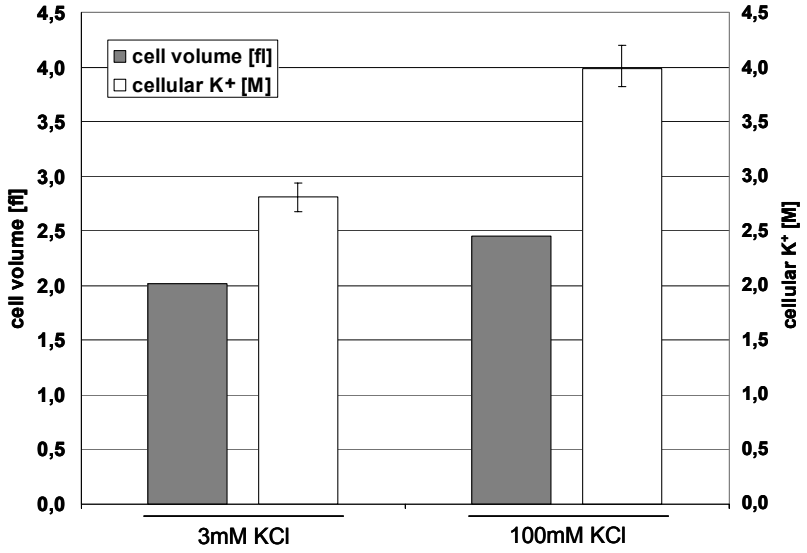

Figure 6: Cellular K^+ concentration and cell volume of *H. salinarum* upon K^+ limitation.
Cellular K^+ concentration and cell volume was measured from stationary growth phase cultures of *H. salinarum* R1 grown in media initially containing 3mM or 100mM KCl.

2.2 Sequence analysis of the halobacterial Kdp system

2.2.1 *kdp* operon organization

The genome sequences of two *Halobacterium* strains revealed the presence of several putative K^+ transport systems potentially involved in observed highly efficient uptake of K^+. Suprisingly, both genomes encode for homologs of the ATP-dependent K^+-uptake system Kdp, which was so far only reported to exist in Bacteria. Based on the genome sequence of *Halobacterium* sp. NRC-1 published by the group of DasSarma (Ng *et al*., 2000), the *kdp* genes are organized in a single operon on one of the two smaller extrachromosomal replicons, pNRC200 (accession number AE004438). An identical genomic composition and sequence with respect to *kdpFABCcat3* is found in the genome sequence of the strain *H. salinarum* R1

(Oesterhelt *et al.,* unpublished; www.halolex.mpg.de). The genome sequence of *H. salinarum* R1 localizes the *kdpFABCcat3*-operon on the extrachromosomal replicon pHS3. Therefore, all sequence analyses were done using the published genomic sequence of *Halobacterium* NRC-1, whereas all experiments were done using the strain *H. salinarum* R1.

Although the *kdpF* gene has not been annotated as such by Ng *et al*., our analysis clearly revealed the presence of *kdpF*, thus resulting in a *kdpFABCcat3* operon (Figure 7). From the initial ATG start codon of *kdpF* at position 147,382, the four genes span a distance of 5,469 bp. The arrangement of the structural genes *kdpFABC* is identical to the corresponding operon from *E. coli* (Siebers & Altendorf, 1993). The operon starts with an ORF corresponding to the *kdpF* gene, followed by the genes *kdpA, kdpB*, and *kdpC*. No homologs of the bacterial regulatory genes *kdpD* and *kdpE* were found, neither organized further downstream in a separate operon directly succeeding *kdpFABC* as in *E. coli*, nor divergently in the opposite direction preceding the structural genes like for example in *Mycobacterium tuberculosis* (Cole *et al*., 1998) or anywhere else in the genome. Instead, an additional 819-bp ORF annotated as *cat3* was found downstream of the *kdpC* gene, with the initial ATG start codon at position 152,033, thereby overlapping with the stop codon of *kdpC*. The initial annotation of this ORF as *cat3* originated from its deduced protein sequence similarity to the C-terminal region of the putative amino acid transporter Cat-1 from *Archaeoglobus fulgidus* (accession number NC_000917.1) (Klenk *et al.,* 1997). Sequence similarity between the deduced proteins Cat3 and Cat-1 with only 22 % identical residues is rather low and primarily due to the presence of two consecutive Usp (universal stress protein) family domain motifs within the C-terminal 250 residues of the 736-residue Cat-1 protein. Since the putative amino acid permease domain determining the function of Cat-1 is located at the N terminus of the polypeptide, the annotation of *cat3* is, thus, misleading and has to be renamed according to its function in the context of the *kdpFABCcat3* operon.

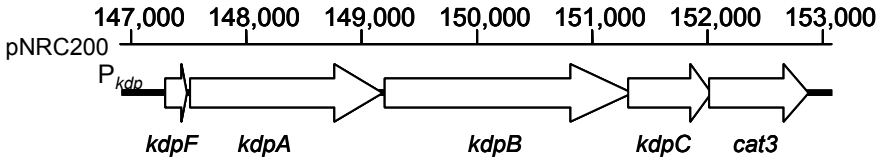

Figure 7: Organization and length of genes within the *kdpFABCcat3* operon.
Numbers indicate positions on the extra chromosomal replicon pNRC200 according to Ng *et al*., (2000).

2.2.2 Phylogenetic relationship of the archaeal Kdp systems

Up to now, six genome sequences of Archaea comprising homologs of the Kdp system have been published. Five of them, namely *Halobacterium* NRC-1 (Ng *et al*., 2000), *Thermoplasma acidophilum* (Ruepp *et al*., 2000), *Thermoplasma volcanicum* (Kawashima *et al*., 2000), *Ferroplasma acidarmanus* (accession number AABC00000000), and *Picrophilus torridus* (Futterer *et al*., 2004) belong to the phylum Euryarchaeota, whereas the sixth, *Thermofilum pedens* (accession number NZ_AASJ00000000), represents a member of the phylum Crenarchaeota. As in case of *H. salinarum*, none of these archaeal genomes features homologs of the bacterial regulatory genes *kdpD* and *kdpE*. Instead, four of these genomes, namely *Halobacterium* NRC-1, *T. acidophilum, T. volcanicum*, and *P. torridus*, comprise ORFs homologous to *cat3*, either as part of the corresponding *kdp* operon or in its immediate vicinity (Figure 8). In the genomes of *F. acidarmanus* and *T. pedens*, potential homologs of *cat3* are also present, although located more distant to the *kdp* operon. Taken together, this argues in favor of the notion, that the composition of the halobacterial *kdpFABCcat3* operon resembles a common archaeal pattern, with a single operon coding for the structural genes. Homologs of the bacterial regulatory genes are absent and replaced by a homolog of a universal stress protein.

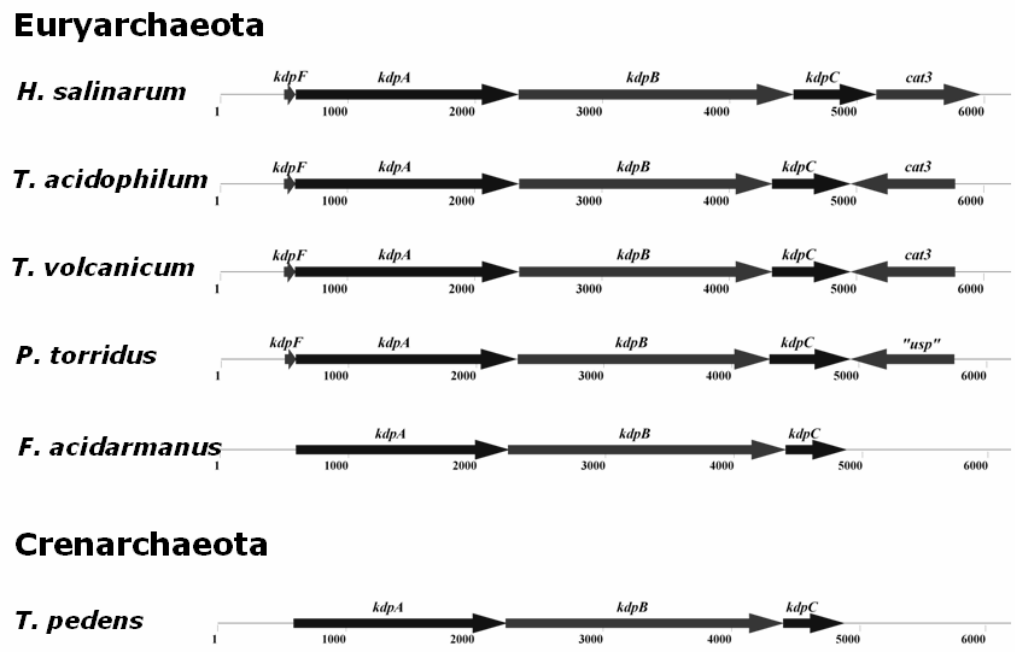

Figure 8: Operon organization of the six known archaeal Kdp systems.

A phylogenetic tree based on the alignment of all so far known putative archaeal KdpB protein sequences as well as of 89 bacterial KdpB sequences of various phyla demonstrates the high degree of sequence homology between archaeal Kdp systems. Furthermore, the archaeal Kdp systems represent an individual clade, thereby clearly separating them from the bacterial Kdp systems (Figure 9). As a concequence, the origin of the Kdp system in Archaea appears to be rooted deeply in the evolution of Archaea, which, in turn, renders the presence of the Kdp system in different Archaea as a result of individual horizontal gene transfer rather unlikely. Thus, the Kdp system is not only widespread within Bacteria but also present in various Archaea, thereby demonstrating that this K^+ uptake system is widely used by all prokaryotes rather than merely by Bacteria. In strong contrast, homologs of the Kdp system have not yet been found in any of the eukaryotic genomes sequenced so far, thereby indicating that this K^+ transport system is unique for prokaryotes. The analysis of the halobacterial Kdp system sharing a common operon organization and a phylogenetic origin with other Archaea could elucidate the role of this K^+ uptake system not only in *H. salinarum* but in other Archaea as well.

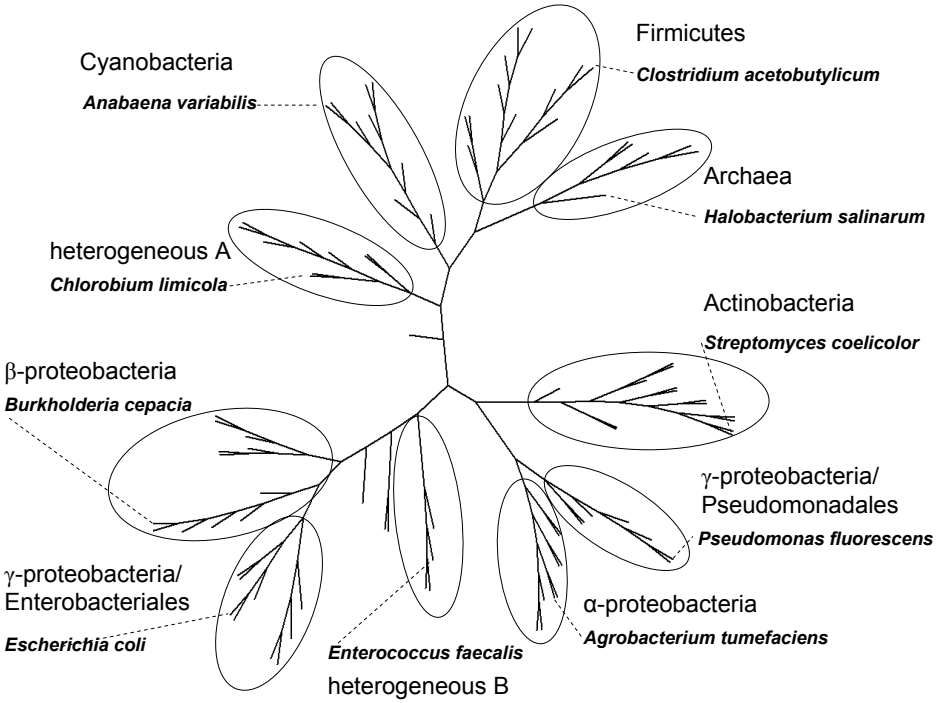

Figure 9: Unrooted radial phylogenetic tree based on a sequence alignment of six archaeal and 89 bacterial deduced KdpB protein sequences.
The domain Archaea, the phyla Firmicutes, Cyanobacteria, and Actinobacteria as well as the classes α- and β-proteobacteria, and the orders Pseudomonadales and Enterobacteriales are indicated as separate clades. The two heterogeneous clades are composed of species of classes γ-proteobacteria, Deinococci, Chlorobia, δ-proteobacteria, Bacteroidetes, and Sphingobacteria (heterogeneous A) and Spirochaetes and Bacilli (heterogeneous B). One characteristic representative of each clade is highlighted with the species name.

2.3 Kdp-dependent K^+ homeostasis of *H. salinarum*

2.3.1 Deletion of *kdpFABCcat3* and *kdpFABC*

In order to study the specific role of the Kdp system and the gene product of *cat3* in the K^+-homeostasis of *H. salinarum*, a deletion of both the entire *kdpFABCcat3* operon as well as of the *kdpFABC* genes was carried out. The resulting deletion strains were viable and exhibited a growth behavior in rich medium essentially similar to thst of the wild type (data not shown). In contrast, both deletion strains showed a different growth phenotype with respect to the wild type regarding their tolerance towards K^+ limitation. As demonstrated above, *H. salinarum* cultivated in medium with an initial K^+ concentration of 3 mM reaches stationary growth phase earlier due to K^+ limitation. In contrast to the wild type, both the *kdpFABCcat3* and *kdpFABC* deletion strains exhibited a similar growth phenotype during the log-phase but entered the stationary phase at a lower optical density (Figure 10A). Although there is apparently only a slight difference, this effect was highly reproducible and, thus, can be considered specific.

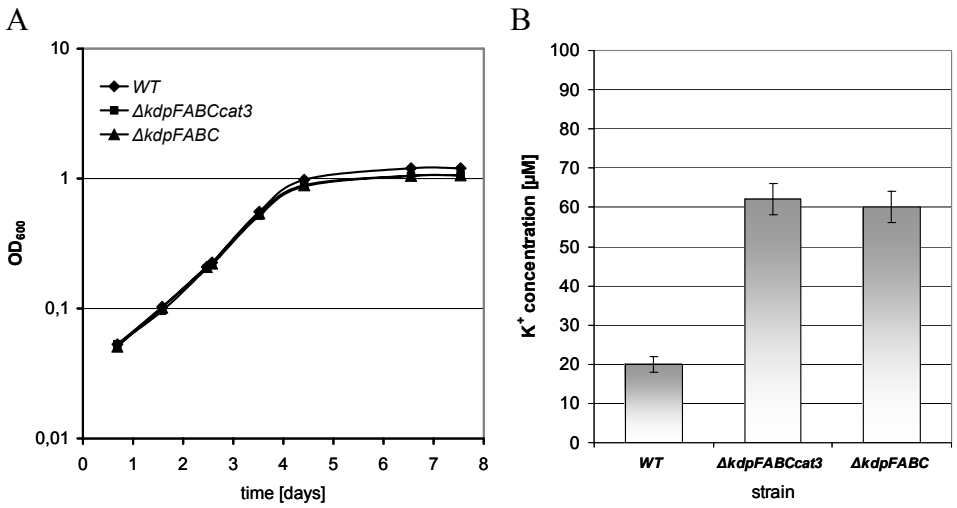

Figure 10: Phenotype of *kdpFABCcat3* and *kdpFABC* deletions.
(A) Cultivation of *H. salinarum* R1, *H. salinarum* Δ*kdpFABCcat3*, and *H. salinarum* Δ*kdpFABC* in media initially containing 3 mM KCl. The growth curves of *H. salinarum* Δ*kdpFABCcat3* and *H. salinarum* Δ*kdpFABC* are virtually congruent. (B) Residual medium K^+ concentration as measured by flame emission photometry in triplicate from stationary growth phase cultures of (A).

The residual K^+ concentration in the medium was measured from the stationary phase cultures. The wild type strain was again able to accumulate K^+ down to 20 µM (Figure 10B). In contrast, both the *kdpFABCcat3* and *kdpFABC* deletion strains were only able to grow in the presence of K^+ concentrations above 60 µM, thereby clearly demonstrating that the altered

growth phenotype is due to the deletion of the high-affinity K^+ uptake system under K^+-limiting conditions.

As shown in figure 6, *H. salinarum* adapts to K^+-limiting conditions by the reduction of both cell volume and cellular K^+ concentration. Under the same conditions, the uptake of K^+ is highly dependent on the presence of the high-affinity Kdp system. In order to analyze the possible role of the Kdp-dependent K^+-uptake in the adaptation of cellular volume and K^+ concentration, both adaptation types were studied in the *kdp*-deletion strain *H. salinarum* Δ*kdpFABCcat3* (Figure 11).

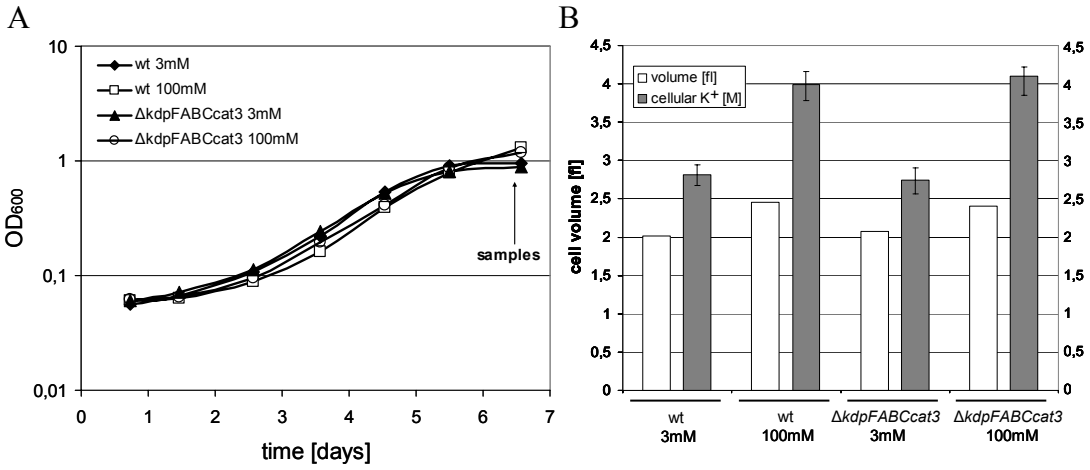

Figure 11: Adaptation of cell volume and cellular K^+ in a *kdpFABCcat3* deletion strain.
(A) Cultivation of *H. salinarum* wild type and *H. salinarum* Δ*kdpFABCcat3* in media initially containing 3 mM KCl. Growth was monitored as optical density of the culture. The time point for sample collection is highlighted by an arrow. (B) Comparison of cellular K^+ concentration and cell volume of *H. salinarum* wild type and Δ*kdpFABCcat3*.

Cellular volumes and K^+ concentrations were measured for wild type cells and a *kdpFABCcat3*-deletion strain grown with initial K^+ concentrations of 100 mM and 3 mM. Similar to the growth phenotypes described above, the cultures of both wild type and deletion strains grown with 3 mM of KCl entered the stationary growth phase at an earlier stage due to K^+ limitation, and the deletion strain *H. salinarum* Δ*kdpFABCcat3* entered the stationary phase at a slightly lower optical density as already described in figure 10. The cultures grown with non-limiting K^+ concentration of 100 mM of KCl exhibited a cellular K^+ concentration of approx. 4 M with no significant difference between wild type and *kdpFABCcat3*-deletion strain (Figure 11B). The cultures grown at an initial K^+ concentration of 3 mM both showed a significantly reduced K^+ concentration of approx. 2.8 M in the stationary phase well in accord with figure 7. However, no significant difference between wild type and *kdpFABCcat3*-

deletion strain could be observed. Furthermore, the determination of cell volumes also resulted in same values independent of the *kdpFABCcat3*-deletion. This data clearly demonstrate the presence of both adaptation types in *H. salinarum* independent of the presence of the *kdpFABCcat3* operon. As a consequence, the adaptation of cell volume and cellular K^+ concentration under K^+ limiting conditions seems to be a Kdp-independent process. The possible role of these adaptation types in the regulation of the Kdp system will be discussed later.

The phenotype of the *kdpFABCcat3* deletion strain could completely be restored and, thus, complemented by the concomitant plasmid-encoded expression of *kdpFABCcat3* (Figure 12). A plasmid-encoded expression of *kdpFABC* without *cat3,* however, did not lead to complementation. These findings further emphasize the specificity of the Kdp system in this effect and already point toward an essential role of the *cat3* gene product, either for the activity of the transport complex itself or for the expression of the corresponding genes.

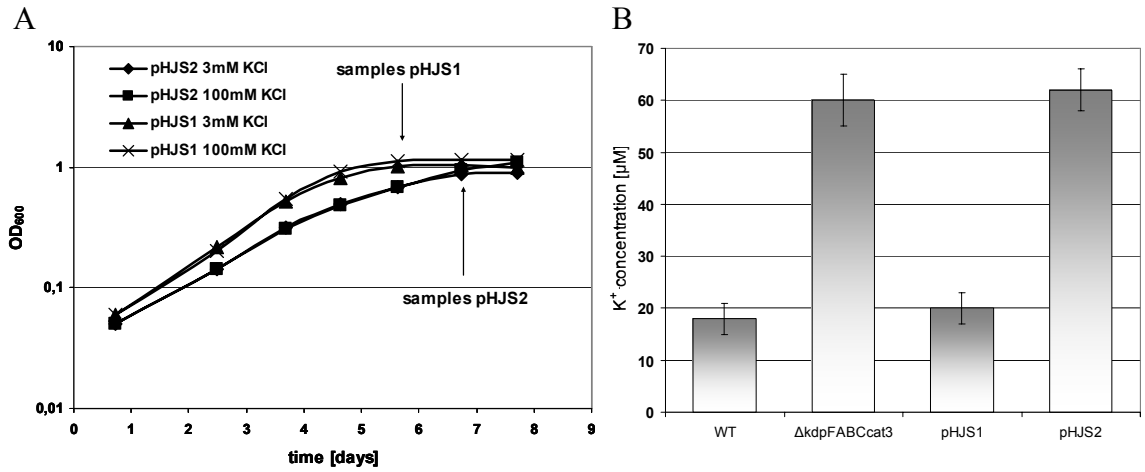

Figure 12: Phenotype of the complementation of Δ*kdpFABCcat3* by plasmid-encoded expression of *kdpFABCcat3* (pHJS1) and *kdpFABC* (pHJS2).
(A) Cultivation of *H. salinarum* Δ*kdpFABCcat3* carrying plasmids pHJS1 or pHJS2 in media initially containing 3 mM or 100 mM KCl, monitored as optical density of the culture. (B) Effect of *cat3* deletion on K^+-uptake. Residual medium K^+ concentrations were measured by flame emission photometry in triplicate from stationary growth phase cultures (sample collection points highlighted in (A) with an arrow).

2.3.2 Expression of the *kdpFABCcat3* operon

To provide first evidence of an active expression of the *kdpFABCcat3* operon, the transcription of the operon was verified by reverse transcriptase PCR. Total RNA of *H. salinarum* R1 was purified from a culture grown in rich medium, and the expression of the *kdpFABCcat3* operon was detected by sequence-specific primers binding in *kdpC* and *cat3* (Figure 13). The use of genomic DNA as a template revealed the presence of the genes and,

thus, served as a positive control (lane 1). No PCR product could be detected with DNaseI–degraded total RNA, serving as a negative control for template purity (lane 2). A specific PCR product exhibiting the expected size could clearly be observed in case of cDNA as template (lane 3), thereby clearly demonstrating the transcription of the corresponding *kdp* genes. Thus, although the Kdp system was so far only reported to exist in Bacteria, *H. salinarum* encodes and also actively expresses genes homologous to the Kdp system. In Bacteria, the expression of Kdp system is highly regulated in a medium K^+ concentration dependent manner. Although expression of the halobacterial *kdp*-operon can be detected in rich medium, quantitative expression level measurements in a casaminoacids-medium permitting better control of medium K^+ concentration are needed to analyze the regulation of gene expression.

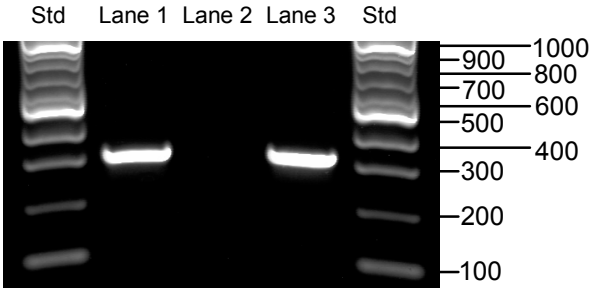

Figure 13: Detection of gene expression of the *kdpFABCcat3* operon by reverse transcriptase PCR. DNA was amplified with sequence-specific primers binding in *kdpC* and *cat3*. Genomic DNA (lane 1), DNaseI-degraded RNA (lane 2), and cDNA (lane 3) were used as template. Std, length standard.

2.3.3 Induced expression of the *kdpFABCcat3* operon

2.3.3.1 Medium K^+ dependent expression of the *kdpFABCcat3* operon

For *H. salinarum*, the expression of a high affinity, ATP-dependent Kdp system is feasible under conditions of a low membrane potential (due to ATP-dependency) and/or low medium K^+ concentrations (due to high affinity), both leading to an increasing $\Delta\psi_{K+}$, under which the other uptake system can no longer supply the cell with K^+ due to either energetic and/or affinity considerations.

Well-detectable levels of *kdp* expression could already be observed under non-limiting conditions using rich medium by reverse transcriptase PCR (compare Figure 13), but without any quantitative means. In order to analyze the effect of the medium K^+ concentration on the expression rate of the *kdpFABCcat3* operon more precisely, *H. salinarum* was cultivated in the presence of different initial K^+ concentrations (3, 5, and 50 mM KCl). K^+ uptake was followed by FEP (Figure 14), and the expression rate of the *kdpFABCcat3* operon was concomitantly measured quantitatively by *real time* RT-PCR (Figure 15).

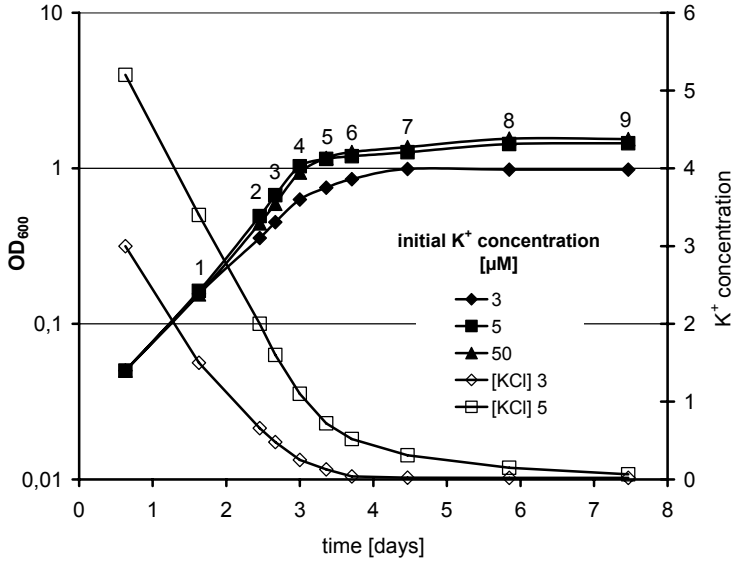

Figure 14: Quantitative analysis of K^+-dependent growth of *H. salinarum*.
Cultivation of *H. salinarum* R1 in media containing different initial K^+ concentrations was monitored as optical density of the culture (left y-axis). Residual medium K^+ concentration measured by flame emission photometry is given for cultures grown at an initial K^+ concentration of 3 mM and 5 mM (right y-axis). Samples were collected from all cultures for *real time* RT-PCR analysis and are numbered correspondingly to sample numbers of Figure 15.

As expected, in a culture grown in non-limiting K^+ concentrations of 50 mM KCl, the expression of the *kdp* operon is on a low but still detectable level, which is in accord with the transcript analysis by reverse transcriptase PCR in rich medium (Figure 13). In contrast, in cultures grown in 5 and 3 mM of KCl (i.e. K^+ limitation), expression is highly induced. The level of expression was found to be clearly dependent on the K^+ concentration in the medium. In cultures grown in in 5 and 3 mM of KCl, the expression in only slightly further stimulated by a decrease of medium K^+ concentration down to approx. 250 µM (samples 1-4 in 3 mM culture and samples 1-5 in 5 mM culture). However, in culture grown in 3 mM of KCl the expression undergoes a strong secondary induction in medium K^+ concentrations below 250 µM (samples 5-7) and reached its maximum at the lowest medium K^+ concentration (20 µM, sample 7). At that point, the *kdp* operon is almost 1000-fold induced with respect to the low expression level in the presence of 50 mM KCl in medium. From this experiment, the relationship between gene expression, residual K^+ concentration in the medium, and K^+-limiting growth conditions becomes evident. Maximal gene expression occurs in case of extremely low K^+ concentrations in the medium, which, in turn, lead to an earlier stationary growth phase. The culture grown in 5 mM KCl still did not exhibit a stationary K^+ depletion level in the medium, which is in accord with the reduced expression rate of the *kdp* operon

with respect to the culture grown in 3 mM KCl. Only at 3 mM initial KCl, the cells reached the minimal K^+ concentration enabling growth (i.e. 20 µl) and, hence, enter the stationary phase due to K^+ depletion with a maximum in *kdp* operon expression. However, in the stationary growth phase, the expression of the *kdp* operon is again down-regulated in an apparently K^+-independent manner. This points in favor to the notion that this stationary phase repression is governed by a more general growth phase-dependent regulation rather than by a putative K^+-specific mechanism.

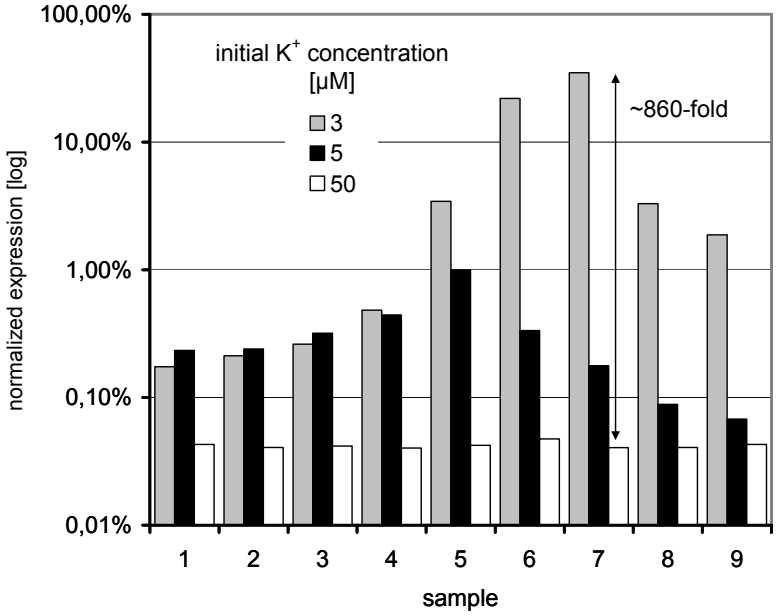

Figure 15: Quantification of K^+-induced *kdpFABCcat3* gene expression.
Normalized expression levels of *kdpFABCcat3* were measured by *real time* RT-PCR in media containing initial K^+ concentrations of 3 mM, 5 mM, and 50 mM. Sample numbering corresponds to sample numbers shown in Figure 14. 100 % represents the expression level of the housekeeping gene *rpoA1* used as expression reference.

2.3.3.2 Medium Na^+ dependent expression of the *kdpFABCcat3* operon

H. salinarum is postulated to maintain an iso-osmotic equilibrium with the medium primary by accumulation of high concentrations of K^+ (Oren 1999). In order to accomplish this function, the cellular K^+ concentration and K^+ uptake needs to be dynamic and adapted to the changing overall salinity of the surrounding medium. For these reasons, the effect of the medium Na^+ concentration on the expression rate of the *kdpFABCcat3* operon was analyzed. *H. salinarum* was cultivated in the presence of different initial K^+ concentrations (3 and 100 mM KCl) in combination with varying NaCl concentrations (2, 3, and 4 M). The expression

rate of the *kdpFABCcat3* operon was measured quantitatively by *real time* RT-PCR in the late logarithmich growth phase (Figure 16).

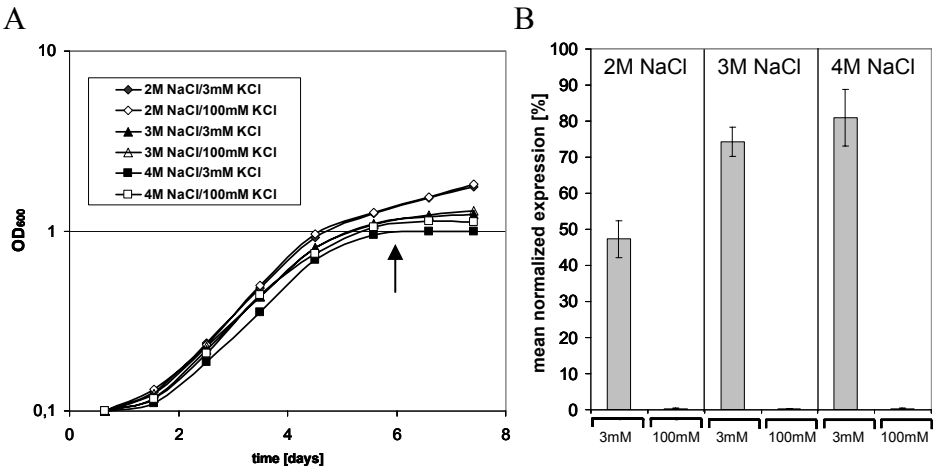

Figure 16: Quantification of K^+-induced *kdpFABCcat3* gene expression in the presence of different medium NaCl concentrations.
(A) Cultivation of *H. salinarum* wild type in media containing 2, 3, and 4 M NaCl together with 3 mM and 100 mM initial K^+, monitored as optical density of the culture. (B) Mean normalized expression levels of *kdpFABCcat3* gene expression in different media measured in the late logarithmic growth phase by *real time* RT-PCR in triplicate (sample collection points highlighted by an arrow). 100 % represents the expression level of the housekeeping gene *rpoA1* used as expression reference.

The cultivation of *H. salinarum* at different NaCl concentrations revealed no significant preference regarding generation time (Figure 16A). However, differences were monitored with respect to maximal optical densities. In the presense of 100 mM KCl, the highest optical density is archieved in the culture grown in 2 M NaCl. In the culture grown in the presence of 3 M NaCl and ever more clearly in the presence of 4 M NaCl, the maximal optical density is significantly reduced. A similar difference was monitored with respect to maximal optical densities upon K^+-depletion. Whereas the culture grown in the presence of 4 M NaCl and initial 3 mM KCl reached K^+-limitation-induced stationary growth at OD_{600} of approx. 1, the corresponding culture grown in the presence of 3M NaCl was able to grow up to an OD_{600} of approx. 1.2. In both cultures, the measured residual medium K^+ concentration was 20 µM as reported above. In culture grown in the presence of 2 M NaCl, even higher optical densities could be measured, although the residual medium K^+ concentration was still above 100 µM, and thus, not limiting. These measurements indicate a significant influence of medium salinity on either amount of K^+ taken up by the culture or on optical properties of the culture (biased by factors like for instance cell size) or both.

All measured strains exhibited highly induced expression levels under inducing conditions (in media containing initial K^+ concentrations of 3 mM) (Figure 16B). Although the expression level is slightly lower in the presence of 2 M NaCl, this is most likely due to higher residual medium K^+ concentrations present at the time point of sample collection. The expression levels under repressing conditions (in media containing initial K^+ concentration of 100 mM) were low but detectable. As a consequence, medium NaCl concentration obviously does not significantly influence the expression level of the *kdpFABCcat3* operon.

2.4 Regulation of *kdpFABCcat3* expression

2.4.1 Sequence-based analysis of the promoter region

The transcriptional apparatus of Archaea more closely resembles that of Eucarya rather than that of Bacteria (Woese *et al*., 1990). This, in turn, leads to a different promoter structure of the *kdpFABCcat3* operon with respect to its bacterial counterpart. For an initial analysis, the putative promoter region of the *kdpFABCcat3* operon (P_{kdp}) was aligned to the well-characterized 53-bp minimal *bop* promoter (P_{bop}) (Gropp *et al*., 1995) (Figure 17). Whereas in P_{bop} there is only a weak homology of the TATA box sequence to the common archaeal TATA-box consensus (Baliga and DasSarma, 1999), P_{kdp} comprises a more distinctive TATA box element located 31 to 25 bp upstream of the transcription start site. Featuring the sequence 5'-TATAAA-3', it is more related to the common archaeal TATA-box consensus sequence of 5'-T/CTTAT/AA-3' (Palmer and Daniels, 1995) and also comprises the formation of TA dinucleotides, which is an additional characteristic feature of highly efficient archaeal promoters (Reiter *et al*., 1990). The INR element marking the start site of transcription is identical in both P_{bop} and P_{kdp} and resembles the relatively weak consensus of 5'-T/CG/A-3' (Palmer and Daniels, 1995), with the transcription starting at the purine base. The location of the transcription initiation site of the *kdpFABCcat3* operon (as highlighted with by an arrow in Figure 17) was verified by primer extension analysis by D. Kixmüller during her diploma thesis (Kixmüller *et al.,* in preparation). Thus, for the *kdpFABCcat3* operon, transcription is supposed to start four nucleotides upstream of the ATG start codon from the postulated *kdpF* gene, resulting in a leaderless mRNA without a ribosomal binding site (RBS). A possible common transcription factor B recognition element (BRE) can be found upstream of the TATA-box region in P_{kdp}. The sequence –36(5'-ACAA-3')–33 closely resembles the –36(5'-gNAA-3')–33 or, more generally, the –36(5'-PuNPu-3')–34 consensus sequence motifs predicted to be involved in TFB interaction in Archaea (Qureshi and Jackson, 1998; Soppa,

1999). Thus, the putative P_{kdp} carries all conserved *cis*-acting elements required in an active archaeal promoter.

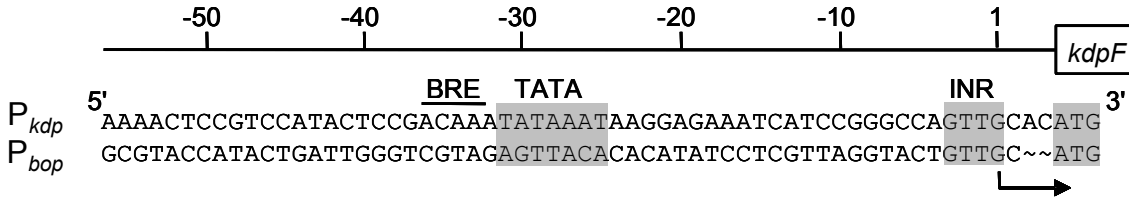

Figure 17: Alignment of the *kdpFABCcat3* promoter (P_{kdp}) to the minimal promoter region of the bacterio-opsin gene (P_{bop}).
The sequence is numbered for P_{bop}, starting with the transcription start point (black arrow) as +1. The translational start codon, transcription initiation region (INR), and TATA-box are shaded. The putative recognition element for transcription factor TFB binding (BRE) is marked for P_{kdp}.

2.4.2 Truncation analysis of the *kdp* promoter

As shown in Figure 15, the expression of the *kdpFABCcat3* operon underlays a complex K^+- and growth phase-dependent regulation. The vast majority of regulated genes are regulated at the level of initiation of transcription by means of transcriptional activators or repressors. Thus, the regulation of the *kdpFABCcat3* operon was studied by site-directed mutagenesis and truncation analysis of the *kdp* promoter. This was done using plasmids, which are coding for a transcriptional fusion of the *kdp* promoter with a halobacterial ß-galactosidase (*bgaH*) as a reporter gene, or using plasmids, which encode for the entire *kdpFABCcat3* operon. The establishment of the *bgaH*-based reporter gene-assay and the preliminary truncation analysis to identify the minimal active promoter was done by E. Özyamak during his diploma thesis (Özyamak, unpublished). A more detailed truncation analysis and the analysis of the regulation of different promoter truncations using the *bgaH* reporter gene-assay were carried out by D. Kixmüller during her diploma thesis (Kixmüller *et al.,* in preparation). Both diploma thesises were carried out under my co-supervision. During these two diploma-thesises, detailed information was obtained about the type of regulation and the localization of *cis*-active elements within the *kdp*-promoter. In summariy, (I) not more than 42 bp upstream of the transcription start is essential for the promoter activity. (II) No essential regulatory *cis*-active elements are present downstream of the start codon of the first gene *kdpF*. (III) The *kdp* promoter underlays a negative regulation. (IV) The minimal fully regulated promoter was identified to be approx. 96 bp long and (V) a potential repressor binding site was located downstream of -96bp.

Based on the truncations analysis, a search for palidromic sequences as potential binding sites for transcriptional regulators of the HTH (helix-turn-helix)–type using ExtraTrain (Pareja *et al.,* 2006) revealed a potential repressor binding site located between -54 bp and -75 bp (Figure 18).

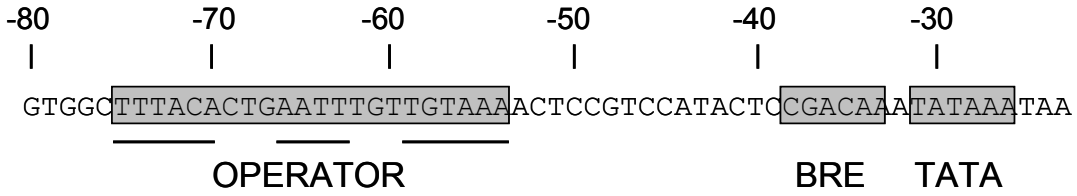

Figure 18: Overview of P_{kdp}. Location of the putative conserved promoter elements and the putative operator sequence. Lines below the putative operator highlight the corresponding palindromic sequence.

In addition, a sequence-based analysis of this putative repressor binding site with the program bend.it® (Munteanu *et al.,* 1998) revealed an intrinsic tendency of this sequence region to bend DNA (Figure 19), which is characteristic of several binding sites for HTH-type repressors (Pérez-Martín & de Lorenzo, 1978; Harrington, 1992).

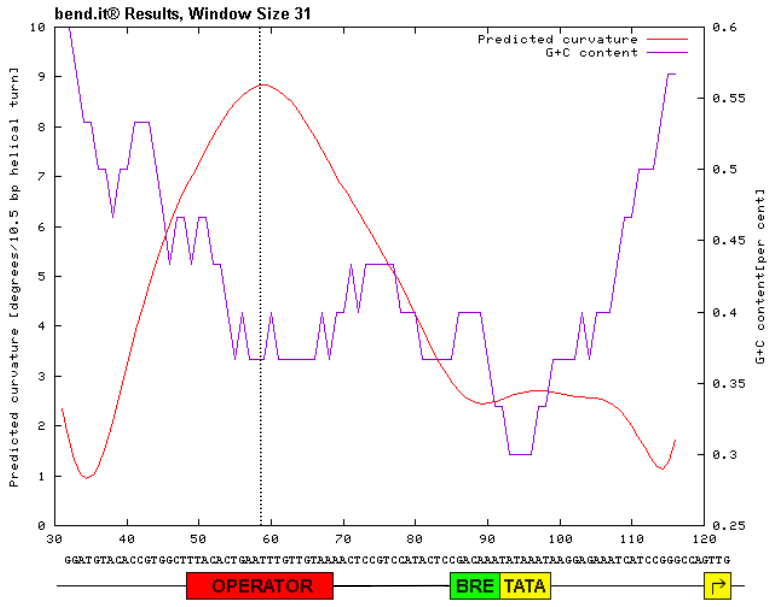

Figure 19: Sequence-based prediction of intrinsic DNA curvature and G+C content of the P_{kdp}-region (-94 to +1) by bend.it®.
The red line indicates the predicted curvature (degrees/helical turn, left-y axis); the purple line indicates the G+C content (right y-axis). The corresponding DNA-sequence with putative conserved promoter elements as well as the putative operator sequence is shown below the plot. The dotted line indicates the maximal predicted curvature in the region of the putative operator. The window size for the calculation was set to be 31.

In order to verify the role of this potential *cis*-active element in the transcriptional regulation of the *kdpFABCcat3* operon, plasmids were constructed carrying the *kdpFABCcat3* operon under control of different truncated *kdp* promoters (-206 bp, -52 bp and -42 bp) as well as a promoter construct with a deletion of the putative *cis*-active element (-54 bp to -75 bp). *H. salinarum* wild type without plasmid and *H. salinarum* Δ*kdpFABCcat3* carrying the corresponding plasmids pHJS9, pHJS10, pHJS11, and pHJS12 were cultivated in medium with an initial K^+ concentrations of 3 mM and 100 mM (Figure 20A). All strains exhibited a growth phenotype similar to that of the wild type. The expression levels of the *kdpFABCcat3* operon under control of the different modified *kdp* promoters were measurered by *real time* RT-PCR (Figure 20B).

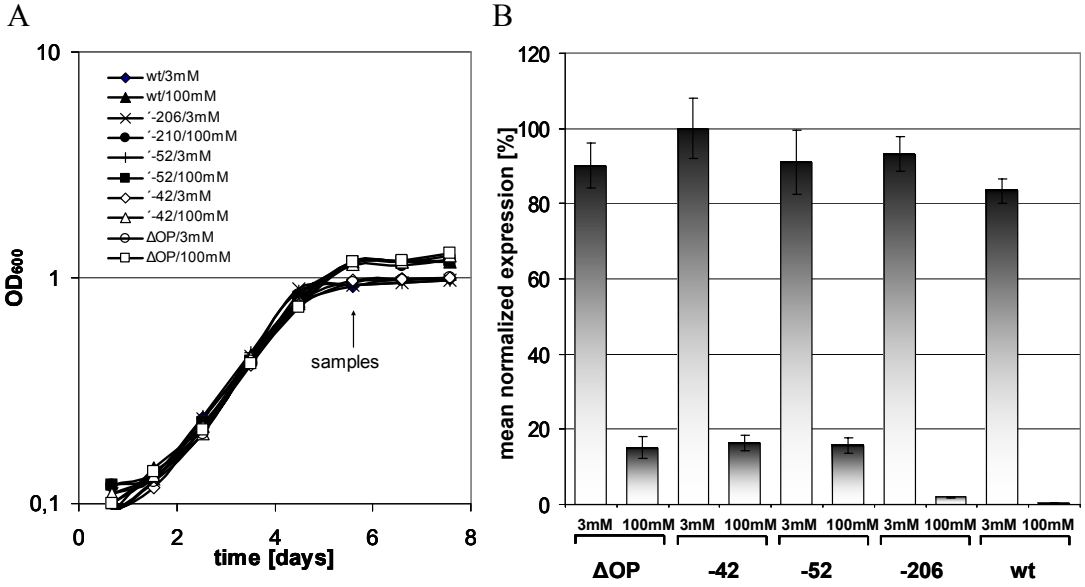

Figure 20: Truncation analysis of the promoter of the *kdpFABCcat3* operon.
(A) Cultivation of *H. salinarum* wild type and Δ*kdpFABCcat3* carrying plasmids coding for *kdpFABCcat3* with different variants of P_{kdp} in media containing 3 mM and 100 mM initial K^+, monitored as optical density of the culture (ΔOP, deletion of the putative operator sequence (pHJS9), -206, 206 bp long promoter (pHJS10), -52, 52 bp long promoter (pHJS11), -42, 42 bp long promoter (pHJS12)). (B) Normalized expression levels of *kdpFABCcat3* gene expression from different promoter variants measured in the late logarithmic growth phase by *real time* RT-PCR in triplicate (sample collection points highlighted by an arrow). 3 mM and 100 mM, initial K^+ concentrations.

As in case of the growth curve, all strains exhibited expression levels comparable to that of the wild type under inducing conditions (in media containing initial K^+ concentrations of 3 mM; Figure 20B). In contrast, the expression levels under repressing conditions (in media containing initial K^+ concentration of 100 mM) were distinctively affected by the mutations in the *kdp* promoter, although the growth curves were virtually congruent. The expression under control of a 206-bp long *kdp* promoter was virtually equal to the wild type. The truncated *kdp*

promoters carrying 42- and 52-bp long *kdp*-promoters, in contrast, exhibited significantly higher expression levels under repressing conditions. This clearly indicates a truncation-mediated loss of a *cis*-active element, which is at least partially responsible for a negative regulation of the *kdp* promoter. The deletion of the putative repressor binding site resulted in a virtually identical effect on the regulation of the *kdp* promoter. This strongly indicates the function of the region between -54 bp to -75 bp as an operator of the *kdp* promoter. Although this region obviously has a function in the negative regulation of transcription, the promoter lacking this sequence is still partially downregulated under repressing conditions. This, together with the fact that the identified potential operator is located clearly upstream of the conserved promoter elements (17 bp), implies the presence of an additional operator located between the transcription start site and the identified potential operator. However, although no homologous sequences serving as potential candidates for the second putative operator could so far be indentified in this region, based on these results, a co-operative action of two different regulatory proteins in the repression of the *kdp* system is likely.

2.4.3 Regulatory function of *cat3*

As demonstrated by the experiments shown in Figure 20, plasmid-encoded expression of *kdpFABCcat3* is sufficient to complement the phenotype of a chromosomal *kdpFABCcat3* deletion strain. However, complementation was not observed by plasmid-encoded expression of *kdpFABC* only. This readily identifies *cat3* as an essential component of the halobacterial Kdp system. In order to distinguish whether *cat3* gene product is involved in a transcriptional regulation of the *kdp*-operon or in activation of the KdpFABC complex, the expression of plasmid-encoded *kdpFABCcat3* (pHJS1) and *kdpFABC* (pHJS2) was studied in a *kdpFABCcat3* deletion background. Both strains were again cultured in media containing 3 or 100 mM KCl, and samples were collected for *real time* RT-PCR measurements in the late logarithmic growth phase (Figure 21A). The corresponding growth phenotypes are interpreted in context of the figure 12A (same data set). The expression of plasmid-encoded *kdpFABCcat3* was found to be essentially comparable to the wild type, with high expression levels in the presence of near-limiting K^+ concentrations and a low expression level in case of non-limiting 100 mM KCl (Figure 21B, compare Figure 20B). In contrast, the plasmid-encoded *kdpFABC* without *cat3* is expressed at a significantly lower level (<10%) even in case of near-limiting K^+ concentrations (Figure 21B), although trancription still was inducible. No differences were observed in case of 100 mM KCl, thereby demonstrating that the *cat3* gene product is not involved in the repression. As a consequence, the *cat3* gene

product appears to have an essential function in the transcriptional regulation of the halobacterial *kdpFABCcat3* operon.

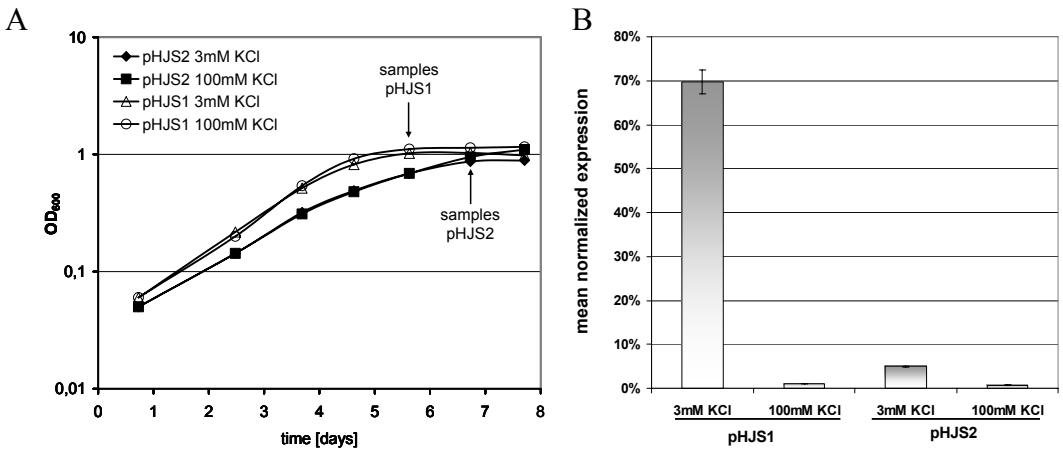

Figure 21: Function of Cat3 in the transcriptional regulation of the *kdpFABCcat3* operon.
(A) Cultivation of *H. salinarum* Δ*kdpFABCcat3*/pHJS1 (*kdpFABCcat3*) and *H. salinarum* Δ*kdpFABCcat3*/pHJS2 (*kdpFABC*Δ*cat3*) in media containing 3 mM and 100 mM initial K^+, monitored as optical density of the culture. (B) Normalized expression levels of *kdpFABC* in *H. salinarum* Δ*kdpFABCcat3*/pHJS1 and *H. salinarum* Δ*kdpFABCcat3*/pHJS2 in the late logarithmic growth phase measured by *real time* RT-PCR in triplicate. 100 % represents the expression level of the housekeeping gene *rpoA1* used as expression reference; sample collection points highlighted by an arrow.

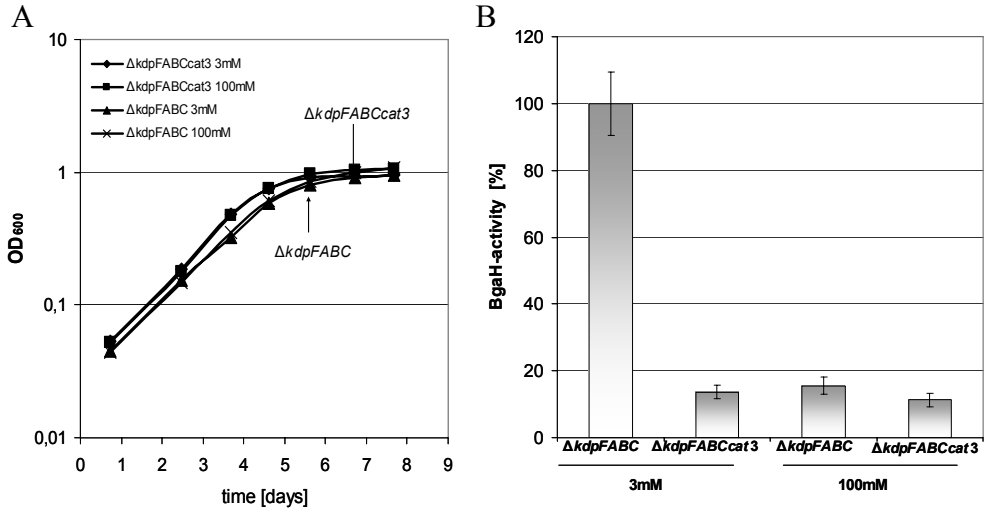

Figure 22: Function of Cat3 in the transcriptional regulation of the *kdpFABCcat3* operon.
(A) Cultivation of *H. salinarum* Δ*kdpFABC* and Δ*kdpFABCcat3* both carrying plasmid pOEZ1 in media containing 3 mM and 100 mM initial K^+, monitored as optical density of the culture. (B) The *kdp*-promoter activity in *H. salinarum* Δ*kdpFABC* and Δ*kdpFABCcat3* in the late logarithmic growth phase measured by a transcriptional fusion with *bgaH* (sample collection points highlighted by an arrow).

A potential *cis*-active function of the *cat3* gene for example on mRNA stability can be ruled out, since the same findings were also obtained from β-galactosidase promoter fusion analyses with Cat3 still encoded on the chromosome and expressed by P_{kdp} (Figure 22A and 22B).

Although *cat3* is obviously essential for a high level expression of the *kdpFABCcat3*-operon, Cat3 can not have a potential function in primary medium K^+-dependent induction of the Kdp system. As discussed later, the expression of the *kdpFABCcat3* operon is already slightly induced in the presence of < 20 mM KCl in the medium. In higher K^+ concentrations, only a low backround expression level of the *kdpFABC* genes as well as *cat3* is detectable. As a consequence, the stimulating effect of Cat3 on the expression of the *kdpFABCcat3* operon must be secondary and occur after initial induction of the whole operon, which takes place in absence of Cat3.

In order to analyze the specific role of Cat3 in the regulation of *kdp* expression, a plasmid (pSH1) was contructed, which expresses *cat3* under the control of a contitutive ferrodoxin promoter (Gregor & Pfeifer, 2005). For this purpose, the vector pJAS35 (Pfeifer *et al*., 1994) was chosen. This plasmid encodes a Nb^R-casette enabling a stable selection in *H. salinarum* even in the presence of additional pMKK100–derivatives. Furthermore, the plasmid pJAS35 carries an Ap^R-resistance cassette and an OriV (enabling cloning and manipulation in *E. coli*) as well as an Ori for replication in *H. salinarum*. The plasmid pJAS35 was a generous gift from F. Pfeifer (TU Darmstadt).

In order to study the function of Cat3 in the transcriptional regulation of the *kdpFABCcat3* operon, the expression of plasmid-encoded *kdpFABC* (pHJS2) was studied in a Δ*kdpFABCcat3 strain* co-transformed with pSH1, thus enabling a contitutive expression of *cat3*. The P_{fxd}-facilitated expression of *cat3* in pSH1 at an adequate K^+-independent level was controlled in earlier measurements (data not shown). The *kdpFABCcat3* deletion strain carrying the plasmid pHJS2 together with pJAS35 was used as a reference. Both strains were cultured in media containing 3 or 100 mM KCl, and samples were collected for *real time* RT-PCR measurements in the late logarithmic growth phase (Figure 23A). In addition, the minimal K^+ concentration enabling growth was measured for cultures grown in the presence of initial 3 mM KCl.

As shown earlier, the cultivation of *H. salinarum* in the presence of initial K^+ concentrations of 3 mM results in an earlier stationary growth phase due to K^+ limitation. In the absence of the *kdpFABC*-genes, slightly lower optical densities are reached due to the inability to take up

K^+ in case of less than approx. 60 µM K^+ in the medium. Furthermore, the expression of *cat3* was shown to be essential to enable growth below 60 µM K^+ in the medium.

As expected, the *kdpFABCcat3* deletion strain carrying plasmids pHJS2 and pJAS35 already entered the stationary growth phase at an optical density of approx. 0,9 at a medium K^+ concentration of approx. 70 µM (Figure 23A and 23B). The combination of the *kdpFABCcat3* deletion strain with plasmid-encoded *kdpFABC* (pHS2) together with the plasmid-encoded constitutive expression of *cat3* (pSH1), in contrast, was able to reach an optical density of approx. 1,0 and was also able to grow with K^+ concentrations down to allmost 20 µM. As a consequence, the constitutive expression of *cat3* in *trans* is obviously sufficient to complement the phaenotype of *cat3*–deletion resulting in growth similar to the wild type (compare Figure 12).

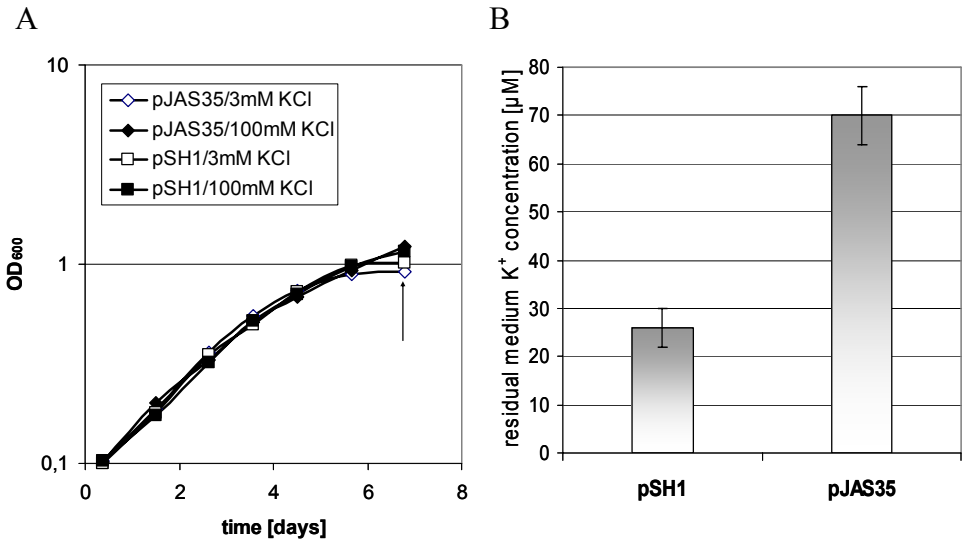

Figure 23: Complementation of Δ*cat3 (ΔkdpFABCcat3 strain* + plasmid encoded *kdpFABC)* by plasmid-encoded constitutive expression of *cat3*.
(A) Cultivation of *H. salinarum ΔkdpFABCcat3* carrying plasmid pHJS2 (*kdpFABC*) together with either pSH1 (contitutive *cat3*) or pJAS35 (negative control) in media initially containing 3 mM or 100 mM KCl, monitored as optical density of the culture. (B) Effect of contitutive expression of *cat3* on K^+-uptake. Residual medium K^+ concentrations were measured by flame emission photometry in triplicate from stationary growth phase cultures (sample collection point indicated by an arrow).

Subsequently, expression levels of *kdpFABC* encoded by plasmid pHS2 together with either plasmid pSH1 (contitutive expression of *cat3*) or the control vector pJAS35 were measured by *real time* RT-PCR (Figure 24). The expression levels of *kdpFABC* encoded by the integrative plasmid pHJS2 in the presence of the control vector pJAS35 highly corresponded to values measured in the absence of pJAS35 (see Figure 21).

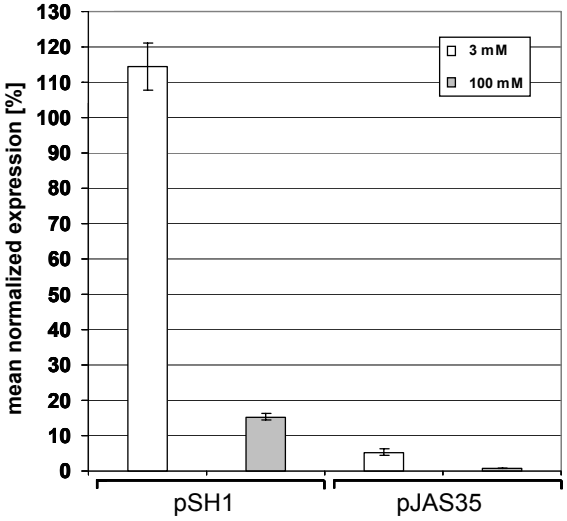

Figure 24: The effect of contitutive expression of *cat3* on the expression of plasmid-encoded *kdpFABC*.
Normalized expression levels of *kdpFABC* in *H.salinarum* Δ*kdpFABCcat3*/pHJS2/pSH1 and *H. salinarum* Δ*kdpFABCcat3*/pHJS2/pJAS35 in the late logarithmic growth phase measured by *real time* RT-PCR in triplicate. 100 % represents the expression level of the housekeeping gene *rpoA1* used as expression reference; sample collection point highlighted by an arrow in Figure 23.

In the presence of initial 3 mM KCl in the culture, the expression of *kdpFABC* exhibits in Δ*kdpFABCcat3* background maximal expression levels of below 10 % of the levels measured in the presence of *cat3*. In the culture grown under non-limiting 100 mM KCl, the uninduced expression level of *kdpFABC* was on a low but still detectable level. However, in the presense of plasmid pSH1, from which *cat3* is expressed constitutively, the expression profile of *kdpFABC* was highly biased. The constitutuve expression of *cat3* in *trans* readily complemented the phaenotype obtained in case of the absence of *cat3* (see Figure 23B). Therefore, the expression of *kdpFABC* was on a high level under K^+-limiting conditions (initial 3 mM KCl). However, the expression level of more than 110 % of the expression level of the housekeeping gene *rpoA1*, revealed to be on a significantly higher level than by plasmid pHS1 (*kdpFABCcat3*; 70 %, see Figure 21) or even in case of wild type (50-80 %, Figures 15 and 16). Furthermore, the constitutive expression of *cat3* resulted in a highly stimulated expression of *kdpFABC* of approx. 15 % even in the presence of repressing conditions. As a consequence, Cat3 obviously has its function in the high level induction of the *kdpFABCcat3*-operon in stimulating the expression after initial lower level induction of the the *kdp*-genes and *cat3* itself.

2.5 Global transcriptional response in *H. salinarum* to K^+ depletion

2.5.1 DNA microarray analysis

Despite the valuable details about changes in cell volume, ion composition and expression of the *kdpFABCcat3* operon in response to K^+ depletion, more global information is needed to understand the cellular response of *H. salinarum* in a more comprehensive manner. In order elucidate the global cellular response of *H. salinarum* to K^+ depletion at the level of gene expression, a DNA microarray study was carried out. The RNA samples needed to identify up- and down-regulated genes as a response to K^+ depletion were collected from *H. salinarum* grown in media with an initial K^+ concentration of 3 mM and 100 mM (Figure 25). Similar to the growth phenotypes described above, the culture grown with 3 mM of KCl entered stationary growth at an earlier stage due to K^+ limitation. The samples were collected at late logarithmic growth phase (OD_{600}=ca.1). At that point, the medium K^+ concentrations exhibited values of 30 µM in a medium with initially 3 mM KCl, and 95 mM in medium with initially 100 mM KCl. Although this rather late sample collection point makes it difficult to differentiate between genes regulated as a response to K^+ depletion and genes regulated as an early response in reaching the stationary growth phase, it is mandatory to ensure adequate K^+ depletion.

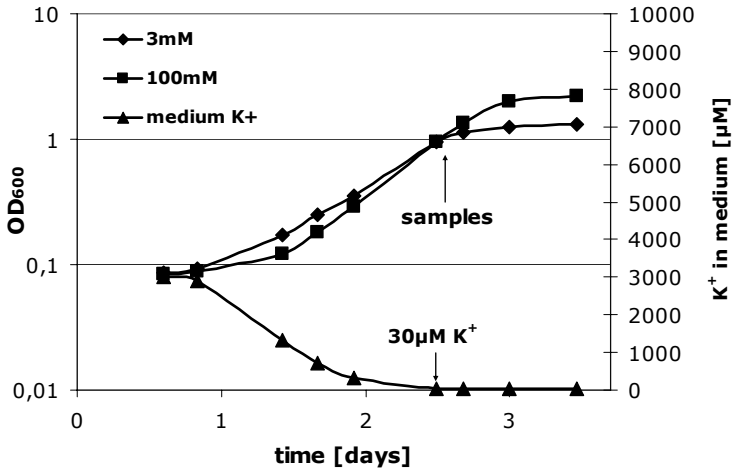

Figure 25: Cell cultivation for DNA microarray studies.
Cultivation of *H. salinarum* wild type in media containing 3mM and 100mM initial K^+, monitored as optical density of the culture (left y-axis). Residual medium K^+ concentration measured by flame emission photometry is given for the culture grown at an initial K^+ concentration of 3 mM (right y-axis). The sample collection point and the corresponding medium K^+ concentration in the K^+-limited culture are highlighted by arrows.

The DNA microarray study was carried out in cooperation with A. Wende (MPI for Biochemistry, Martinsried). Two independent sets of microarray slides were hybridized with the samples collected as described above. During the analysis, only changes in expression levels fulfilling the following parameters were considered significant. (I) The values from two

individual sets of microarray chips had to pass a permutation–based t-test. (II) The difference between log2 mean median values of microarray slides hybridized with different samples had to be higher than 0,7. (III) The mean standard deviation of both arrays had to be less than the mean median values thereof. In table 1, the genes down-regulated upon K^+ depletion are listed in the order of the measured expression level difference. Table 2 represents the up-regulated genes in a corresponding order. A total number of 35 genes down-regulated and 26 genes up-regulated in repsonse to K^+ limitation were identified. As expected, *kdpA*, *kdpB*, *kdpC*, and *cat3* were among genes that are highly induced under K^+ limiting conditions. In addition to *kdp*-genes, a remarkably high number of unknown genes are coinduced under these conditions. A high number of transposons together with several genes of an operon coding for a A_1A_o ATPase are among genes that are downregulated. Interestingly, *orc3*/*cdc6* gene homologs regulating initiation of replication and, as a consequence, cell division are also regulated in response to changes in medium K^+ concentration.

Table 1: List of genes down-regulated under K^+ limiting conditions as identified by DNA-microarray analysis.

ID*	gene name**	predicted function***	mean of medians****	mean of stddevs*****
OE3644F	*nadA*	quinolinate synthetase A	-1.55E+00	8.52E-02
OE3949R	-	glutaredoxin homolog	-1.24E+00	6.12E-02
OE1102R	-	transposase	-1.13E+00	5.19E-02
OE1019R	-	transposase	-1.12E+00	7.43E-02
OE1472F	*fba2*	fructose-bisphosphate aldolase	-1.08E+00	6.56E-02
OE1173F	-	transposase	-1.07E+00	5.04E-02
OE7198F	-	transposase	-1.05E+00	5.49E-02
OE1679R	*phoX2*	ABC-type phosphate transport system	-1.02E+00	1.65E-01
OE5340R	-	transposase	-1.01E+00	4.77E-02
OE3732R	-	Phosphoribosylformylglycinamidine synthase	-9.86E-01	4.03E-02
OE5162R	*orc5*	cell division control protein orc/cdc6	-9.64E-01	1.38E-01
OE6296R	-	transposase	-9.47E-01	7.80E-02
OE5406R	-	transposase	-9.15E-01	4.97E-02
OE1471F	*trpA*	tryptophan synthase, chain alpha	-8.67E-01	5.12E-02
OE3731R	*purQ*	phosphoribosylformylglycinamidine synthase	-8.66E-01	5.04E-02
OE3989R	*atpK*	A1Ao-ATPase, chain K	-8.63E-01	5.80E-02
OE2600R	*rpl12*	ribosomal protein L12	-8.58E-01	1.20E-01
OE5407F	-	transposase	-8.52E-01	5.54E-02
OE1440F	-	transposase	-8.42E-01	1.60E-01
OE4613F	*acn*	aconitate hydratase	-8.32E-01	6.90E-02
OE2458R	*guaB*	IMP dehydrogenase	-8.01E-01	5.54E-02
OE1040R	-	transposase	-7.90E-01	4.18E-02
OE3582F	*cspD2*	cold shock protein	-7.84E-01	2.90E-02
OE7046R	-	transposase	-7.79E-01	5.41E-02
OE1102R	-	transposase	-7.71E-01	8.90E-02

Table 1: List of genes down-regulated under K^+ limiting conditions as identified by DNA-microarray analysis (continuation).

ID*	gene name**	predicted function***	mean of medians****	mean of stddevs*****
OE2601R	*rpl10*	ribosomal protein L10	-7.64E-01	7.55E-02
OE1981R	-	hypothetical protein, 2TM	-7.59E-01	6.47E-02
OE2622R	*porB*	pyruvate-ferredoxin oxidoreductase, beta chain	-7.50E-01	1.72E-01
OE3985R	*atpA*	A_1A_o-ATPase, chain A	-7.46E-01	6.60E-02
OE7169A	-	transposase	-7.46E-01	4.58E-02
OE3986R	*atpF*	A_1A_o-ATPase, chain F	-7.35E-01	2.22E-02
OE2274R	*purL*	phosphoribosylformylglycinamidine synthase	-7.31E-01	9.33E-02
OE3984R	*atpB*	A_1A_o-ATPase, chain B	-7.11E-01	8.31E-02
OE4122R	*cctA*	Thermosome, chain alpha	-7.07E-01	7.87E-02
OE1470F	*trpB*	tryptophan synthase, chain beta	-7.04E-01	1.23E-01

Table 2: List of genes up-regulated under K^+ limiting conditions as identified by DNA-microarray analysis.

ID*	gene name**	predicted function***	mean of medians****	mean of stddevs*****
OE5052F	*kdpA*	KdpA	4.50E+00	1.49E-01
OE5053F	*kdpB*	KdpB	4.35E+00	1.93E-01
OE5054F	*kdpC*	KdpC	4.28E+00	2.13E-01
OE5066R	-	hypothetical protein	3.75E+00	2.84E-01
OE5051R	*trkA2*	TrkA	2.77E+00	3.60E-01
OE5055F	*cat3*	universal stress protein	2.56E+00	1.50E-01
OE5065R	-	DHH + DHHA1 domain protein	1.47E+00	1.21E-01
OE2450F	*acs2*	acetate-CoA ligase	1.43E+00	6.99E-02
OE5067R	-	hypothetical protein	1.26E+00	8.79E-02
OE3822R	-	hypothetical protein	1.23E+00	8.79E-02
OE2838R	*trkA5*	TrkA	1.16E+00	7.31E-02
OE2173F	*cgs*	cystathionine gamma-lyase	1.03E+00	3.34E-02
OE3942R	-	hypothetical protein	9.79E-01	3.61E-02
OE5134F	-	hypothetical protein, 1TM	9.49E-01	9.83E-02
OE5068F	-	Superfamily: DNA/RNA polymerases	9.47E-01	3.33E-01
OE4306F	-	hypothetical protein, 4 CBS domains	9.09E-01	5.69E-02
OE1789R	-	hypothetical protein	8.15E-01	3.23E-02
OE4384R	-	hypothetical protein, 4TM	7.82E-01	6.30E-02
OE5037R	*orc2*	cell division control protein orc/cdc6	7.75E-01	3.00E-01
OE5063R	-	IS200-type transposase	7.75E-01	6.73E-02
OE2333R	*ark*	signal-transducing histidine kinase	7.65E-01	6.81E-02
OE4382R	-	hypothetical protein , 2TM	7.53E-01	7.69E-02
OE5165R	-	hypothetical protein, 2TM	7.42E-01	1.64E-01
OE2442R	-	hypothetical protein , 3TM	7.40E-01	7.17E-02
OE3542R	-	unknown	7.40E-01	3.34E-02
OE4509F	-	nonhistone chromosomal protein	7.21E-01	5.06E-02

*Locus names and **gene names as annoteted for *H. salinarum* R1, *** predicted function (blast/PFAM/JNET), ****mean of medians from two independent arrays, *****mean of standard deviations from two independent arrays. All given values are log2-values. stddevs, standard deviations.

2.5.2 Cluster of up-regulated genes

The analysis of the localization of the genes up-regulated upon K^+ depletion uncovered a significant gene clustering. Whereas 66 % of the up-regulated genes are dispersed, 44 % are located in a small region of the extra-chromosomal replicons pNRC200 (*Halobacterium* NRC-1) or pHS3 (*H. salinarum* R1) (Figure 26). Including the *kdpFABCcat3* operon, most of these clustered genes show the strongest induction of all up-regulated genes. Several of the genes directly next to the *kdpFABCcat3* operon (compare Figure 30) were identified as highly up-regulated genes (*orc2, trkA2*, *kdpA*, *kdpB*, *kdpC*, *cat3*, VNG6182H, VNG6183C, *cat4*, VNG6185H, VNG6186H).

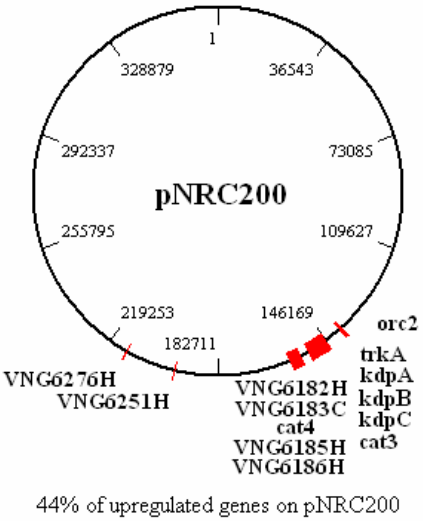

Figure 26: Clustering of genes up-regulated upon K^+ depletion.
Location of up-regulated genes on the extrachromosomal replicon pNRC200. Loci names and locations as annotated for *Halobacterium* NRC-1 in Ng *et al.* (2000).

Due to this significant clustering of genes up-regulated upon K^+ depletion, a possible role of the chromosomal location in the K^+ depletion dependent regulation of the *kdpFACcat3* operon was studied. This was carried out by use of the integration of a transcriptional fusion between the *kdp* promoter and the halobacterial ß-galactosidase (*bgaH*) in different regions of the genome. All plasmids based on pMKK100 do nut comprise an own origin of replication in *H. salinarum* and the stability of the plasmids is only ensured by the integration into the chromosome. Since the prerequisite for an effective integration via recombination is a homologous sequence region, the integration point can be influenced by the variation of this region on the plasmid. This was used to construct three plasmids carrying variable regions for integration together with a transcriptional fusion of the *kdp* promoter with the reporter gene

bgaH. Three non-coding regions were chosen for the integration: (I) A 300 bp-region immediately downstream of *cat3* (pHJS6), (II) a 300 bp-region immediately upstream of *rpoA1* (pHJS7), and (III) a 300 bp-region immediately upstream of *bop* (pHJS8). These regions were selected to ensure integration in the up-regulated cluster as well as within a region of two genes known not to be regulated in response the K^+ depletion as a negative control. Since the deletion strain *H. salinarum* Δ*kdpFABC,* in which the plasmids were used, still encoded for the *kdp* promoter followed by *cat3*, a compromise needed to be accepted with respect to the length of the *kdp* promoter. In order to prevent integration via the *kdp* promoter region, a 54 bp-long truncated *kdp* promoter lacking one operator but still exhibiting strong response to K^+ depletion was used.

Following transformation of *H. salinarum* Δ*kdpFABC* with all three plasmids, the correct integration was controlled by PCR (data not shown). All strains were cultured in media containing 3 or 100 mM KCl, and samples were collected for ONPG measurements in the late logarithmic growth phase (Figure 27A). ß-galactosidase activities were found to be essentially comparable independent of the integration site, with high activities in the presence of near-limiting K^+ concentrations and low activities in case of non-limiting 100 mM KCl (Figure 27B). As a consequence, although the *kdpFABCcat3* operon is located within a cluster of genes up-regulated upon K^+ depletion, the regulation of gene expression is obviously not dependent on the chromosomal location of the genes.

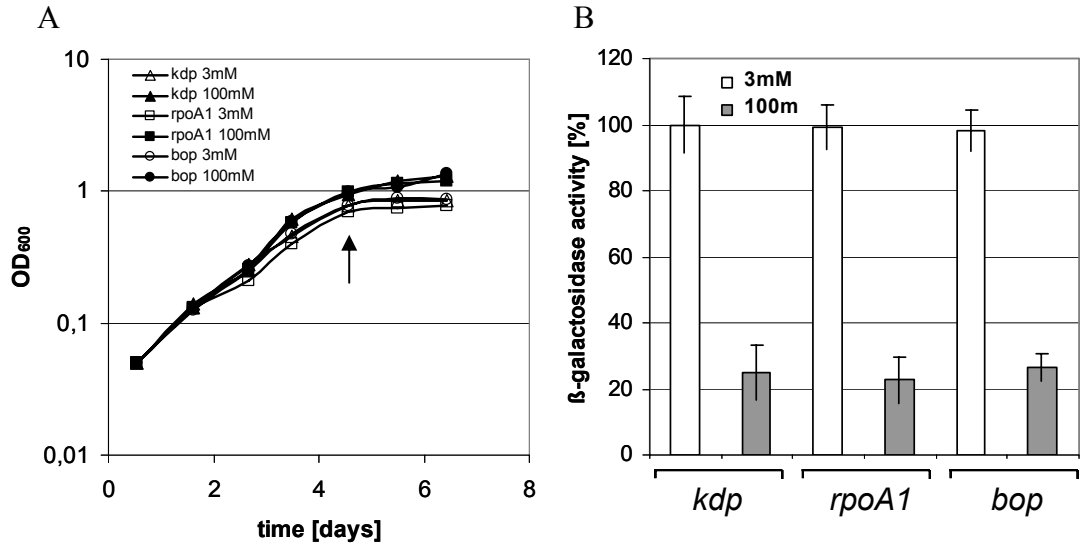

Figure 27: Location dependent expression of *kdpFABCcat3*.
(A) Cultivation of *H. salinarum* Δ*kdpFABC* carrying plasmids pHJS6 (*kdp*), pHJS7 (*rpoA1*) or pHJS8 (*bop*) in media containing 3 mM and 100 mM initial K^+, monitored as optical density of the culture. (B) Activity of the *kdp* promoter integrated at different locations in the genome, measured by a transcriptional fusion with *bgaH* (sample collection points highlighted by an arrow) .

2.5.3 DNA replication and replicon copy number

The genome of *H. salinarum* is reported to carry multiple origins of replication, from which the replication is initiated during cell division (Zhang & Zhang; 2003; Berquist & DasSarma, 2003). A crucial step in the initiation of replication is the sequence specific binding of an Orc1/Cdc6 protein homog at the replication initiation site. This is supposed to be followed by the subsequent binding of additional proteins in order to build up a functional replication initiation complex (Grainge *et al.,* 2003). The genome of *H. salinarum* comprises for ten *orc1*/*cdc6* homogues although only two of them (*orc2* and *orc10*) are reported to be essential (Berquist *et al*., 2007). Furthermore, several *orc/cdc6* homogs are located in the near vicinity of a postulated origin of replication, and this co-localization is discussed as a conserved character of archaeal origins of replication (Norais *et al.,* 2007). One of the reported essential *orc1/cdc6* homogs (*orc2*) is located only ~7 kb upstream of the *kdpFABCcat3* operon and, thus, in the near vicinity of the gene cluster up-regulated upon K^+ depletion. Two additional nonessential *orc/cdc6* homologs (*orc3* and *orc5*) are also located within this region. In the course of the DNA microarray analysis, *orc2* was identified as a gene, which is significantly up-regulated and *orc5* as a gene down-regulated under conditions of K^+-depletion (compare tables 1 and 2). Although *orc3* was not identified itself, it most likely builds up an operon together with VNG6186 which was shown to be highly up-regulated. These findings indicate a putative linkage between the regulation within the discussed gene cluster and the regulation of replication initiation. Whereas replication-mediated gene amplification plays a fundamental role in the gene regulation processes in Eucarya (Tower, 2004; Claycomb & Orr-Weaver, 2005), the utilization of a corresponding mechanism has not yet been reported in Archaea. Since the replication in *H. salinarum* is reported to be a highly dynamic process resulting in variations in the copy number of different replicons depending on at least growth conditions and growth phase (Breuert *et al.,* 2006), the potential role of replication-mediated gene amplification in the regulation of *kdpFABCcat3* and in the regulation of the up-regulated gene cluster was analyzed.

In order to identify the potential role of a local induction of replication and the resulting higher copy number of clustered genes upon K^+ depletion, *H. salinarum* was grown in media containing 3 or 100 mM KCl, and samples of genomic DNA were collected for *real time* PCR measurements in the late logarithmic growth phase (Figure 28A). The relative copy number of the genomic region, in which the *kdpFABCcat3* operon is located, was determined to detect possible fluctuations upon K^+ depletion (Figure 28B). As a control, the relative copy number of *rpoA1* was taken as a gene unaffected by K^+ depletion. The obtained values for the region

coding for *rpoA1* and *kdpFABCcat3* indicate only a slightly higher copy number for the *rpoA1* region. The measured overall difference (<10%) in copy number of the chromosome region (*rpoA1*) and the extra chromosomal replicon pHS3 (*kdpC*/*cat3*) is significantly lower than reported earlier (Breuert *et al.,* 2006). However, no difference could be detected between cultures grown in the presence of sufficient K^+ concentrations and upon K^+ depletion. As a concequence, the copy number of the genomic region coding for the *kdpFABCcat3* and most likely several additional up-regulated genes under conditions of K^+ depletion is unaffected. Thus, a replication-mediated gene amplifiction obviosly does not play a notable role in the regulation of the corresponding genes.

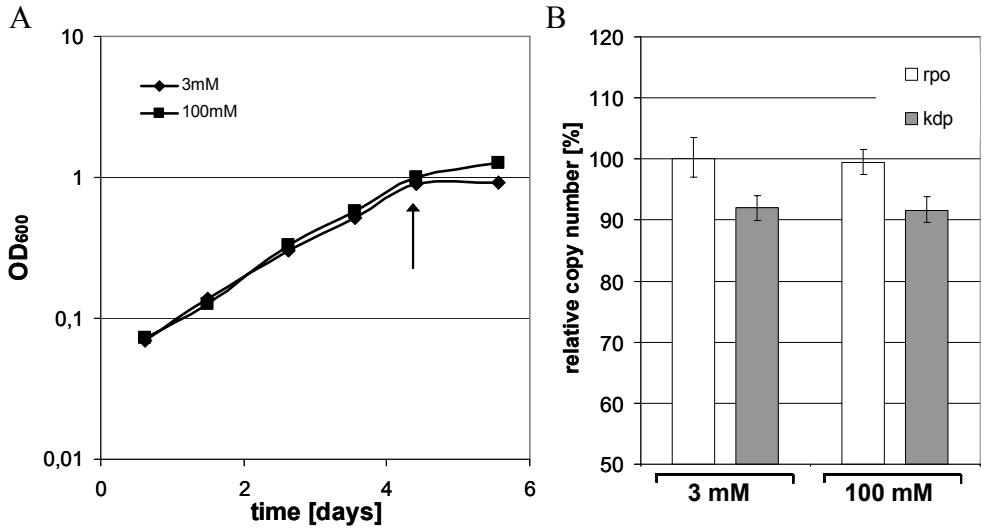

Figure 28: K^+ limitation-dependent analysis of the relative copy number of *kdpFABCcat3*.
(A) Cultivation of *H. salinarum* wild type in media containing 3mM and 100mM initial K^+, monitored as optical density of the culture. (B) Relative copy number of genomic DNA coding for *kdpFABCcat3* and *rpoA1* in *H. salinarum* wild type in the late logarithmic growth phase measured by *real time* PCR in triplicate (sample collection points highlighted by an arrow) .

2.6 Search for transcriptional regulators of the *kdp* system

2.6.1 Two-component systems

As described earlier, the expression of bacterial Kdp systems is governed by the two component system KdpD/KdpE. In contrast, none of the Archaea coding for homologs of the transporter genes *kdp(F)ABC* also comprises homologs of *kdpD* or *kdpE*. In the genome of *H. salinarum*, however, three response regulators have been identified, for which the corresponding regulated genes are unknown. In order to study a potential function of these two-component systems in the transcriptional regulation of the Kdp system, deletion strains of

all three response regulators, namely OE3854, OE2334, and OE2086 were studied with respect to their ability to regulate the expression of the *kdpFABCcat3* operon. The deletion strains were a generous gift from A. Wende (MPI for Biochemistry, Martinsried). All three deletion strains and *H. salinarum* wild type were cultured in media containing 3 or 100 mM KCl, and samples were collected for *real time* RT-PCR measurements in the late logarithmic growth phase (Figure 29A). The expression levels of *kdpFABCcat3* in all three deletions strains under both inducing and repressing conditions were comparable to those of the wild type strain (Figure 29B). As a consequence, the transcriptional regulation of the halobacterial Kdp system is not only independent of KdpD/KdpE but also independent of any additional identified response regulator, thereby most likely representing a regulatory system essentially different from the bacterial counterparts.

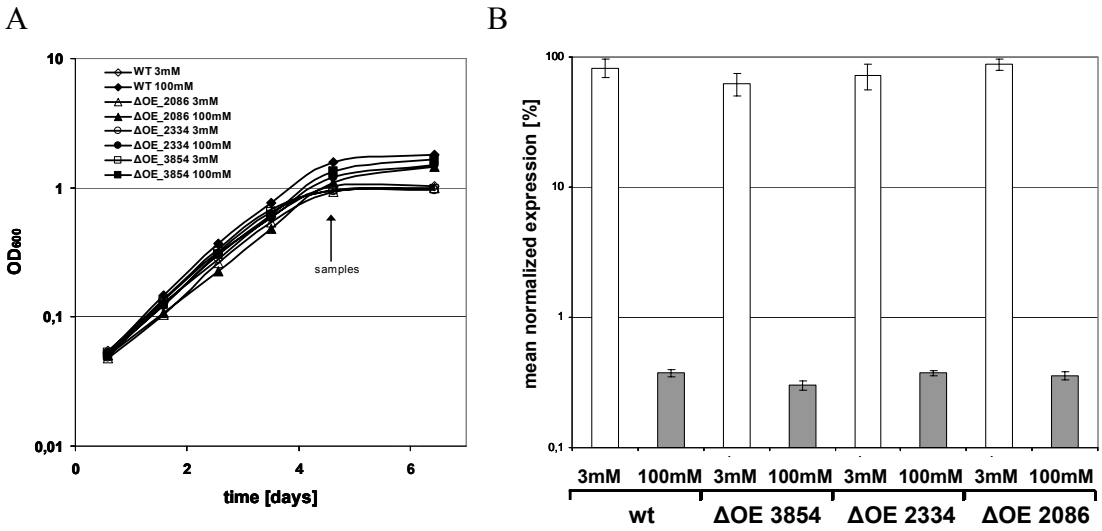

Figure 29: Function of three putative response regulators in the transcriptional regulation of the *kdpFABCcat3* operon.
(A) Cultivation of *H. salinarum* wild type, ΔOE 3854, ΔOE 2334 and ΔOE 2086 in media containing 3 mM and 100 mM initial K^+. (B) Normalized expression of *kdpFABCcat3* in *H. salinarum* wild type, ΔOE 3854, ΔOE 2334, and ΔOE 2086 in the late logarithmic growth phase measured by *real time* RT-PCR in triplicate. 100 % represents the expression level of the housekeeping gene *rpoA1* used as expression reference; sample collection points highlighted by an arrow.

2.6.2 Neighboring genes

Several transcriptional regulators are located on the chromosome in the near vicinity of the genes they regulate. This is particularly true for the bacterial Kdp systems. For this reason, the sequences of genes located up- und downstream of the *kdpFABCcat3* operon (+/- ca. 10,000 bp) were analyzed by pfam pattern search for their potential ability to act as a transcriptional regulator. However, no potential transcriptional regulators could be identified on pNRC200

surrounding the *kdpFABCcat3* operon. Nevertheless, the region immediately downstream of the *kdpFABCcat3* operon encodes two putative open reading frames (orf´s) with unknown function (Figure 30). One of them, namely OE5061, was annotated only for *H. salinarum* R1 (Oesterhelt *et al.,* unpublished; www.halolex.mpg.de) and encodes a putative orf without any known homologs. The second, namely VNG6180 as annotated for *Halobacterium* NRC-1 (Ng *et al.,* 2000) or OE5058F as annotated for *H. salinarum* R1, encodes a conserved putative orf with unknown function.

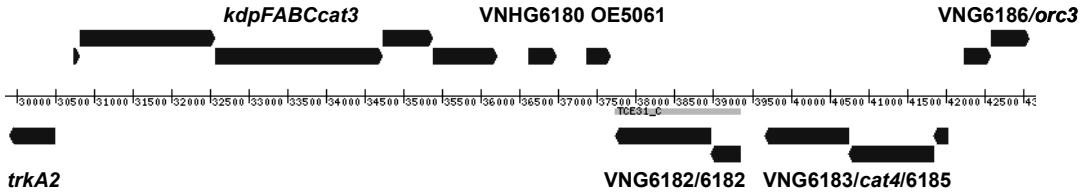

Figure 30: Genomic organization of genes neighboring the *kdpFABCcat3* operon.
Locus name and location of OE5061 as annotated for *H. salinarum* R1 (Oesterhelt *et al.,* unpublished; www.halolex.mpg.de). All additional loci are as annotated for *Halobacterium* NRC-1 according to Ng *et al.* (2000).

Although both orf´s do not comprise sequence homology to any known transcriptional regulators, an array was carried out to verify the expression of these orf´s. In order to analyse their expression, *H. salinarum* wild type was cultured in media containing 3 or 100 mM KCl, and samples were collected for *real time* RT-PCR measurements in the late logarithmic growth phase (Figure 31A). *Real time* RT-PCR measurements were carried out by use of primers binding in *kdpC/cat3* (primers 12 and 13) and *rpoA1* (primers 14 and 15) as positive and negative controls, respectivly, and in OE5061 (primers 18 and 19) or VNG6180 (primers 20 and 21)(Figure 31B). Under these conditions, the reference gene *rpoA1* showed a strong constitutive expression (ct-values of ~20), whereas the *kdpFABCcat3* operon exhibited an induction of expression in the culture grown at initial K^+ concentration of 3 mM (from a ct-value of ~31 to 23). Hardly any expression could be detected for OE5061F. In contrast, an induced transcription of VNH6183 was clearly detectable (ct-value of ~23 in the culture grown at initial K^+ concentration of 3 mM and a ct-value of ~26,5 in the culture grown at initial K^+ concentration of 100 mM). Both orf´s exhibited a slight induction under conditions, in which the *kdpFABCcat3* operon is highly induced. This, however, could also be due to transcriptional read-thru from the *kdpFABCcat3* operon located directly upstream. Although a transcriptional terminator is located downstream of the *kdpFABCcat3* operon, it only

terminates transcription with an efficiency of ~90 % (Kixmüller *et al.,* in preparation). Thus, a reliable induced expression could only be detected for VNH6183. Even though highly hypothetical, a role of this conserved putative orf in the transcriptional regulation of the halobacterial *kdpFABCcat3* operon can not be ruled out.

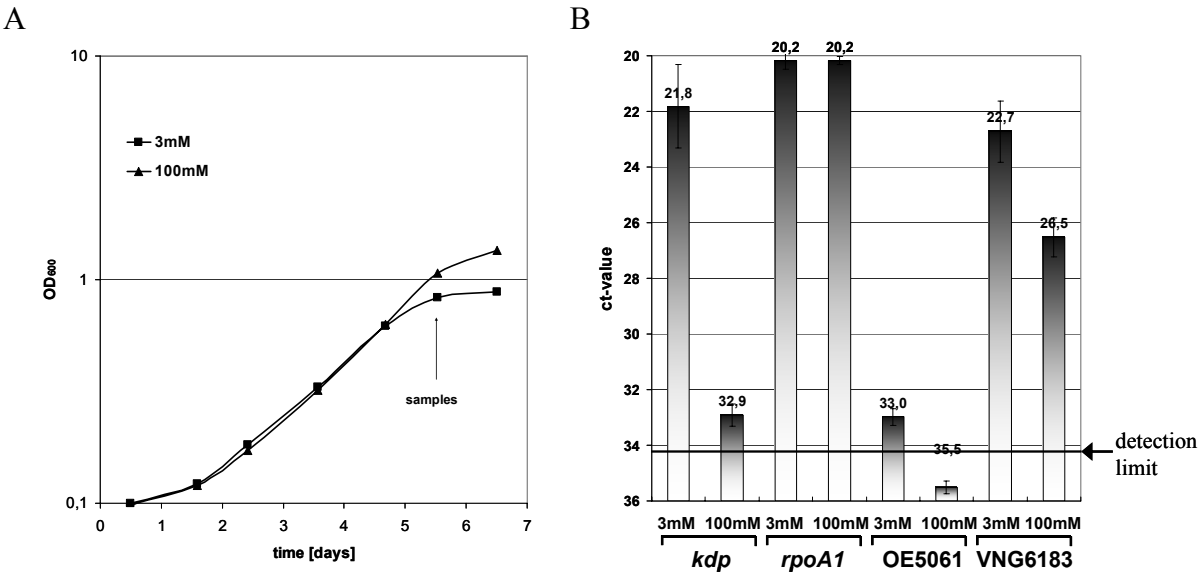

Figure 31: Expression of two putative orf's located downstream of *cat3*.
(A) Cultivation of *H. salinarum* wild type in media containing 3 mM and 100mM initial K^+, monitored as optical density of the culture (sample collection point highlighted by an arrow).
(B) Ct values of *real time* RT-PCR analysis applying primers binding in *kdp* (primers 12 and 13), in *rpoA1* (primers 14 and 15), in VNG6183 (primers 16 and 17), and in OE5061 (primers 18 and 19). The expression detection limit indicates the lowest detectable expression level .

2.6.3 Genomic library screen

In addition to the studies described above, an attempt was carried out to identify the transcriptional regulatory proteins of the halobacterial *kdp* system by means of a genomic library screen. This approach was enabled by the development of sophisticated molecular biological methods (knock out, vector systems, selectable markers etc.) for an additional halobacterial species, *Haloferax volcanii*. This strain does not encode homologs of the *kdp* system, thereby justifying the assumption that homologs of the corresponding regulatory proteins of the halobacterial *kdp* system are absent as well. The basic idea of the genomic library screen was to construct a plasmid carrying a transcriptional fusion of the *kdp* promoter to the selectable reportegen *pyrE2*. *pyrE2* encodes an essential protein of the uracil biosynthesis pathway of *H. volcanii,* resulting in uracil auxotrophy in the absence of *pyrE2* or in absence of *pyrE2* expression. As a consequence, the expression of plasmid-encoded *pyrE2* under the control of the halobacterial *kdp* promoter in *H. volcanii* Δ*pyrE2* could, if active in

H. volcanii, result in the ability to grow without supplemented uracil. The expression of *pyrE2* is, however, counter-selectable. In the presence of uracil, *H. volcanii* is able to take up uracil from medium, resulting in growth behaviour similar to the wild type, even in absence of PyrE2. An analog of uracil, 5-FOA (5-fluoro orotic acid), can also be taken up by *H. volcanii* and serves as an additional substrate for PyrE2. The enzymatic activity of PyrE2, however, converts 5-FOA to a toxic form. This enables the selection for the absence of *pyrE2* expression in the presence of uracil and 5-FOA. In an initial experiment, the activity of the *kdp* promoter in *H. volcanii* was analyzed. For this purpose, a plasmid pTA425 was chosen. This plasmid carries a *trpA* gene under control of a constitutive P_{fdx}–promoter, thus enabling a stable selection in a *H. volcanii* Δ*trpA* strain in the absence of tryptophane in the medium. Furthermore, the plasmid pTA425 carries an Ap^R–resistance cassette and an OriV (enabling cloning and manipulation in *E. coli*) as well as a pHV4-Ori (for replication in *H. volcanii*). The original plasmid pTA425, in which *pyrE2* is not expressed due to the absence of an appropriate promoter, was manipulated to encode a transcriptional fusion between P_{kdp} and *pyrE2* (pHJS23, Figure 32A). The combination of *H. volcanii* H53 (Δ*trpA* Δ*pyrE2*) and pHJS23 enabled a screen for the activity of the halobacterial *kdp* promoter in *H. volcanii* by the ability to complement the uracil auxotrophy. Both the *H. volcanii* H53 strain and plasmid pTA425 were a generous gift from T. Allers (University of Nottingham).

The activity of the *kdp* promoter in *H. volcanii* was controlled via the ability of *H. volcanii* H53/pHJS23 to grow on agar plates with and without supplemented uracil in the presence of 3 mM or 100 mM KCl. Strain *H. volcanii* H53 carrying either no plasmid or plasmid pTA425 were used as controls (Please note that casaminoacids used as the sole carbon source do not contain tryptophane). As reported earlier (Allers *et al.,* 2004), *H. volcanii* H53 was only able to grow in casaminoacids-medium if supplemented with uracil and tryptophane (Figure 32B). In contrast, *H. volcanii* H53 carrying plasmid pTA425 was able to grow without tryptophane but was still uracil auxotroph due to absence of *pyrE2*-expression. In contrast, *H. volcanii* H53 carrying plasmid pHJS23 was able to grow without both supplemented uracil and tryptophane, thereby demonstrating that *pyrE2* is expressed in *H. volcanii* by the halobacterial *kdp* promoter at levels sufficient to complement uracil auxotrophy. This complementation was found to be independent of the K^+ concentration in the medium. This indicates the *per se* ability of the *kdp* promoter to initiate transcription even in the absence of any *kdp*-specific regulatory proteins in a constitutive manner.

A

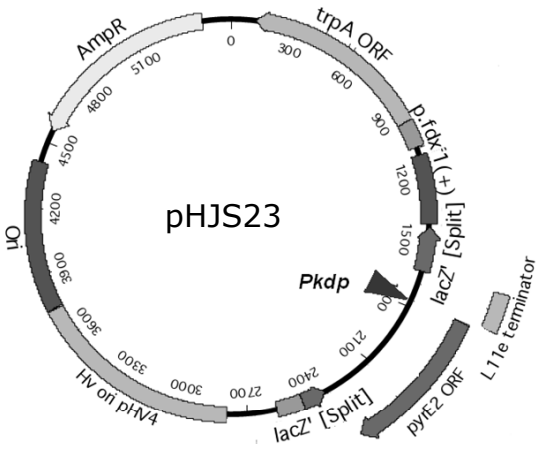

B

Ability to grow in casaminoacids (CAA)-medium

CAA supplemented with	*H. volcanii* H53 ΔtrpA ΔpyrE2	*H. volcanii* H53 pTA425	*H. volcanii* H53 pHJS23 *Pkdp:pyrE2*
+Trp +Ura	+++	+++	+++
-Trp +Ura	-	+++	+++
-Trp -Ura 3mM KCl	-	-	+++
-Trp -Ura 100mM KCl	-	-	+++

Figure 32: Expression of the counter-selectable reporter gene *pyrE2* under control of the halobacterial P_{kdp} in *Haloferax volcanii* H53.
(A) Plasmid map of plasmid pHJS23. Location of all genes is indicated with arrows and *cis*-active elements with boxes. Location of P_{kdp} is highlighted. (B) Growth of *H. volcanii* H53, *H. volcanii* H53/pTA425 and *H. volcanii* H53/pHJS23 in casaminoacids-medium with and without tryptophane and uracil in initial medium K^+ concentrations of 3 and 100 mM. No growth is documented with (-), growth like *H. volcanii* H53 with uracil and tryptophane is documented with (+++).

In the following experiment, this counter-selectable expression system was used for a genomic library screen. The combination of *H. volcanii* H53 together with plasmid pHJS23 was highly sensitive to presence of 5-FOA (10 µg/ml 5-FOA abolished any detectable growth on agar plates). This property was used for a screen applying a genomic library of *H. salinarum.* The used genomic library was constructed based on plasmid pWL-Nov carrying an Ori compatible to the Ori used in pHJS23 together with a novobiocin resistance cassette for the selection of transformants. This library was a generous gift from M. Mevarech (Tel Aviv University; Giladi *et al.,* 2002). The library has a coverage of ~90 % of the genome of *H. salinarum*, whereas the individual plasmids carry genomic fragments of ~8 kb (Mevarech, personal correspondence).

The screen was set up by a combination of *H. volcanii* H53/pHJS23 transformed with the genomic library and the selection of clones by their ability to grow on casaminoacid plates, which were supplemented with uracil and 5-FOA. Assuming that the repressor (or repressors) of the halobacterial Kdp system is (are) located on an individual fragment of the library and that the repressor (or repressors) is (are) expressed and active in *H. volcanii*, the repressor should be able to repress the *kdp* promoter-driven expression of *pyrE2.* This clone is then selectable by the ability to grow in the presence of 5-FOA. Although the screen was carried

out several times with different concentrations of 5-FOA, no clones with significant growth in the presence of 5-FOA could be isolated.

Even though the identification of the transcriptional regulators of the halobacterial Kdp system was not successful in this case, the established expression system in *H. volcanii* provides a promising test system in general. In the comparison of alternative methods like for instance knock-out analyse, with little effort, this system could be used to verify the identity of potential repressors of the halobacterial Kdp system.

2.6.4 The halobacterial *kdpFABCcat3* operon as part of a regulon

As discussed earlier, several genes are up- und down-regulated in response to K^+ depletion. With the exception of the *kdp* promoter, none of the up-regulated genes or putative operons were so far analyzed with respect to their mode of gene regulation. In order to information about a potential linkage of these genes in a hypothetical K^+-responsive regulon, the putative promoter sequences of all up-regulated genes were analyzed. In addition to overall sequence similarity, the putative promoter regions were analyzed with respect to the presence of palindromic sequences as putative regulatory protein binding sites. Several of the analyzed potential promoter regions comprised palindromic sequences that could serve as regulatory protein binding sites. Most of these potential *cis*-active elements, however, exhibit no significant sequence homology (data not shown). The only exception was the putative *cis*-active element that was already identified to be involved in the negative regulation of the *kdp* promoter (see Figures 18, 19, and 20). A sequence highly homologous to this putative *cis*-active element of the *kdp* promoter was found to be located in the promoter region of a putative operon build up by the genes VNG6183 (accession number NP_395715), *cat4* (accession number NP_395716), and VNG6185 (accession number NP_395717) (Figure 30). This homologous putative binding site is located at -22 to -41 bp upstream of the start codon of the first gene VNG6185, thereby comprising a position to inhere with the transcription initiation or elongation.

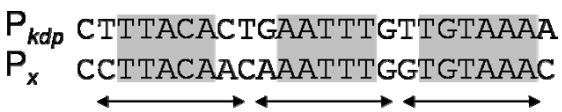

Figure 33: Potential binding sites of a shared transcriptional regulator.
The potential repressor binding site of the *kdp* promoter is indicated with P_{kdp}. The potential binding site in promoter region of a potential operon build up by genes VNG6183, *cat4* and VNG6185 is indicated as P_X. The arrows indicate the range of one helical turn of DNA thereby locating the conserved regions on one side of the DNA double helix.

Although the identity of a putative regulatory protein is still highly hypothetical, it is tempting to speculate about the linkage of these two operons into a regulon by use of a shared regulatory protein. The corresponding second putative operon is located ~3.4 – 5.8 kb downstream of *cat3* in the reverse complementary direction (see Figure 30). It is separated from the *kdpFABCcat3* operon only by the conserved putative orf located directly downstream of *cat3* (VNH6183; see Figure 31) and a transposon (VNG6182/VNG6182). The function of all three genes located in the putative operon is unknown. Two of the genes, namely VNG6183 and VNG6185, were identified in the course of a DNA microarray study as one of the most up-regulated genes. VNG6185 encodes a conserved hypothetical protein, whereas VNG6183 carries sequence homologies to DHH+DHHA1 protein domain family which is characterized by a phosphoesterase activity. The third gene of the potential operon (*cat4*), located in between VNG6183 and VNG6185, encodes a member of the universal stress protein family and, thus, a homolog of *cat3*.

3. Discussion

3.1 K^+ homeostasis in *H. salinarum*

H. salinarum exhibits a high tolerance with respect to the environmental potassium concentrations supporting growth, although K^+ is of vital importance for the cell's life. Even though K^+ is accumulated inside the cell in a molar range, growth occurs in case of very low K^+ concentrations down to 20 µM. *H. salinarum* responds to these conditions by an adapted lower cellular K^+ concentration as well as by a lower cell volume and, thus, higher cell densities can be achieved with limited K^+. For another reason, similar shifts in the cellular K^+ concentration have already been reported as a result of changes in illumination conditions (Wagner *et al*., 1978, Lanyi, 1978). During illumination, K^+ was shown to be accumulated in high concentrations most probably as a result of the increased membrane potential generated by the activity of the light-driven proton pump bacteriorhodopsin. In the absence of illumination, this high K^+ concentration was supposed to be used as an energy converter, and the extrusion of K^+ coupled to the uptake of Na^+ via a Na^+/H^+-antiporter could be used to increase the membrane potential under conditions of low H^+-pumping activity (Wagner *et al*., 1978, Lanyi 1978, Brown *et al.,* 1983). However, since the required K^+-extruding system has not yet been found in this context, this scenario remains hypothetic.

Anyway, *H. salinarum* is postulated to maintain an iso-osmotic equilibrium with the medium (Oren 1999). In order to accomplish this, the cellular ion concentration needs to be dynamic and adapted to the changing overall salinity of the surrounding medium. In the course of the bachelor thesis of Stefan Thiele (carried out under my supervision), first experimental evidence supporting the highly dynamic character of cytoplasmic K^+ and Na^+ in balancing the osmolality was obtained. The cytoplasmic K^+ concentration indeed shows a significant correlation to the osmolality of the medium. In the presence of adequate levels of K^+, the rising osmolality of the medium is compensated by a concomitant increase in cellular K^+ concentration. The adaptation of the cellular K^+ concentration upon changes in medium salinity is, however, combined with unexpectedly large and yet unreported changes in cell volume. Whereas the rising medium osmolality is compensated by an elevated cellular K^+ concentration, a parallel strong reduction of the cell volume can be monitored. If, however, cultivated under near limiting K^+ concentrations, a highly sophisticated interplay between cellular K^+ and Na^+ as well as cell volume can be observed. As shown earlier (see results), *H. salinarum* adapts to K^+ depletion by reducing both the cellular K^+ concentration (~30 %) and

the cell volume (~20 %) if cultivated in the presence of 3 M NaCl. In the presence of 4 M NaCl, the cells exhibit a higher cellular K^+ concentration and a lower cell volume. Upon K^+ depletion, the adaptation in case of a reduced K^+ availability is mainly achieved by the reduction of the cellular K^+ concentration (>40 %), whereas the reduction of cell volume is subordinate (<15 %). Independent of the medium salinity, the reduction of the cellular K^+ concentration is compensated by a concomitantly increased uptake of Na^+ (Stefan Thiele, bachelor thesis, 2007). As a concequence, a highly dynamic interplay between the balancing of cell volume and osmolality of the cytoplasm with the medium and an adaptation of cell volume and cellular ion composition as a response to K^+ depletion ensures the ability to grow under variable Na^+ and K^+ concentrations in the medium.

In our studies, the decrease in the cellular K^+ concentration to a stationary value of about 70% with respect to the non-limited potassium level, appears to represent the minimal internal K^+ threshold *H. salinarum* can tolerate. The most likely reason for this effect resides in the specific adaptation of halophilic proteins to high salt conditions. Most proteins of *H. salinarum* exhibit their activity only in the presence of molar concentrations of Na^+ or K^+ (Kennedy *et al.*, 2001, Madern *et al*., 2000, Elcock & McCammon 1998), demonstrating that the proteome is essentially adapted to the high cellular salt concentration. Since K^+ is the dominant cation in the cytoplasm of *H. salinarum*, the presence of a minimum of cellular K^+ concentration supporting activity of at least many essential proteins, is more than just feasible. The presence of a minimal cellular K^+ concentration, which cannot be substituted by Na^+, would, in turn, have a drastic effect on the physiology and ecology of *H. salinarum*. As discussed earlier, *H. salinarum* maintains an iso-osmotic equilibrium with the environment, and a decline in the external salinity results in a reduced concentration of K^+ inside the cell. If the external salinity decreases below the internal minimal threshold for potassium, this would result in an elevated hydrostatic pressure and, thus, in cell lysis. It is tempting to speculate that this intracellular K^+ threshold primarily determines the lower level of salt tolerance of *H. salinarum*. This, however, hast to be further verified.

3.2 Sequence analysis of the halobacterial Kdp system

The analysis of the genome sequence of *H. salinarum* revealed the presence several putative K^+ transport systems potentially able to facilitate the discussed higly efficient uptake of K^+. In cource of this thesis, a special care and attention was laid on the analysis of the ATP-dependent high affinity K^+ uptake system Kdp. The genes coding for the halobacterial Kdp system were initially identifed in the course of the automated annotation of the *Halobacterium*

NRC-1 genome sequence (Ng *et al.,* 2000). Although only the genes *kdpA*, *kdpB,* and *kdpC* were originally annotated, the genome of *Halobacterium* NRC-1 also encodes a conserved but unannotated gene *kdpF* located at a conserved position between *kdpA* and the promoter of the corresponding operon. An additional 819 bp-Orf annotated as *cat3* was found downstream of the *kdpC* gene. Thus, the genes coding for a halobacterial ATP-dependent K^+ uptake system Kdp are organized in a single operon comprising the genes *kdpFABC* and *cat3*. The corresponding *kdpFABCcat3* operon is located on one of the extrachromosomal replicons (pHS3 in *H. salinarum* R1 and pNRC200 in *Halobacterium* NRC-1). Interestingly, although most genes linked to K^+ and Na^+ homeostasis are encoded on the main chromosome, several genes (*nhaC3*, *trkH4* and *kdpFABCcat3*) are located on the same extrachromosomal replicon (pHS3 respectivly pNRC200). A putative role of the characteristic extrachromosomal replicons of *Halobacterium* species in genome evolution assisting in acquisition of new genes via lateral gene transfer has been discussed (Ng *et al.,* 1998; Ng *et al.,* 2000). Although speculative, this could indicate the existence of the Kdp system in *Halobacterium* as a result of a lateral gene transfer thereby broadening the capacity of *H. salinarum* to deal with changing environmental conditions. This hypothesis might be further supported by the absence of a corresponding system in other halophilic Archaea, of which genome sequence is available (*Haloarcula marismortui*, Goo *et al.,* 2004; *Natronomonas pharaonis*, Falb *et al.,* 2005; *Haloquadratum walsbyi*, Bolhuis *et al.,* 2006; *Haloferax volcanii*, unpublished; *Halorubrum lacusprofundi*, unpublished). However, genes conding for homologs of the halobacterial Kdp system are present in genomes of several additional members of the phylum Euryarchaeota as well as in the genome of *Thermofilum pedens* as a single representative of the phylum Crenarchaeota. As a consequence, the Kdp system is not only widely distributed among Bacteria but also present in various phylogenetically rather distant Archaea. In order to elucidate the relationship of the Kdp systems present in Archaea and in Bacteria, a phylogenetic analysis of 89 bacterial and six archaeal KdpB-protein homologs was carried out. As mentioned earlier, the bacterial Kdp system is widely distributed and the analyzed phylogenetic relationships of the KdpB homologs closely resemble the universal bacterial phylogenetic tree (Daubin *et al.,* 2002). The archaeal Kdp systems, at least on basis of the KdpB protein sequence, represent an individual clade clearly separated from the bacterial counterparts. Although the archaeal Kdp systems seem to exhibit slightly higher homology to systems present in Firmicutes and Cyanobacteria, the data offers no clear evidence for an extended lateral gene transfer between Archaea and Bacteria regarding at least KdpB. It can be speculated, that the Kdp system are present in Archaea as a product of lateral gene transfer

from Bacteria. If so, however, this gene transfer must have occurred at an early stage in the evolution of Archaea, and the six analyzed archaeal Kdp systems in Euryarchaeota and Crenarchaeota have all emerged from this one precursor.

During the finalization of this work, the genome sequence of an additional Archaeon *Candidatus Methanoregula boonei* 6A8 (unpublished) became available. The genome of this methanogenic Euryarchaeon encodes a rather atypical putative Kdp system, featuring two distinct *kdp* operons carrying genes for KdpB and for a fusion of KdpA and KdpC. As a first known Archaeon, *Candidatus Methanoregula boonei* 6A8 also encodes a gene homologue of *kdpD*. Although this Archaeon is not included in the phylogenetic tree presented in this work, a preliminary analysis revealed a high homology between the two KdpB-protein homologs present in *Candidatus Methanoregula boonei* and members of the heteregenous group B. Thus, the Kdp system in this Archaeon is clearly different from all other Kdp systems found in Archaea and is most likely a product of an individual lateral gene transfer from Bacteria.

3.3 Kdp-dependent K^+ homeostasis in *H. salinarum*

Our analyses revealed that the halobacterial Kdp system is essential for growth in case of K^+ concentrations below 60 µM, and under these conditions, the corresponding genes *kdpFABCcat3* are highly expressed. Expression is induced by a decrease of the K^+ concentration in the medium and reaches its highest level in depleated K^+ concentrations of below 200 µM. These findings are in good accord with the reported characteristics of bacterial Kdp systems. Also in *E. coli*, the deletion of the *kdp* genes results in an elevated minimal K^+ concentration supporting growth, which is due to the higer K^+-affinity of the Kdp system with respect to other K^+ uptake systems. In the absence of the KdpFABC complex, the minimal K^+ concentration supporting growth of *E. coli* is determined by the lower-affinity Trk systems (Rhoads *et al.,* 1976). At first glance, these results support the notion that the Kdp complex of *H. salinarum* is used accordingly as a high-affinity K^+ uptake system induced under conditions, in which either affinity and/or driving force of the other K^+ uptake systems are not sufficient to facilitate K^+ uptake. As soon as $\Delta\psi_{K+}$ is more negative than $\Delta\psi_m$, K^+ transport has to be energized either by symport or antiport with other ions or by ATP hydrolysis. Molar concentrations of K^+ inside the cell vs. very low extracellular K^+ concentrations in a µM range result in a steep K^+ gradient of over a 100,000-fold. The resulting calculated $\Delta\psi_{K+}$ of >300 mV in case of 20 µM KCl in the medium and 2,5 M inside the cell readily excludes K^+ uptake taking place merely via the $\Delta\psi_m$-driven K^+ channels (PchA1-2) as postulated earlier (Wagner *et al.,* 1978; Lanyi, 1979).

The driving force for K^+ uptake has been studied for *Haloferax volcanii*, an additional member of the family *Halobacteriaceae* (Meury & Kohiyama, 1989). In this study, the K^+ uptake for this organism was shown to be both $\Delta\psi_m$ and ATP –dependent. In addition, the $\Delta\psi_{K+}$ generated by the uptake of K^+ was shown not to be in equilibrium with $\Delta\psi_m$. At least in case of K^+ concentrations below 20 mM in the medium, the $\Delta\psi_m$ was calculated to be higher than $\Delta\psi_m$. Although not yet published, the available genome sequence of *H. volcanii* opens room for discussion of these results with respect to the K^+ uptake systems present. For these reasons, the draft genome sequence of *H. volcanii* was screened for the presence of homologs for all known K^+ uptake systems. As in case of *H. salinarum*, the genome of *H. volcanii* encodes one K^+ channel of the KcsA-type, for a second K^+ channel of the Shaker-type as well as K^+ uptake systems of the Trk–type (Durell *et al.,* 1999; Bakker, 1993; Stumpe *et al*., 1996). Whereas the genome of *H. salinarum* encodes four copies of the TrkH-homolog, the genome of *H. volcanii* encodes only two copies. Furthermore, the Kdp system is not present in *H. volcanii*.

Several conclusions potentially valuable for the understanding K^+ uptake in *H. salinarum* as well can be concluded from this data. Although *H. volcanii* encodes K^+ channels most likely catalyzing a $\Delta\psi_m$–driven K^+ uptake, the uptake of K^+ was measured to be an utterly ATP-dependent process. Since K^+ uptake was shown to be $\Delta\psi_m$–dependent as well, this ATP-dependency was discussed by Meury and Kohiyama (1989) as a regulatory effect on the Trk-system. As a consequence, the absence of a $\Delta\psi_m$–driven channel mediated K^+ uptake in *H. volcanii* is is in clear discrepancy to the presence of homologs of such systems in the genome. Although this could be discussed as an indication for the absence expression of the corresponding genes, a closer look on the sequence of these genes opens an additional potential explanation for this apparent discrepancy. As the potential homolog in *H. salinarum* (PchA2), the predicted KcsA-type K^+ channel of *H. volcanii* carries an additional C-terminal domain exhibiting high homology to TrkA. Although found as a fused domain in several proteins, this so called RCK-domain was first characterized as a subunit of the Trk-system regulating K^+ transport activity in an ATP-dependent manner (Stumpe *et al*., 1996). Although hypothetical, a similar function in the regulation of the K^+ channel activity, in this case rather as a fused domain than as an independent subunit, could explain the strict ATP-dependency of K^+ uptake via this channel in *H. volcanii*. This is further supported by the fact, that the RCK-domain present in this putative channel protein exhibits a GXGXXG-motif conserved in RCK-domains which are able to bind ATP (Kröning *et al.,* 2007). The growth and buffer conditions used by Meury and Kohiyama (1989) for the measurements of ATP- and $\Delta\psi_m$–

dependency of K^+-uptake could also provide an explanation for the discrepancy. The corresponding measurements were carried out in buffer K^+ concentrations below 20 mM. Under these conditions, *H. volcanii* was shown to generate a $\Delta\psi_{K+}$ higher than $\Delta\psi_m$, thereby ruling out the mere presence of a $\Delta\psi_m$-driven transport of K^+. As a consequence, an active transport of K^+ must take plase, which is most likely driven by the TrkH-homologs. In addition, the presence of a $\Delta\psi_{K+}$ higher than $\Delta\psi_m$ presupposes either the absence of K^+ channels or a voltage-dependent gating mechanism of the K^+ channels preventing K^+ efflux in case high $\Delta\psi K^+$. For these reasons, the measured K^+ uptake in the presence of <20 mM KCl was most likely dominated by the Trk-systems and, therefore, the ATP-independent $\Delta\psi_m$–driven K^+ uptake activity of the encoded K^+ channels of *H. volcanii* might have been overlooked.

A similar K^+ uptake mechanism composed of voltage-gated K^+ channels able to take up K^+ in the presence of $\Delta\psi_{K+}$ lower than $\Delta\psi_m$ and Trk-systems capable of taking up K^+ in symport with H^+ even in presence of $\Delta\psi_{K+}$ higher than $\Delta\psi_m$ could be present in *H. salinarum* as well. Although a similar composition of K^+ channels and transporters is present in *H. salinarum* and *H. volcanii*, K^+ uptake was, in contrast to *H. volcanii,* reported to be an utterly ATP-independent process in *H. salinarum* (Wagner *et al.,* 1978; Lanyi, 1979). *H. salinarum*, however, is able to generate high $\Delta\psi_m$–levels (up to -270 mV, Michel & Oesterhelt, 1980) by a joint activity of bacteriorhodopsin and the respiratory chain, whereas *H. volcanii* does not possess bacteriorhodopsin, and the $\Delta\psi_m$ generated by the respiratory chain exhibits only lower values (up to -140 mV, Meury & Kohiyama, 1989). As a consequence, the limit of extracellular K^+ concentration, in which the $\Delta\psi_{K+}$ is more negative than $\Delta\psi_m$ and an active transport of K^+ becomes mandatory, is presumably lower for *H. salinarum*. According to the Nernst equation, the calculated $\Delta\psi_{K+}$ for *H. salinarum* is more negative than $\Delta\psi_m$ already in the presence of approx. 70 µM of extracellular K^+ (in case of cellular 2,8 M K^+, see results, and -270 mV (Michel & Oesterhelt, 1980)). The experiments performed by Wagner *et al.,* (1978), however, were performed in the presence of 2 mM KCl and above. Under these conditions ($\Delta\psi_m > \Delta\psi_{K+}$), K^+ uptake is most likely dominated by the $\Delta\psi_m$-driven K^+ channels, thereby potentially explaining the absence of an ATP-dependent component in K^+ uptake, either at the level of regulation or as primary energy source. As discussed earlier, the Kdp system is essential for *H. salinarum* at K^+ concentrations below 60 µM. As a consequence, at least under condition of high $\Delta\psi_m$ during illumination, *H. salinarum* seem to be able to generate a $\Delta\psi_{K+}$ significantly higher than the $\Delta\psi_m$ only in presence of the Kdp

system. The question wether the inability of the Trk systems to transport K^+ under these conditions is due to limitations of the Trk system concerning the generation of such high $\Delta\psi_{K+}$ or limitations concerning K^+ binding affinity, remains unclear.

It is tempting to speculate that in case of a low $\Delta\psi_m$, as for example during aerobic growth or in the absence of light, the Kdp system is induced as an ATP-dependent K^+ uptake system able to work against the high $\Delta\psi_{K+}$. On the other hand, extreme K^+ limitation as the primary stimulus is also a possibility, although it has so far been disregarded in the ecology of *Halobacterium*. Usually, the K^+ concentration in the hypersaline environment is above 100 mM and, thus, not limiting. However, *Halobacterium* is reported to persist also on or even within salt crystals, i. e. conditions, under which the concentration of free K^+ is close to zero, which obviously implicates the need for a high-affinity K^+ uptake system. However, both the change in $\Delta\psi_m$ and the external K^+ limitation could initially lead to a decrease in the intracellular K^+ level due to insufficient K^+ uptake via the channel proteins as well as via Trk systems. Thus, both initial stimuli conjoin in the same effect then serving as the primary stimulus for *kdpFABCcat3* expression.

3.4 Induction of the halobacterial Kdp system

Sofar it is unknown, at which level the necessity to express a $\Delta\psi_m$–independent high affinity K^+ -uptake system is sensed. Although the extracellular K^+ itself could serve as stimulus, this would require the presence of an integral membrane protein able to sense the extracellular K^+ concentration together with an additional signaling pathway to enable a response at the level of transcription. However, the expression of the *kdpFABCcat3*-operon is stimulated by medium K^+ concentrations over a broad range (20 mM - 20 µM, Özyamak, diploma thesis, 2004). As a consequence, a specific sensing of K^+ over this broad range in the presence of high Na^+ concentrations would be required to explain the observed transcriptional response. Although unlikely, the presence of a such novel sensing mechanism and a corresponding signal pathway can not be ruled out.

As discussed above, cellular K^+ concentrations in the molar range in the presence of low medium K^+ concentration results in the generation of a high $\Delta\psi_{K+}$. As a consequence, the K^+ concentration in the medium directly influences the driving force of $\Delta\psi_m$. Upon K^+ limitation, the calculated $\Delta\psi_{K+}$ of >300 mV can potentially significantly depolarize the membrane, even if all additional major ions (Na^+, Mg^{2+}, Cl^-) are taken into account. Whereas membrane depolarization is a major signal for transcriptional regulation in Eucarya, very little is known about the cellular response to membrane depolarisation at the level of transcription in

Archaea. Although a transcriptional response of the Kdp system in range of 20 mM - 20 µM merely as a result of changes in the membrane depolarization seems to be unlikely at first view, the presence of approx. 4 M KCl in the cell readily results in a $\Delta\psi_{K+}$ of approx. 140 mV in case of medium K^+ concentrations of 20 mM. As a concequence, the first measurable expression of the *kdpFABCcat3* operon takes place under conditions, in which $\Delta\psi_{K+}$ has already reached values of half of $\Delta\psi_m$ and rises as $\Delta\psi_{K+}$ becomes more dominant. In an other context, *H. salinarum* has been reported to exhibit phototaxis mediated by sensory rhodopsin I (Krah *et al.,* 1994). More recently, a transducer (MpcT) mediating phototaxis in response to changes in membrane potential was discovered (Koch & Oesterhelt, 2005), thereby demonstrating the presence of membrane potential-sensing proteins in *H. salinarum*. Interestingly, a homolog of a putative membrane potential-sensing domain of MpcT was found to be present in a putative histidine kinase (VNG1193C) as well. Although highly hypothetical, this uncharacterized histidine kinase with unknown function and signal transduction pathway could serve as a potential candidate inducing the Kdp system as a result of changes in membrane potential.

The observed decrease in the cellular K^+ concentration upon K^+ depletion as well as the parallel reduction of cell volume can be challenged as an primary stimulus for several reasons. Whereas both types of adaptation to K^+ depletion only take place in the presence of extracellular K^+ concentrations of approx. 250 µM and below (see Figure 34), the expression of the *kdpFABCcat3* operon is readily stimulated in the presence of the medium K^+ concentrations of 20 mM and below. Furthermore, if cultivated in the presence of 4 M NaCl, *H. salinarum* exhibits a cell volume comparable to the reduced cell volume measured in the presence of lower osmolality and K^+ depletion (Stefan Thiele, bachelor thesis, 2007). In the presence of 4 M NaCl, however, the *kdpFABCcat3* operon is still expressed in a medium K^+-dependent manner. The same line of reasoning can be used to rule out changes in the cellular K^+ concentrations as a primary stimulus. The reduced intracellular K^+ level measurable upon K^+ depletion can also be observed in the presence of a lower overall osmolality in the growth medium. If grown in the presence of 2 M NaCl, *H. salinarum* exhibits cellular K^+ concentrations similar to the reduced K^+ concentrations measured in cultures grown in the presence of higher osmolality and K^+ depletion (Stefan Thiele, bachelor thesis, 2007). Under these growth conditions, again the expression of the *kdpFABCcat3* operon still exhibits a strict dependency on medium K^+ concentrations. A significant difference, however, exists between the reduction of cellular K^+ concentration as a result of K^+ depletion or lower medium salinity. Whereas *H. salinarum* adapts to lower medium salinity solely by the

reduction of cellular K^+, the reduction of cellular K^+ is accompanied with a parallel increase in cellular Na^+ concentration as a response to K^+-depletion. Hence, the decrease in intracellular K^+ as a result of K^+ depletion entails drastic consequences for the electrophysiological conditions of the cell. Given that the internal salt concentration in *H. salinarum* is close to the saturation level, there is a drastically reduced water activity due to each water molecule being coordinated by salt ions, either Na^+ or K^+. Thus, proteins are strongly competing with the ions for water molecules to gain a proper hydration shell. Although halobacterial proteins are highly adapted to this environment, the availability of surface water is essential for protein function (Tehei *et al.,* 2007). In this respect there is a great difference if there is more K^+ than Na^+ or vice versa. NaCl-saturated salt brines comprise a water activity (a_W) of 0.75. Saturated KCl, in contrast, features an a_W value of 0.86, resulting in significantly more free water molecules due to less coordination events. Under conditions of K^+ limitation, the internal K^+ concentration is decreased by approx. 30 % (i.e. from 4 M to about 2.8 M). In this reduction, the cellular K^+ most likely is replaced by Na^+, which, in turn, readily leads to a significant loss in internal water molecules in order to coordinate the increasing Na^+. As a consequence, proteins are supposed to release low entropy surface water at increasing amounts of Na^+ when K^+ concentration decreases, which may have a great impact on protein structure and function and may lead to either inhibition or activation. In mesophiles, this effect is neglegible due to the relative low ion content with respect to approx. 55 M H_2O concentration together with the high water permeability of the cell envelope. In *H. salinarum*, however, the internal salts sum up to the tenth part of the molar composition with respect to water, rendering these ion shifts to be of great importance due to the coordination of many water molecules per ion. It is tempting to speculate that the reduced cellular water activity could be sensed as a signal finally leading to the induction of the *kdpFABCcat3* operon. The reduction of the cellular K^+ concentration and the resulting changes in cell water activity take plase in medium K^+ concentrations significantly lower than needed for the initial induction of the *kdpFABCcat3* operon. Nevertheless, this potential regulatory mechanism might play a significant role in the context of a potential multi-level regulation of the *kdpFABCcat3* operon.

Although the expression of the *kdpFABCcat3* operon is already slightly induced at medium K^+ concentrations of 20 mM and below, a decrease in the medium K^+ concentration below approx. 250 µM results in an additional strong induction of expression (see Figure 34). The non-linearity in K^+ dependency implicates the presence of a possible dual-level transcriptional regulation of the *kdpFABCcat3* operon. In the range between 20 mM and approx. 250 µM, the

expression exhibits a fairly linear dependency to the medium K^+ concentration (Özyamak, diploma thesis, 2004). If the concentration, however, decreases below 250 µM, the expression level undergoes a remarkable secondary induction. Interestingly, this secondary induction occurs virtually parallel to the discussed adaptation of cell volume and cellular K^+ concentration.

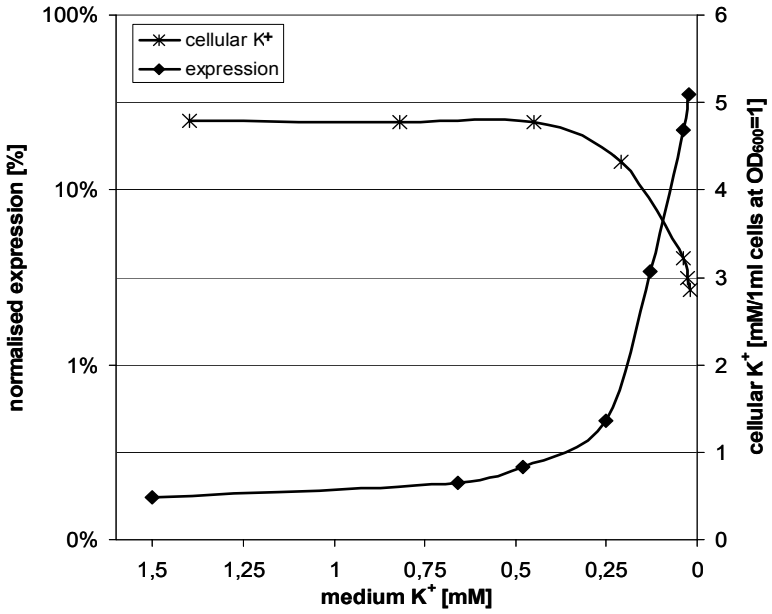

Figure 34: The dependency of cellular K^+-content and *kdpFABCcat3*-expression on the medium K^+ concentration.
The expression values and the corresponding medium K^+ concentrations are as in figures 14 and 15. The cellular K^+ content is represented as K^+ released from 1ml cells at OD_{600}=1. Due to missing cell counts and cell volume measurements, the amount of cellular K^+ is plotted as a function of optical density (data not shown elsewhere). Although indirect, the given data illustrate the dynamic shift in cellular K^+/OD_{600}-ratio influenced by adaptation of cell volume and cellular K^+ concentration.

It is tempting to speculate, that the expression of the *kdpFABCcat3* operon is regulated at two different levels. The primary induction could occur as a response to a decrease in the medium K^+ concentration as discussed above, whereas the secondary strong induction could be linked to either primary or secondary effects of a very high $\Delta\psi_{K+}$ or to changes in water activity in the cell, as already discussed.

In addition, the expression *kdpFABCcat3* operon was shown to be regulated in a growth phase-dependent manner, resulting in a repression of gene expression in the stationary growth phase. This down-regulation of an ATP-consuming K^+ uptake system in the stationary growth phase is most likely linked to the absence of the necessity to perform significant K^+ uptake during arrested cell growth. Whereas the induction of the *kdpFABCcat3* genes is most likely performed at the level of an operon or possibly a regulon (discussed later), this repression in the stationary growth phase could represent a more global and K^+ independent level of

regulation. The genome of *H. salinarum* encodes multiple copies of the general archaeal transcription factors (6 copies of TBP and seven copies of TFB). A role of the different TBP, TFB and combinations thereof in a global transcriptional regulation in *H. salinarum* has already been discussed (Baliga *et al.,* 2000) and could also apply in case of the *kdpFABCcat3* operon.

3.5 Regulation of gene expression of *the kdpFABCcat3* operon

The sequence-based analysis of the promoter region disclosed together with the putative TATA-box and BRE (TFB-binding site) sequences, which are highly similar to conserved archaeal promoter elements. Although initially identified on the basis of sequence homology to the well-characterized bacterioopsin-promoter, the transcription start site of the *kdpFABCcat3*-operon was later confirmed to be located in a conserved distance of 28 bp downstream of the postulated TATA-box. Assuming the presence of a conserved, although nonannotated *kdpF* gene, the transcript of the *kdpFABCcat3* operon features an only 4 bp long 5´-UTR. The absence of a significant 5´-UTR is a phenomenon widely found in Archaea (Tolstrup *et al.,* 2000; Sartorius-Neef & Pfeifer, 2004), although the detailed mechanism of the recruitment of leaderless mRNA´s in Archaea is so far unknown. The truncation analysis of the P_{kdp} demonstrated that the minimal active promoter extends 42 bp upstream of the transcription start site. This strongly supports the identification of the postulated TATA-box and BRE.

Truncation analysis of P_{kdp}, however, additionally indicated the presence of a potential operator located downstream of -96 position. Extended sequence analysis of the corresponding region revealed a palindromic sequence typical of binding sites of transcriptional regulators of the HTH-type. Finally, via site directed mutagenesis, this region was identified to participate in a negative regulation of the *kdpFABCcat3* operon. This putative binding site for a transcriptional repressor, however, is located atypically far upstream of the conserved promoter elements. Given the distance of 15-20 bp upstream of BRE, it is questionable if a repressor bound to this putative operator could directly inhibit the initiation of transcription. However, the deletion of this putative operator, as it is true for all truncations affecting this region, is not sufficient to abolish repression entirely. For these reasons, the existence of a second yet unknown operator located between -42 bp and +4 bp is postulated. This second putative operator would be located in the region of the conserved promoter elements, in which the inhibition of transcription initiation by bound repressor is reasonable. Even though most likely not being capable to inhibit transcription by itself, the binding of a repressor in the sequence region upstream of the conserved promoter elements

could stabilize the binding of a second putative repressor, resulting in a cooperative repression of P_{kdp} (see Figure 35). Although highly hypothetical, a dimerization of the two putative bound repressors could even result in a strong loop-like bend of DNA being responsible for the atypical strong repression of P_{kdp}.

Although several approaches were carried out in order to identify the cellular components participating in the regulation of expression of the *kdpFABCcat3* operon, the protein(s) responsible for the primary medium K^+ concentration-dependent induction and the postulated related repressors could not be indentified yet. Although the hypothetical role of two candidates (VNH6183C, VNG1193C) is discussed, the function of these proteins in the regulation of gene expression has to be verified by further studies. Although the *kdpFABCcat3* operon is localised in a cluster of genes up-regulated in response to K^+ depletion, this location was shown not to be essential for medium K^+-dependent regulation of the corresponding genes. Furthermore, the role of a potential replication-mediated gene amplification in the induction of the halobacterial Kdp system as well as the in induction of the discussed up-regulated gene cluster can be ruled out.

The halobacterial Kdp system was shown to exhibit a transcriptional regulation not only independent of the common KdpD/KdpE regulators but also independent of any additional response regulator. As a consequence, the gene regulation of the halobacterial Kdp system is apparently essentially different from that found in Bacteria. In most Archaea encoding a Kdp system, however, a strong connection can be found between the *kdp(F)ABC* genes and *cat3* at least with respect to their location on the chromosome. Although this favors a function of Cat3 in the context of the Kdp system, it was quite surprising to find *cat3* to be essential for high-level induction of the *kdpFABCcat3* operon. Since *cat3* is co-induced together with *kdpFABC* genes, and the expression of *cat3* is under noninducing conditions of >20 mM K^+ in the medium as low as for other genes of the Kdp system, the gene product of *cat3* can exhibit its function apparently only after an initial induction of the whole operon. As a consequence, *cat3* can not exhibit its regulatory function in the initial K^+-dependent induction of the *kdpFABCcat3* operon. The residual expression level found in the absence of *cat3* of approx. 5 % of the induced level measured in the presence of *cat3*, however, is virtually congruent with expression levels measured in the wild type in the presence of approx. 250 µM K^+ in the medium. In other words, the deletion of *cat3* results in expression levels similar to those measured just before the secondary induction of the *kdpFABCcat3* operon. It is tempting to speculate, that after the primary K^+-dependent induction of *kdpFABCcat3* operon, Cat3 could

have its function in enabling the secondary high-level induction of the *kdpFABCcat3* operon by an interaction with the postulated, but yet unknown repressors.

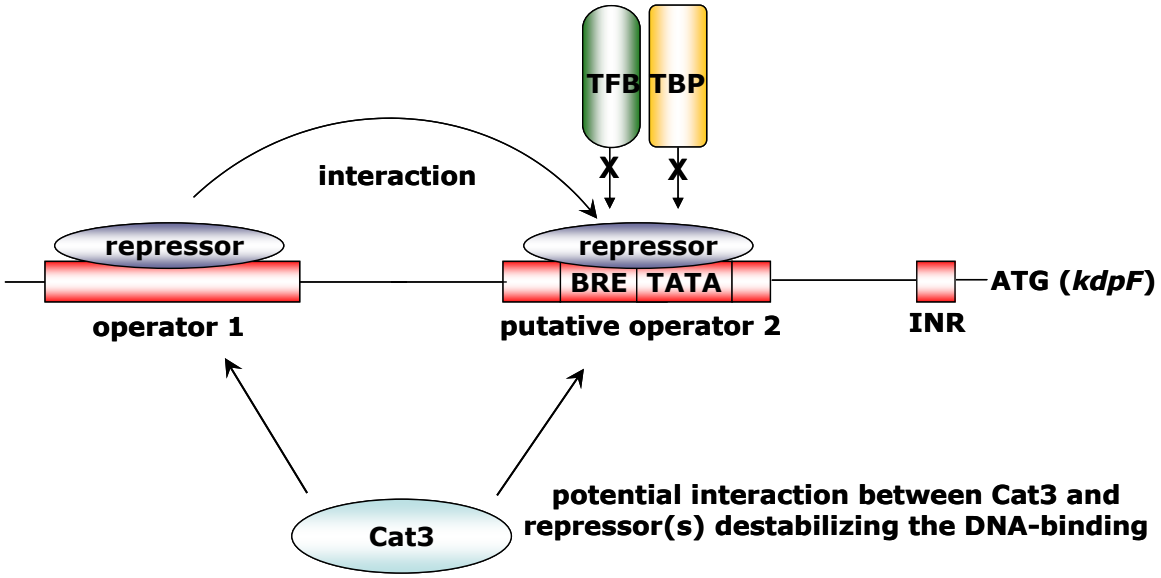

Figure 35: Model of the putative mode of function of the *kdp* promoter.
The repressor bound to a yet unknown but postulated operator 2 represses the initiation of transcription by sterical hindrance. The binding of a repressor to operator 1 stabilizes the repressor/operator 2- complex by a direct interaction. Upon primary induction, the DNA-binding of either one of the repressors or both is destabilized. Alternatively, the interaction between bound repressors could be altered. Upon the secondary strong induction, Cat3 interacts with the bound repressor(s), thereby inhibiting DNA-binding and allowing a fully derepressed expression.

This hypothetical model of *kdp* regulation and of the regulatory function of Cat3 is highly supported by the observed expression profile of *kdpFABC* if *cat3* is constitutivly expressed in *trans*. The deletion of *cat3* and the recovery of high-level *kdpFABC* expression by the plasmid-encoded expression of *cat3* in *trans* clearly demonstrates the function of the *cat3* gene product itself rather than that of the mere *cat3* coding region in the regulation of the *kdpFABCcat3* operon. Furthermore, the stimulation of *kdp* expression by the constitutive expression of *cat3* under noninducing and even inducing conditions highly supports the notion, that Cat3 exerts its influence through the negative regulation of the *kdp* promoter. The significantly elevated expression level in the presence of 100 mM KCl in the medium could, thereby, mimic the K^+-independent inhibition of repression carried out by Cat3 in the secondary induction phase of *kdp* expression. However, the observed expression levels under inducing conditions being significantly higher than the levels measured in the wild type strain appearently puzzles this view. This could be interpreted as an indication that Cat3 directly acts as a transcriptional activator rather than in the modulation of the negative regulation carried out by the putative repressors. The absence of a sequence similarity to any known DNA-binding proteins, however, supports an alternative explanation. In the wild type, the

expression of *kdpFABCcat3* on a high level occurs in a relativly short growth period characterized by a decrease in the medium K^+ concentration from approx. 250 µM to 20 µM. The corresponding increase in optical density from 0.75 to approx. 1.0 does permit the induction of gene expression to a high level but the accumulation of the produced proteins in the cell most likely requires considerably more time. In the presence of a constitutive expression of *cat3*, however, the gene product of *cat3* is readily accumulated on a high level only influenced by the equilibrium between the strength of the corresponding ferrodoxin promoter and the stability of Cat3 in the cell. As a consequence, the constitutive expression of *cat3* could result in a fraction of Cat3 in the cell considerably higher than present in the wild type. This excess of Cat3 could be sufficient to eliminate repression of the *kdp* promoter, even stronger than observed in wild type and, thus explains the observed phenomenon.

At first glance, the discussed type of gene regulation present in *Halobacterium* obviously represents a novel type highly different from that found to regulate the Kdp system in Bacteria. However, remarkable similarities can be found regarding Cat3. In Bacteria, *kdpFABC* expression is normally governed in response to K^+ limitation and high osmolality. Since halobacteria are osmotically balanced with their environment, the KdpFABC complex is not required to be involved in turgor regulation and, hence, there is no need for an corresponding complex sensory system analogous to the *E. coli* KdpD/KdpE sensor kinase/response regulator. However, although alterations in ion concentration and external osmolality are thought to trigger KdpD-dependent signal perception in *E. coli*, it has recently been discussed that the primary stimulus rather resides in changes of intracellular parameters (Jung and Altendorf, 2002). The possibility of an ATP-activated molecular switch involved in stimulus perception gives rise to speculations about an according more basic signal transduction mechanism in *Halobacterium*, although the primary stimulus is most likely different from that of *E. coli*. The framework of this kind of regulation relying on ATP as the primary activator of a Cat3-dependent secondary control of *kdpFABC* expression is not thus far away from its more complex bacterial counterpart. Based on sequence analysis, the deduced Cat3 protein clearly consists of a tandem Usp domain motif with no further domains or extensions. A sequence based and homology modelling analysis of Cat3 revealed a significant structural homology to a class of Usp-proteins able to bind ATP (Aravind *et al*., 2002; see Figure 36). Furthermore, at least the C-terminal Usp-domain of Cat3 exhibits high sequence and structural homology to a ATP binding site identified within the Usp-homolog MJ0577 (Zarembinski *et al.,* 1998).

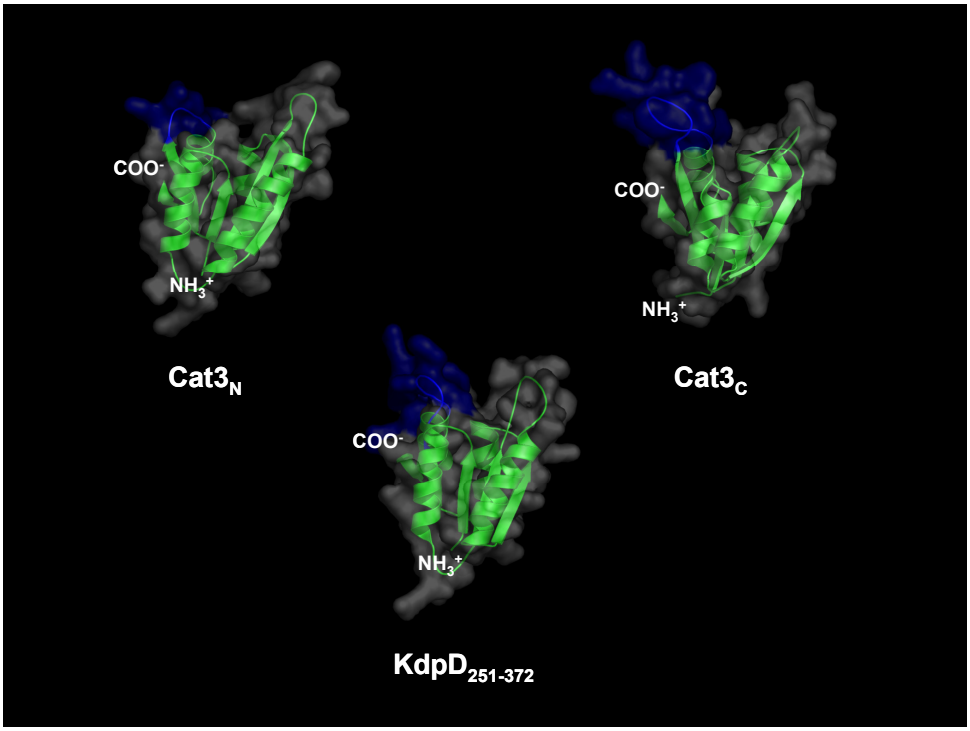

Figure 36: Structural model of the putative Usp-domains of Cat3 and *E. coli* KdpD.
Usp domains were modeled against the structural coordinates of MJ0577 (1MJH, Zarembinski *et al.,* 1998). The putative ATP-binding loop of the Usp domains of Cat3 and *E. coli* KdpD are highlighted in blue.

In working as a possible ATP-activated molecular switch, Cat3 would obviously correspond to the bacterial KdpD, since it closely resembles a structural pattern of the N-terminal part of KdpD ($KdpD_{251-372}$). A regulatory effect of ATP binding has already been reported for the N-terminal part of KdpD although the exact binding site is unknown (Heermann *et al*., 2000). In addition, ATP-dependent signaling via this Usp domain influencing the kinase activity of KdpD has already been discussed in the context with structure-related functional features of Usp domain family members (Aravind *et al*., 2002). A functional homology of Cat3 and $KdpD_{251-372}$ is further favored by the fact that the N-terminal domain of KdpD bearing the Usp motif is rather unique and can not be found in any other sensor kinase proteins sequenced so far (Jung and Altendorf, 2002).

The primary K^+-dependent induction of the *kdpFABCcat3* operon via yet unknown transcriptional regulators together with a secondary induction via Cat3 potentially working as an ATP-dependent modulating switch would reasonably connect active K^+ uptake to alterations in both $\Delta\psi_m$ and intracellular ATP level. Since $\Delta\psi_{K+}$ itself obviously contributes to $\Delta\psi_m$, the potassium gradient across the membrane directly influences the level of the equilibrium between the phosphate potential and the proton motive force and, as a consequence, the intracellular ATP/ADP ratio (Wagner *et al*., 1978; Michel & Oesterhelt,

1980; Brown *et al*., 1983). Thereby, the combination of steep K^+ and the Na^+ gradients are thought to stabilize both $\Delta\psi_m$ and the ATP pool of the cell during periods of darkness and anaerobiosis (Brown *et al*., 1983). An ATP-mediated activation of a regulatory protein by Cat3 would, thus, be an attractive model integrating both the intracellular ATP/ADP ratio and $\Delta\psi_m$. This rather sophisticated regulatory pattern would well correspond to the physiological capabilities of halobacteria including facultative anaerobic and phototrophic growth. Interestingly, also bacterial KdpD is supposed to work at least in part as an electrostatic switch responding to changes in ionic strength (Jung & Altendorf, 2002), thus further supporting an analogous function of KdpD and Cat3. However, a direct sensing of cytoplasmic K^+, as it is true for the halobacterial Kdp system as well, can be ruled out (Hamann et al, 2007).

3.6 Global transcriptional response to K^+ depletion

The analysis of the global trancriptional response of *H. salinarum* identified 26 genes significantly being up-regulated and 35 genes being down-regulated as a response to K^+ depletion. The genes encoded by the *kdpFABCcat3* operon were found to exhibit the strongest measured transcriptional response, thereby indicating the crucial role of the Kdp system for the cell´s ability to grow with low K^+ concentrations. As an independent method, these findings further support the expression level measurements carried out by use of reporter gene fusions and *real-time* RT-PCR. The additional K^+ uptake systems present in *H. salinarum* (PchA1-2 and TrkH1-4) do not seem to be regulated in a K^+-dependent manner. However, two potential homologs of *trkA* (*trkA2* and *trkA5*) are significantly up-regulated. TrkA proteins are reported to exhibit their function as a TrkHA complex in modulating the K^+ transport via TrkH. (Schlösser *et al.,* 1993, Nakamura *et al.,* 1998; Harms *et al.,* 2001). Thus, a function of these *trkA* homologs in modulating the activity of Trk transport systems under conditions of high $\Delta\psi_{K+}$ and/or low extracellular K^+ is possible.

In the framework of a high $\Delta\psi_{K+}$ it is interesting that also the *atp* operon was found to be repressed, thus leading to a reduced amount of A_1A_O ATP synthase. Since this enzyme utilizes the $\Delta\psi_m$ for the synthesis of ATP, a reduction in the fraction of active enzymes readily increases the $\Delta\psi_m$, which can then be used to re-inforce the channel-mediated K^+ uptake in case of an increasing opposing $\Delta\psi_{K+}$. In the context of the regulation of the Kdp system via Cat3, the down-regulation of the *atp* operon and, as a consequence, the lower cellular ATP level further emphasises the link between the Kdp system and changes in $\Delta\psi_m$ and the cellular ATP/ADP balance. Although out of the scope of this work, the K^+ concentration-dependent

regulation of pyruvate-ferredoxin oxidoreductase (*porB*) as well as of fructose-bisphosphate aldolase (*fba2*) genes could also mirror the strong influence of high $\Delta\psi_{K+}$ on the central energy homeostasis of *H. salinarum*.

As discussed earlier, 44 % of the genes up-regulated in response to K^+-depletion are located in a rather narrow region on the extrachromosomal replicon pHS3 or pNRC200. This obviosly groups a subset of the up-regulated genes in a K^+-responsive cluster. Since the expression of at least the *kdpFABCcat3* operon is clearly independent of the chromosomal location of the genes, the reason for this phenomenon remains unclear. The postulated co-localisation of *orc1/cdc6* gene homologs with origins of replication (Norais *et al.,* 2007) and the presence of several *orc1*/*cdc6* homologs in the corresponding K^+-responsive cluster implicates an interesting correlation between the discussed clustering and the replication processes. However, no significant influence of the K^+ concentration on the copy number of the corresponding genome region was observed. Alternatively, replication could be inhibited by changes in expression of the *orc1/cdc6* gene homologues *orc2*, *orc3,* and *orc5* at the level of the whole genome rather than in the discussed specific region. As a consequence, the inhibition of this initial step of replication and the resulting inhibition of the following cell division could represent a rather sofisticated mechanism initiating the stationary growth phase mode in order to avoid cell division in the absence of adequate K^+ supply. However, because of the sample collection the a late logarythmic growth phase and a possible intermixture of K^+-dependent and growth phase-dependent effects, this hypothesis needs to be verified by further studies.

The observed induction of a putative operon built up by the genes VNG6183, *cat4,* and VNG6185 and the discovery of a sequence highly homologous to the identified operator of the *kdp* promotor in the putative promotor region of this operon opens the room for discussion about a different way how the clustered genes could be linked to each other. Although this has to be verified in further experiments, the *kdpFABCcat3* operon could share a common repressor with this putative operon and, thus, represent a part of a K^+-responsive regulon. Although not obligatory and as in case of the *kdpFABCcat3* operon without any measurable influence on the regulation of gene expression, operons arranged in a regulon have a considerable tendency to be located in a near vicinity to each other. To which extend other genes up-regulated upon K^+ depletion participate in this potential regulon or build up own independent regulons would be an interesting subject for further studies and would significantly broaden our understanding of K^+ homeostasis in *H. salinarum*.

4. Materials and Methods

All chemicals used were of analytical grade. Concentrations listed in percentage are given as weight/volume [w/v]. The list below contains all the suppliers of chemicals unless stated otherwise.

BioRad	(Müchen, Germany)	iQ SYBR Green Supermix
Becton Dickinson	(Oxnard, USA)	Falcon Flexible PVC 96-Well Microplate, Difco Peptone
Fermentas	(St.Leon-Rot, Germany)	First Strand cDNA Synthesis Kit, GeneRuler™ 100bp DNA Ladder, GeneRuler™ DNA Ladder Mix
Finnzymes	(Espoo, Finland)	Phusion™ High-Fidelity DNA Polymerase
Oxoid	(Wesel, Germany)	Yeast Extract, Casaminoacids
Invitrogen	(Carlsbad, USA)	TOPO TA Cloning® Kit, Agar
NEB	(Schwalbach, Germany)	Restriction Enzymes, RNase free DNase, T-4 ligase, DNA Polymerase I Large (Klenow)
Qiagen	(Hilden, Germany)	RNeasy mini kit, QIAquick Gel Extraction Kit, QIAGEN Plasmid Mini Kit
Ratiopharm	(Ulm, Germany)	Simvastatin 40mg
Sigma-Aldrich	(Deisenhofen, Germany)	Novobiocin, Uracil, 5-FOA, Tryptophan, ONPG
Stratagene	(Amsterdam, Netherlands)	Herculase® DNA Polymerase

All other chemicals were purchased from Sigma-Aldrich (Deisenhofen, Germany), Fluka (Neu-Ulm, Germany), Riedel-De-Haen (Seelze, Germany), Roth (Karlsruhe, Germany), or Serva (Heidelberg) unless stated otherwise.

4.1 *H. salinarum* media, and cultivation

The genotypes of *H. salinarum* strains and plasmids used in this work are described in tables 6 and 7. For physiological and gene expression analyses, strains were grown in media as described in Kauri *et al.,* (1990) with the following modifications: The total salt concentration

was shifted to 25 % according the growth requirements of *H. salinarum.* Potassium salts were substituted with sodium salts to obtain a K^+-free medium, whereas potassium was added as KCl in required concentrations. 0.5 % Casaminoacids was used as carbon source (Table 3). For all other experiments, strains were grown in rich media as described for *Halobacterium* sp. NRC-1 in the American Type Culture Collection (ATCC medium 2185). If needed, media were supplemented with 20 µg/ml of Simvastatin, which was extracted from solid tablets (Ratiopharm) by dissolving in ethanol, or with 0,2 µg/ml Novobiocin. All strains were grown under illumination with shaking at 37°C. Optical densities were monitored at 600 nm.

Table 3: *H. salinarum* casaminoacids medium

Casaminoacids medium	**1000 ml**
NaCl	174 g
$MgCl_2 \cdot 6\ H_2O$	69 g
Na_2SO_4	5,68 g
$CaCl_2 \cdot 2\ H_2O$	0,36 g
NH_4Cl [1M]	5 ml
KCl	variable
trace elements solution	1 ml
Na_2HPO_4-Puffer [0,5M; pH 7,2]	2 ml
Glycerin [87%]	58 ml
Thiamin [1mg/ml]	1,6 ml
Biotin [1mg/ml]	100 µl
Casaminoacids	5 g

trace elements solution	**100 ml**
$ZnSO_4 \cdot 7\ H_2O$	36 mg
$MnSO_4 \cdot 1\ H_2O$	44 mg
$FeSO_4 \cdot 6\ H_2O$	230 mg
$CuSO_4 \cdot 5\ H_2O$	5 mg

Table 4: *H. salinarum* ATCC medium

***Halobacterium* ATTC**	**1000 ml**
NaCl	250 g
$MgSO_4 \cdot 7\ H_2O$	20 g
Na_3-citrate	3 g
KCl	2 g
Peptone	5 g
Yeast extract	3 g
trace elements solution	100 µl
Agar (optional)	16 g

trace elements solution	**200 ml**
$ZnSO_4 \cdot 7\ H_2O$	660 mg
$MnSO_4 \cdot 1\ H_2O$	170 mg
$FeSO_4 \cdot 6\ H_2O$	390 mg
$CuSO_4 \cdot 5\ H_2O$	70 mg

4.2 *H. volcanii* media, and cultivation

The genotypes of *H. volcanii* strains and plasmids used in this work are described in tables 6 and 7. For physiological and complementation analyses, strains were grown in media as described in table 5. If needed, media were supplemented with 2 µg/ml of Novobiocin, 50 µg/ml tryptophan, 50 µg/ml uracil or 50 µg/ml 5-FOA.

Table 5: *H. volcanii* casaminoacids medium

Casaminoacids medium	1000 ml
NaCl	144 g
$MgCl_2 \cdot 6\ H_2O$	18 g
$MgSO_4 \cdot 7\ H_2O$	21 g
KCl	variable
Tris HCl [1 M; pH 7,5]	12 ml
Casaminoacids	0,8 g
$CaCl_2$ [0.5 M]	6 ml
Thiamine [1 mg/ml]	266 µl
Biotin [1 mg/ml]	33 µl
Uracil [50 mg/ml]	340 µl
5-FOA [50 mg/ml]	340 µl
Agar	16 g

4.3 Strains, plasmids, and oligonucleotides

Table 6: Strains used in this study

Strains	relevant genotype	relevant characteristics	reference[(a)]
H. salinarum R1	wild type	gas vesicle deficient	Stockenius & Kunau (1968)
H. salinarum Δ*kdpFABCcat3*	Δ*kdpFABCcat3*	deletion of *kdpFABCcat3* *R1*-derivative	
H. salinarum Δ*kdpFABC*	Δ*kdpFABC*	deletion of *kdpFABC* R1-derivative	
H. salinarum ΔOE3854	ΔOE3854	deletion OE3854 R1-derivative	A. Wende, unpublished
H. salinarum ΔOE2334	ΔOE2334	deletion OE2334 R1-derivative	A. Wende, unpublished
H. salinarum ΔOE3854	ΔOE2083	deletion OE2083 R1-derivative	A. Wende, unpublished
H. volcanii H53	Δ*pyrE2* Δ*trpA*	deletion of *pyrE2* and *trpA*	Allers *et al.* (2004)
E. coli DH5α	F-, ø80d*lacZ*Δ*M15*, Δ(*lacZYA-argF*)U169, *deoR*, *recA1*, *endA1*, *hsdR*17(rK^-, mK^+), *phoA*, *supE44*, λ–, *thi-1*, *gyrA96*, *relA1*	cloning strain	Hanahan (1983)
E. coli TOP10 OneShot	F- *mcrA* Δ*(mrr-hsdRMS-mcrBC*) ø80*lacZ*Δ*M15* Δ*lacX74 deoR recA1 araD139* Δ(ara-leu)7697 *galU galK rpsL* (StrR) *endA1 nupG*	cloning strain	Invitrogen

[a] unless otherwise stated, strains were constructed in this work

Table 7: Plasmids used in this study

Plasmids	genotype[(a)]	characteristics	reference[(a)]
pMKK100	Ap^R, Mv^R, *bgaH, ColE1*	*H. salinarum*/*E. coli* shuttle vector	Koch & Oesterhelt (2005)
pTA425	Ap^R, *Col*E1, pHV4 *pyrE2*	*H. volcanii/E. coli* shuttle vector	T. Allers, unpublished
pJAS35	Ap^R , Nb^R, *ColE1*	*H. salinarum* expression vector	Pfeifer *et al.,* (1994)
pHJS1	Ap^R, Mv^R, *bgaH, ColE1, kdpFABCcat3*	expression of *kdpFABCcat3*	
pHJS2	Ap^R, Mv^R, *bgaH, ColE1, kdpFABC*	expression of *kdpFABC*	
pHJS3	Ap^R, Mv^R, *bgaH, ColE1*	knock-out plasmid for Δ*kdpFABC*	
pHJS4	Ap^R, Mv^R, *bgaH, ColE1*	knock-out plasmid for Δ*kdpFABCcat3*	
pOEZ1	Ap^R, Mv^R, *ColE1* P_{kdp}:: *bgaH*	reportergen-fusion P_{kdp}:: *bgaH*	Özyamak (Diploma, 2004)
pHJS6	Ap^R, Mv^R, *ColE1* P_{kdp56}::*bgaH*	reportergen-fusion, truncated promotor (52bp), intergration 300 bp downstream of *cat3*	
pHJS7	Ap^R, Mv^R, *Col*E1 P_{kdp56}::*bgaH*	reportergen-fusion, truncated promotor (52bp), intergration 300bp upstream of *rpoA1*	
pHJS8	Ap^R, Mv^R, *ColE1* P_{kdp56}::*bgaH*	reportergen-fusion, truncated promotor (52bp), intergration 300bp upstream of *bop*	
pHJS9	Ap^R, Mv^R, *bgaH, ColE1, kdpFABCcat3*	expression of *kdpFABCcat3,* deletion of operator 1	
pHJS10	Ap^R, Mv^R, *bgaH, ColE1, kdpFABCcat3*	expression of *kdpFABCcat3,* truncated promotor (206bp)	
pHJS11	Ap^R, Mv^R, *bgaH, ColE1, kdpFABCcat3*	expression of *kdpFABCcat3,* truncated promotor (52bp)	
pHJS12	Ap^R, Mv^R, *bgaH, ColE1, kdpFABCcat3*	expression of *kdpFABCcat3,* truncated promotor (42bp)	
pHJS23	*trpA*, P_{kdp}::*pyrE2*	reportergen-fusion P_{kdp}::*pyrE2*	
pSH1	P_{fdx}::*cat3,* Nb^R	constitutive expression of *cat3*	Hockemeyer (Lab course, 2007)
pBAD24	Ap^R, *ColE1*	*E. coli* expression vector	Guzman *et al.* (1995)

[a] Abbreviations: Ap^R, Ampicillin resistance; Mv^R, Mevinolin/Simvastatin resistance, Nb^R, Novobiocin resistance. [b] Unless otherwise stated, plasmids were constructed during this work.

Table 8: Primers used in this study

primer	sequence	purpose
# 1	CTCGGAGGAGTGAGGGATTCGACGACCC	cloning of the *kdpFABCcat3*
# 2	GACTTCTTGTGCAACGGACATCCACCGG	cloning of the *kdpFABCcat3*
# 3	CGACGCCCACATTTCCCCGGCG	Δ*cat3*
# 4	GTCACGGCGGCCCTTAGTGGTCACCGTTCGCTATTTCG	Δ*cat3*
# 5	CGGTGACCACTAAGGGCCGCCGTGACAGACTCA	Δ*cat3*
# 6	GCCCACCTCAGCCTCGTGCGCGCCATGGGCAGC	Δ*kdpFABC*/Δ*kdpFABCcat3*
# 7	GTTTCGTGCTGACATGTGCAACTGGCCCGGATGATTTC	Δ*kdpFABC*
# 8	CGGGCCAGTTGCACATGTCAGCACGAAACGAAACCGG	Δ*kdpFABC*
# 9	GCGCGAAGCTTGACGACCACTGGCACCAGTATC	Δ*kdpFABC*/Δ*kdpFABCcat3*
# 10	GGTCACGGCGGCCCCATGTGCAACTGGCCCGGATGATTTC	Δ*kdpFABCcat3*
# 11	CGGGCCAGTTGCACGGGCCGCCGTGACCGCCTCAC	Δ*kdpFABCcat3*
# 12	CGACGCCCACATTTCCCCGGCG	*real time* RT-PCR *kdpC*/*cat3*
# 13	GTCTACGAGGATGCTCGACAGCTC	*real time* RT-PCR *kdpC*/*cat3*
# 14	CGGGCGGCTGCAACGGCCAC	*real time* RT-PCR *rpoA1*
# 15	CATCGACGCCGCGATGCGCTC	*real time* RT-PCR *rpoA1*
# 16	CCTGGAAAGGGTACCTAAAGGCGG	*real time* RT-PCR *kdpA*
# 17	GTCTACGAGGATGCTCGACAGCTC	*real time* RT-PCR *kdpA*
# 18	CGATCTTGATATCGAACCCGG	*real time* RT-PCR OE5061
# 19	GGGCGGCTCGGATTTCTCTC	*real time* RT-PCR OE5061
# 20	GCTGTTGAATGGAGCACAGAC	*real time* RT-PCR VNG6180
# 21	GCAGTCCCACGGGTTGCTG	*real time* RT-PCR VNG6180
# 22	GCGCGCCATGGGCCAGAACTGTGGCAGCGAG	206 bp long P_{kdp}
# 23	CAACACCCAGATAGACACG	206 bp long P_{kdp}
# 24	GCGCGCCATGGGCTCCGTCCATACTCCGACAAATATAAA TAAGG	52 bp long P_{kdp}
# 25	CAACACCCAGATAGACACG	52 bp long P_{kdp}
# 26	GCGCGCCATGGACTCCGACAAATATAAATAAGGAG	42 bp long P_{kdp}
# 27	CAACACCCAGATAGACACG	42 bp long P_{kdp}
# 28	GCGCGCCATGGGCCAGAACTGTGGCAGCGAG	P_{kdp}, deletion of operator 1
# 29	CACCGTGGCTAACTCCGTCCATACTCCG	P_{kdp}, deletion of operator 1
# 30	CCTACATGTGGTGGCACCGATTGAGGCAGG	P_{kdp}, deletion of operator 1
# 31	CAACACCCAGATAGACACG	P_{kdp}, deletion of operator 1
# 32	GCGCGCTGCAGCGTGCAGAGCCTCAGTGAGAG	1000 bp integration region
# 33	GCGCGCCATGGCGTTGGTGCCGGCAGAATAGG	1000 bp integration region
# 34	GCGCGCCATGGGCCAGAACTGTGGCAGCGAG	P_{kdp}::*bgaH*
# 35	GCAGACACCAACTGTCATGTGCAACTGGCCCGG	P_{kdp}::*bgaH*
# 36	CCGGGCCAGTTGCACATGACAGTTGGTGTCTGC	P_{kdp}::*bgaH*
# 37	GCCTCGCCACAGTCCTCGCAG	P_{kdp}::*bgaH*
# 38	GCGCGCCATGGCGCGGCCGACGCTATCAAC	integration near *cat3*
# 39	GCGCGAAGCTTCCCTGAGGGGTGAGCGGG	integration near *cat3*
# 40	GCGCGCCATGGGCTCCCGATGGGTGCAACC	integration near *bop*
# 41	GCGCGAAGCTTGACCGATGAACCGTCAGACAC	integration near *bop*
# 42	GCGCGCATGGGGCCTGGTCCCGTCGGTTG	integration near *rpoA1*
# 43	GCGCGAAGCTTGAGATACTACAGGCCAGTTGC	integration near *rpoA1*
# 44	GCGCGATCGATCCAGAACTGTGGCAGCGAG	P_{kdp}::*pyrE2*
# 45	GATGAGTGCTGCGTTCGCCATGTGCAACTGGCCCGG	P_{kdp}::*pyrE2*
# 46	CCGGGCCAGTTGCACATGGCGAACGCAGCACTCATC	P_{kdp}::*pyrE2*
# 47	CTGGAGCTCCACCGCGGTG	P_{kdp}::*pyrE2*
# 48	GCGCGCCATGGGCTCAGCACGAAACGAAACCGG	P_{fdx}::*cat3*
# 49	GCGCGGGTACCTCAGGACTCCGGTGGCACC	P_{fdx}::*cat3*

4.4 Cloning of the *kdpFABCcat3* operon

Unless stated otherwise, all molecular biological methods were performed according to the protocols described in Sambrock *et al*. (1989). Genomic DNA of *H. salinarum* R1 was isolated by phenol/chloroform extraction followed by ethanol precipitation. A 6735-bp genomic fragment carrying the *kdpFABCcat3* genes was isolated via PCR using Herculase™ enhanced DNA polymerase (Stratagene) together with primers 1 and 2 (table 8). The resulting PCR product was cloned into pCR2.1-TOPO by use of the TOPO TA Cloning® Kit (Invitrogen). A 5914-bp *Eco*RV/*Xba*I restriction fragment of pCR2.1-TOPO carrying the *kdpFABCcat3* genes was then subcloned in pBAD24 using *Sma*I/*Xba*I restriction sites. Using the restriction sites *Nco*I and *Hind*III of the pBAD24 multi cloning site, a 5944-bp *Nco*I/*Hind*III fragment carrying the *kdpFABCcat3* operon was subsequently cloned in pMKK100, finally resulting in plasmid pHJS1.

4.5 Construction of plasmids, transformation, and knock-out mutagenesis

Transformation of *H. salinarum* strains was carried out as described in Cline *et al*. (1989) and transformation of *H. volcanii* strains as described in Allers *et al*. (2004).

Plasmids used for the knock-out mutagenesis of chromosomally encoded *kdpFABCcat3* and *kdpFABC* were constructed by two-step PCR technique using Herculase™ Enhanced DNA polymerase and primers 6, 7, 8, 9, 10, and 11 (table 8). The resulting PCR products carrying 900 bp sequences framing the *kdpFABC* and *kdpFABCcat3* genes were cloned in plasmid pMKK100 using the restriction sites *Nco*I and *Hin*dIII, resulting in pHJS3 and pHJS4, respectively.

Knock-out mutagenesis by recombination for the deletion of *kdpFABC* and *kdpFABCcat3* in *H. salinarum* R1 was carried out using the knock-out plasmids pHJS3 and pHJS4, respectively, as described in Krebs *et al*. (1993). The deletion of the *kdpFABC* and *kdpFABCcat3* genes was controlled by PCR. In addition, the absence of expression was confirmed by RT-PCR.

The plasmid carrying the *kdpFABC* operon without the *cat3* gene was constructed by two-step PCR with Herculase™ Enhanced DNA polymerase by use of primers 2, 3, 4, and 5 (table 8). The resulting PCR product was subcloned into the pBAD24 derivative carrying the *kdpFABCcat3* genes described above using the *Apa*I/*Xba*I restriction sites. An *Nco*I/*Hin*dIII-fragment carrying *kdpFABC* genes was subsequently cloned in pMKK100 resulting in plasmid pHJS2.

The plasmids carrying the *kdpFABCcat3* operon with different variations of the *kdp*-promoter were constructed by PCR with Herculase™ Enhanced DNA polymerase by use of primers 22 and 23 (206 bp promoter), primers 24 and 25 (52 bp promoter), primers 26 and 27 (42 bp promoter), and by two step PCR using primers 28, 29, 30, and 31 (deletion of operator 1). The resulting PCR product was subcloned into the pBAD24 derivative carrying the *kdpFABCcat3* genes described above using the *Nco*I/*Kpn*I restriction sites. To to ensure integration into the chromosome, a 1000 bp fragment homologous to a region 240 bp to 1240 bp upstream of *kdpF* was amplified by PCR with Herculase™ Enhanced DNA polymerase using primers 32 and 33. The corresponding PCR product was incubated with DNA Polymerase I Large (Klenow) to create blunt ends. In the following, pMKK100 was linearised using the restriction site *Pst*I, blunt ends created by incubation with DNA Polymerase I Large (Klenow) and the 1000 bp PCR product was inserted by ligation. The *Nco*I/*Hin*dIII-fragments carrying *kdpFABCcat3* genes and different variations of the *kdp*-promoter were subsequently cloned in pMKK100 carrying additional 1000 bp essential for effective integration, resulting in plasmids pHS10-12.

The plasmid carrying a transcriptional fusion between P_{kdp} and *bgaH* was constructed by two-step PCR with Herculase™ Enhanced DNA polymerase by use of primers 34, 35, 36, and 37. The PCR product was cloned into pHJS4 using *Pst*I/*Eco*R1 restriction sites resulting in plasmid pOZ1.

The plasmids carrying a transcriptional fusion between P_{kdp} and *bgaH* as well additional sequences ensuring integration in different regions of the chromsome were constructed by PCR with Herculase™ Enhanced DNA polymerase by use of primers 38 and 39 (integration downstream of *cat3*), primers 40 and 41 (integration upstream of *bop*) and primers 42 and 43 (integration upstream of *rpoA1*). The resulting PCR products were cloned into pOZ1 using *Nco*I/*Hind*III restriction sites resulting in plasmids pHJS6-8.

The plasmid carrying a transcriptional fusion between P_{kdp} and *pyrE2* was constructed by two-step PCR with Phusion™ High-Fidelity DNA Polymerase by use of primers 44, 45, 46, and 47. The resulting PCR products were cloned into pTA425 using the *Cla*I/*Sac*I restriction sites, resulting in plasmid pHJS23.

The plasmid carrying a transcriptional fusion between P_{fdx} and *cat3* was constructed by PCR with Phusion™ High-Fidelity DNA Polymerase by use of primers 48 and 49. The resulting PCR products was cloned into pJAS35 using the *Nco*I/*Acc*65I restriction sites resulting in plasmid pSH1.

4.6 Measurements of medium and cell K^+ concentrations and cell volume

The concentration of medium K^+ was measured by flame emission photometry (FEP) using an Eppendorf ELEX 6361 flame photometer in a buffer containing 5 mM CsCl and 1.5 % TCA. The amount of cytoplasmic K^+ was determined after centrifugation of 1 ml of culture and subsequent cell lysis in 1 ml ddH_2O by flame emission photometry as described above. Residual K^+ outside of the cell can be neglected, since the K^+ content of the medium is far below the intracellular K^+ level. Cell volume was determined by conversion of cells into spheroplasts as described in Cline *et al.* (1989) followed by migrographic imaging using a Zeiss Axioskop 40 FL microscope with an attached CCD-camera (Diagnostic Instruments SPOT RT Slider). The pixel area of approx. 500 individual cells per sample was measured using the ImageJ software version 1.37 (http://rsb.info.nih.gov/ij/) and converted into metric units using a microscopy calibration slide (Motic) and the Flow Cytometry Size Calibration Kit (Molecular Probes) as size standards. The cell volume was calculated from the mean area assuming that spheroplasts are round inductile spheres. Total cell counts were measured with the aid of a Neubauer haemocytometer (Marienfeld, Germany).

4.7 Sequence analysis and phylogenetic computation

Genes coding for the halobacterial *kdpFABCcat3* operon as well as homologues in other archaeal genomes were identified by use of the BLAST program (Altschul *et al*., 1990) using KdpFABC from *E. coli* as query. Multiple sequence alignments and pairwise distance matrices of 89 bacterial and six archaeal homologs of KdpB were calculated using ClustalW (Thompson *et al.,* 1994). The unrooted radial phylogenetic tree was genereted with the Phylodraw software (Choi *et al.,* 2000) using the ClustalW distance matrix and the neighbour joining algorithm (Saitou *et al*., 1987). All additional sequence analysis methods used are descibed in the corresponding context.

4.8 RNA extraction, RT-PCR, and *real time* RT-PCR

Total RNA of *H. salinarum* was isolated from cultures grown in rich medium or in casaminoacids medium with varying K^+ concentrations with the RNeasy mini kit (Qiagen) following the manufacturer's instructions. RNA was diluted to a concentration of 20 µg/ml and subsequently treated with DNaseI (Fermentas) following the manufacturer's instructions in order to remove residual DNA contaminations. 70 ng of total RNA was reversely transcribed by use of the First Strand cDNA Synthesis Kit (Fermentas) together with random hexamer primers following the manufacturer's instructions. Detection of gene expression was

carried out by RT-PCR with Sawady-Taq DNA Polymerase (PeqLab), 1 µl of cDNA, and 0.2 nM of each primer. For gene expression level measurements, *real-time* RT-PCR was carried out on a BioRad iCycler with Biorad iQ SYBR Green Supermix, 1 µl of cDNA, and 0.2 nM of each primer. The primers used for RT- and for *real time* RT-PCR (primers 12 and 13, table 8) are located in *kdpC* and *cat3*, respectively, and the reaction results in a specific 300-bp PCR-product. Both PCRs were carried out using an initial denaturation at 98 °C for 3 min, followed by 40 cycles of denaturation at 98 °C for 1 min, annealing at 64 °C for 30 sec, and extension at 72 °C for 30 sec. In case of *real time* RT-PCR, the calculated Ct-values were normalised against Ct-values of reactions using primers binding within the *rpoAI* gene as a non-regulated housekeeping gene (primers 14 and 15, table 8). The normalization and the calculation of normalized expression levels were carried out using the Q-Gene software (Simon, 2003). Reactions without template and DNaseI-treated RNA as template were included as negative controls.

The gene expression level measurements using the *H. salinarum* Δ*kdpFABCcat3* strain complemented with plasmid-encoded expression of *kdpFABC* and *kdpFABCcat3* were carried out as described for wild type with the following modification. The primers used for the detection of the *kdpFABC(cat3)*-transcript in *real time* RT-PCR (primers 16 and 17, table 8) are located in *kdpA*.

The *real time* RT-PCR gene expression level measurements of the two putative orf´s OE5058F and VNG6180 were carried out as described for the wild type with following modifications. Primers 18 and 19 were used for the detection of OE5061 and primers 20 and 21 for detection of VNG6180. The corresponding ct-values were not normalized or calculated using Q-Gene software (Simon, 2003).

4.9 β-galactosidase activity assay

β-galactosidase activity measurements applying plasmids pOEZ1 and pHJS6-8 were carried out as descibed in Holmes *et al*. (1998) with following modifications: Measurements were carried out using 96-well microtiter plates (Falcon Flexible PVC Microplate) in an ELISA-Reader (SLT 340; ATTC). After preliminary controls for the dependency between optical density and whole protein concentration, the culture optical density measurements were used as estimation for the amount of cell material used in the assay.

4.10 DNA microarrays

Isolation of RNA for hybridisation of DNA microarrays was carried out as disribed for RT-PCR analysis with the following modifications. RNA was isolated from a total amount of 5 ml of culture. RNA was not diluted for DNase degradation, and an additional purification step using the RNeasy mini kit (Qiagen) was applied after DNase degradation. The hybridisation of DNA microarrays was essentally carried out as described in Twellmyer (2007). The primary analysis of the raw fluorescence data was performed with Genepix Pro V4 and V6 (Molecular Devices, Sunnyvale, USA). The t-tests to identify the significance of the measured fluorescence differences were performed using TIGR-MEV (Rockville, USA). The hybridization and analysis of DNA microarrays were carried out by A. Wende (MPI for Biochemistry, Martinsried) and should, therefore, not be regarded as a personal contribution of the author. The prediction of function of the identified genes was carried out using Blast, Pfam (Bateman *et al*., 2002) and JNET (Cuff & Baron (1999)).

4.11 Copy number measurements

The relative DNA copy number measurements were carried out essentially as described for the relative expression level measurements applying *real-time* RT-PCR. However, in place of cDNA, genomic DNA was applied as a template. The corresponding DNA templates were obtained by centrifugation of 1 ml of culture followed by lysis in 1 ml H_2O and homogenization of the sample by sonification. A sample volume of 1 µl was used in triplicate to measure the relative abundance of chromosomal DNA coding for *rpoA1* (primers 14 and 15) as well as for pHS3-DNA coding for *kdpC/cat3* (primers 12 and 13). The normalization and the calculation of relative copy levels were carried out using the Q-Gene software.

5. References

Alam, M. and Oesterhelt, D. (1984) Morphology, function and isolation of halobacterial flagella. *J. Mol. Biol.* **176**:459-475.

Allers, T., Ngo, H.-P., Mevarech, M., and Lloyd, R.G. (2004) Development of Additional Selectable Markers for the Halophilic Archaeon Haloferax volcanii Based on the leuB and trpA *Genes Appl Environ Microbiol*. **70**:943–953.

Allers, T., and Mevarech, M. (2005) Archaeal genetics - the third way. *Nat Rev Genet*. **6**:58-73.

Altendorf, K., Gaßel, M., Puppe, W., Möllenkamp, T., Zeeck, A., Boddien, C. *et al*. (1998) Structure and function of the Kdp-ATPase of *Escherichia coli*. *Acta Physiol Scand Suppl* **643**:137-146.

Altschul, S.F., Gish, W. Miller, W., Myers, E.W., and Lipman, D.J. (1990) Basic local alignment search tool. *J Mol Biol* **215**:403-410.

Aravind, L., and Koonin, E. V. (1999) DNA-binding proteins and evolution of transcription regulation in the archaea. *Nucleic Acids Res*.**27**:4658–4670.

Aravind, L., Anantharaman, V., and Koonin, E.V. (2002) Monophyly of class I aminoacyl tRNA synthetase, USPA, ETFP, photolyase, and PP-ATPase nucleotide-binding domains: implications for protein evolution in the RNA. *Proteins* **48**:1-14.

Bakker, E.P. (1993) Low-affinity K^+ uptake systems. In Alkali cation transport systems in prokaryotes. Bakker, E.P. (ed.). Boca Raton, Fla: CRC Press, Inc., pp. 253-276.

Baliga, N.S., and DasSarma, S. (1999) Saturation mutagenesis of the TATA box and upstream activator sequence in the haloarchaeal *bop* gene promoter. *J Bacteriol* **181**:2513-2518.

Baliga, N.S., Goo, Y.A., Ng, W.V., Hood, L., Daniels, C.J., DasSarma, S. (2000) Is gene expression in Halobacterium NRC-1 regulated by multiple TBP and TFB transcription factors? *Mol Microbiol.* **36**:1184-5.

Ballal, A., Basu, B., and Apte, S.K. (2007) The Kdp-ATPase system and its regulation. *J Biosci*. **32**:559-68.

Bateman, A., Birney, E., Durbin, R., Eddy, S.R., Howe, K.L., and Sonnhammer, E.L. (2000) The Pfam protein families database. *Nucleic Acids Res* **28**:263-266.

Bell, S. D., Cairns, S. S., Robson, R. L. and Jackson, S. P. (1999) Transcriptional regulation of an archaeal operon in vivo and in vitro. *Mol. Cell* **4**:971–982.

Bell, S.D., and Jackson, S.P. (2000) Mechanism of autoregulation by an archaeal transcriptional repressor. *J Biol Chem.* **275**:31624-9.

Bell, S. D. and Jackson, S. P. (2003) Mechanism and regulation of transcription in archaea. *Curr. Opin. Microbiol*.**4**:208–213.

Berquist, B.R., and DasSarma, S. (2003) An Archaeal Chromosomal Autonomously Replicating Sequence Element from an Extreme Halophile, *Halobacterium* sp. Strain NRC-1 *J Bacteriol*. **185**:5959–5966.

Berquist, B.R., DasSarma, P. and DasSarma, S. (2007) Essential and non-essential DNA replication genes in the model halophilic Archaeon, Halobacterium sp. NRC-1. *BMC Genet*. **8**:31.

Bolhuis, H., Palm, P., Wende, A., Falb, M., Rampp, M., Rodriguez-Valera, F., Pfeiffer, F., and Oesterhelt, D. (2006) The genome of the square archaeon Haloquadratum walsbyi : life at the limits of water activity. *BMC Genomics*, **7**:169.

Bramkamp, M, Altendorf, K., and Greie. J.-C. (2007) Common patterns and unique features of P-type ATPases: a comparative view on the KdpFABC complex from Escherichia coli. *Mol Membr Biol,* **24**:375-86.

Breuert, S., Allers, T., Spohn, G., and Soppa, J. (2006) Regulated polyploidy in halophilic archaea. *PLoS ONE.* **1**:e92.

Brown, I.I., Galperin, M.Y., Glagolev, A.N., and Skulachev, V.P. (1983) Utilization of energy stored in the form of Na^+ and K^+ ion gradients by bacterial cells. *Eur J Biochem* **134**:345-349.

Choi, J.H., Jung, H.Y., Kim, H.S., and Cho, H.G. (2000) PhyloDraw: a phylogenetic tree drawing system. *Bioinformatics* **16**:1056-8.

Claycomb, J.M., and Orr-Weaver, T.L. (2005) Developmental gene amplification: insights into DNA replication and gene expression. *Trends Genet.* **21**:149-62.

Cohen-Kupiec, R., Blank, C. & Leigh, J. A. (1997) Transcriptional regulation in Archaea: in vivo demonstration of a repressor binding site in a methanogen. *Proc. Natl Acad. Sci. USA* **94**:1316–1320.

Cole, S.T., Brosch, R., Parkhill, J., Garnier, T., Churcher, C., Harris, D., *et al.* (1998) Deciphering the biology of *Mycobacterium tuberculosis* from the complete genome sequence. *Nature* **393**:537-544.

Cuff, J.A. and Baron, G.J. (1999) Application of enhanced multiple sequence alignment profiles to improve protein secondary structure prediction. *Proteins* **40**:502-511.

Danon, A., and Stoeckenius, W. (1974) Photophosphorylation in Halobacterium halobium. *Proc Natl Acad Sci U S A*. **71**:1234-8.

Daubin, V., Gouy, M., and Perriere, G. (2002) A Phylogenomic Approach to Bacterial Phylogeny: Evidence of a Core of Genes Sharing a Common History. Genome Res. 12:1080-1090.

Desmarais, D., Jablonski, P.E., Fedarko N. S. und Roberts, M. F.(1997) 2-Sulfotrehalose, a novel osmolyte in haloalkaliphilic Archaea. *J Bact*. **179**:3146-53.

Doyle, D.A., Cabral, J.M., Pfuetzner, R.A., Kuo, A., Gulbis, J.M., Cohen, S.L., *et al.* (1998) The structure of the potassium channel: molecular basis of K+ conduction and selectivity. Science **280**:69-77.

Durell, S.R., Hao, Y., Nakamura, T., Bakker, E.P., and Guy, H.R. (1999) Evolutionary relationship between K+ channels and Symporters. *Biophys. J.* **77**:775-788.

Elcock, A.H., and McCammon, J.A. (1978) Electrostatic contributions to the stability of halophilic proteins. *J Mol Biol* **24**:731-48.

Eugster, H.P. and Hardie, L.A. (1978) Saline lakes. *In*: Lerman, A. (ed.) *Chemistry, Geology and Physics of Lakes,* Springer-Verlag, New York, 237–293.

Falb, M., Pfeiffer, F., Palm, P., Rodewald, K., Hickmann, V., Tittor, J., and Oesterhelt, D. (2005) Living with two extremes: conclusions from the genome sequence of Natronomonas pharaonis. *Genome Res.* **15**:1336-43.

Futterer, O., Angelov, A., Liesegang, H., Gottschalk, G., Schleper, C., Schepers, B. *et al.* (2004) Genome sequence of Picrophilus torridus and its implications for life around pH 0. *Proc Natl Acad Sci U S A* **15**:9091-6.

Gandbhir, M., Rashed, I., Marliere, P., und Mutzel, R. (1995) Convergent evolution of amino acid usage in archaebacterial and eubacterial lineages adapted to high salt. *Res Microbiol.* **146**:113-20.

Giladi, M., Bitan-Banin, G., Mevarech, M., and Ortenberg, R. (2002) Genetic evidence for a novel thymidylate synthase in the halophilic archaeon Halobacterium salinarum and in Campylobacter jejuni *FEMS Microbiol Lett*. **216**:105-9.

Ginzburg, M., and Ginzburg, B.Z. (1975) Factors influencing the retention of K in a Halobacterium. *Biomembranes.* **7**:219-251.

Golyshina, O.V., Pivovarova, T.A., Karavaiko, G.I., Kondrateva, T.F., Moore, E.R., Abraham, W.R. *et al.* (2000) Ferroplasma acidiphilum gen. nov., sp. nov., an acidophilic, autotrophic, ferrous-iron-oxidizing, cell-wall-lacking, mesophilic member of the Ferroplasmaceae fam. nov., comprising a distinct lineage of the Archaea. *Int J Syst Evol Microbiol* **3**:997-1006.

Goo, Y.A., Roach, J., Glusman,G., Baliga, N.S., Deutsch, K., Pan, M., Kennedy, S., DasSarma, S., Ng, W.V., and Hood, L. (2004) Low-pass sequencing for microbial comparative genomics. *BMC Genomics*, **5**:3.

Grabowski, B., and Kelman, Z. (2003) Archeal DNA replication: eukaryal proteins in a bacterial context. *Annu Rev Microbiol*. **57**:487-516.

Grainge, I., Scaife, S., and Wigley, D.B. (2003) Biochemical analysis of components of the pre-replication complex of Archaeoglobus fulgidus. *Nucleic Acids Res.* **31**:4888-98.

Grant, W. D. (2004) Life at low water activity. *Philos Trans R Soc Lond B Biol Sci.* **359**:1249–1267.

Gregor, D., and Pfeifer, F. (2005) In vivo analyses of constitutive and regulated promoters in halophilic archaea. *Microbiology.* **151**:25-33.

Gropp, F., Gropp, R., and Betlach, M.C. (1995) Effects of upstream deletions on light- and oxygen-regulated bacterio-opsin gene expression in *Halobacterium halobium*. *Mol Microbiol* **16**:357-364.

Guzman, L.M., Belin, D., Carson, M.J., and Beckwith, J. (1995) Tight regulation, modulation, and high-level expression by vectors containing the arabinose PBAD promoter. *J Bacteriol* **177**:4121-30.

Hanahan, D. (1983) Studies on Transformation of Escherichia coli with Plasmids. *J. Mol. Biol.* **166**:557-580.

Hamann, K., Zimmann, P., and Altendorf, K. (2007) Changes of turgor are not the stimulus for the sensor kinase KdpD of *Escherichia coli*. (submitted).

Harms, S., Domoto, Y., Celik, C., Rahe, E., Stumpe, S., Schmid, R., Nakamura, T., and Bakker, E.P. (2001) Identification of the ABC protein SapD as the subunit that confers ATP dependence to the K+-uptake system TrkH and TrkG from Escherichia coli K-12. *Microbiology* **147**:2991-3003.

Harrington. R.E. (1992) DNA curving and bending in protein-DNA recognition. *Mol Microbiol.* **6**:2549–2555.

Heermann, R., Altendorf, K., and Jung, K. (2000) The hydrophilic N-terminal domain complements the membrane-anchored C-terminal domain of the sensor kinase KdpD of *Escherichia coli*. *J Biol Chem* **275**:17080-17085.

Heermann, R., Fohrmann, A., Altendorf, K., and Jung, K. (2003) The transmembrane domains of the sensor kinase KdpD of Escherichia coli are not essential for sensing K+ limitation. *Mol Microbiol.* **47**:839-48.

Hofacker, A., Schmitz, K. M., Cichonczyk, A., Sartorius-Neef, S. and Pfeifer, F. (2004) GvpE- and GvpD-mediated transcription regulation of the p-gvp genes encoding gas vesicles in Halobacterium salinarum. *Microbiology* **150**:1829–1838.

Holmes, M. L., Scopes, R., Moritz, R., Simpson, R., Englert, C., Pfeifer, F. and Dyall-Smith, M. (1997). Purification and analysis of an extremely halophilic ß-galactosidase from Haloferax alicantei. *Biochim Biophys Acta* **1337**:276-286.

Huet, J., Schnabel, R., Sentenac, A. and Zillig, W. (1983) Archaebacteria and eukaryotes possess DNA-dependent RNA polymerases of a common type. *EMBO J.* **2**:291–1294.

Ito, M., A.A. Guffanti, J. Zemsky, D.M. Ivey, and T.A. Krulwich. (1997). Role of the *nhaC*-encoded Na^+/H^+ antiporter of alkaliphilic *Bacillus firmus* OF4. J. Bacteriol. **179**:3851-3857.

Jung, K., Veen, M., Altendorf, K. (2000) K+ and ionic strength directly influence the autophosphorylation activity of the putative turgor sensor KdpD of Escherichia coli. *J Biol Chem.* **275**:40142-7.

Jung, K., and Altendorf, K. (2002) Towards an understanding of the molecular mechanisms of stimulus perception and signal transduction by the KdpD/KdpE system of *Escherichia coli*. *J Mol Microbiol Biotechnol* **4**:223-228.

Kamo, N., Racanelli, T., and Packer, L. (1982) Light-dependent delta pH and membrane potential changes in halobacterial vesicles coupled to sodium transport. *Membr Biochem*. **4**:175-88.

Kauri, T., Wallace, R., and Kushner, D.J. (1990) Nutrition of the halophilic archaebacterium, *Haloferax volcanii*. *Syst Appl Microbiol* **13**:14–18.

Kawashima, T., Amano, N., Koike, H., Makino, S.-I., Higuchi, S., Kawashima-Oya, Y., *et al.* (2000) Archaeal adaptation to higher temperatures revealed by genomic sequence of *Thermoplasma volcanium*. *Proc Natl Acad Sci USA* **97**:14257-14262.

Kayushin, L.P., and Skulachev, V.P. (1974) Bacteriorhodopsin as an electrogenic proton pump: reconstitution of bacteriorhodopsin proteoliposomes generating delta psi and delta pH. *FEBS Lett.* **39**:39-42.

Kelman, Z. (2000) DNA replication in the third domain (of life). *Curr Protein Pept Sci.* **1**:139-54.

Kennedy, S.P., Ng, W.V., Salzberg, S.L., Hood, L., and DasSarma, S. (2001) Understanding the adaptation of *Halobacterium* species NRC-1 to its extreme environment through computational analysis of its genome sequence. *Genome Res* **11**:1641-1650.

Kixmüller, D. (2006) Untersuchungen zur Promotorstruktur des kdpFABCcat3-Operons von Halobacterium salinarum. Diploma Thesis, University of Osnabrück

Klenk, H.P., Clayton, R.A., Tomb, J.-F., White, O., Nelson, K.E., Ketchum, K.A., *et al.* (1997) The complete genome sequence of the hyperthermophilic, sulphate-reducing archaeon *Archaeoglobus fulgidus*. *Nature* **390**:364-370.

Koch, M..K., and Oesterhelt, D. (2005) MpcT is the transducer for membrane potential changes in *Halobacterium salinarum*. *Mol Microbiol* **55**:1681–1694.

Kokoeva, M.V., Storch, K.F., Klein, C., and Oesterhelt, D. (2002) A novel mode of sensory transduction in archaea: binding protein-mediated chemotaxis towards osmoprotectants and amino acids. *EMBO J* **15**:2312-22.

Krah, M., Marwan, W., Verméglio, A., and Oesterhelt, D. (1994) Phototaxis of Halobacterium salinarium requires a signalling complex of sensory rhodopsin I and its methyl-accepting transducer HtrI. *EMBO J.* **13**:2150–2155.

Krebs, M.P., Mollaaghababa, R., and Khorana, H.G. (1993) Gene replacement in *Halobacterium halobium* and expression of bacteriorhodopsin mutants. *Proc Natl Acad Sci USA* **90**:1987–1991.

Kröning, N., Willenborg, M., Tholema, N., Hanelt, I., Schmid, R., and Bakker E.P. (2007) ATP binding to the KTN/RCK subunit KtrA from the K+ -uptake system KtrAB of Vibrio alginolyticus: its role in the formation of the KtrAB complex and its requirement in vivo. *J Biol Chem.* **282**:14018-27.

Lanyi, J.K., Hilliker, K. (1976) Passive potassium ion permeability of Halobacterium halobium cell envelope membranes. *Biochim Biophys Acta.* **448**:181-4.
Lanyi, J.K. (1978) Light energy conversion in *Halobacterium halobium. Microbiol Rev.* **42**:682–706.

Lanyi, J.K., Helgerson, S.L., and Silverman, M.P. (1979) Relationship between proton motive force and potassium ion transport in *Halobacterium halobium* envelope vesicles. *Arch Biochem Biophys* **193**:329-339.

Lie, T.J., Wood, G.E., and Leigh, J.A. (2005) Regulation of nif expression in Methanococcus maripaludis: roles of the euryarchaeal repressor NrpR, 2-oxoglutarate, and two operators. *J Biol Chem*. **280**:5236-41.

Luisi, B.F., Lanyi, J.K,. and Weber, H.J. (1080) Na+ transport via Na+/H+ antiport in Halobacterium halobium envelope vesicles. *FEBS Lett*. **117**:354-8.

Madern, D., Ebel, C., and Zaccai, G. (2000) Halophilic adaptation of enzymes. *Extremophiles* **4**:91-8.

Meury, J., and Kohiyama, M. (1989) ATP is required for K^+ active transport in the archaebacterium *Haloferax volcanii*. *Arch Microbiol* **151**:530-536.

Michel, H., and Oesterhelt, D. (1980) Electrochemical proton gradient across the cell membrane of *Halobacterium halobium*: effect of N,N'-dicyclohexylcarbodiimide, relation to intracellular adenosine triphosphate, adenosine diphosphate, and phosphate concentration, and influence of the potassium gradient. *Biochemistry* **19**:4607-4614.

Munteanu, M. G., Vlahovicek, K., Parthasaraty, S., Simon, I. and Pongor, S. (1998): Rod models of DNA: sequence-dependent anisotropic elastic modelling of local bending phenomena. *Trends Biochem. Sci.* **23**:341-346.

Murakami, N., and Konishi, T. (1985) DCCD-sensitive, Na+-dependent H+-influx process coupled to membrane potential formation in membrane vesicles of Halobacterium halobium. *J Biochem*. **98**:897-907.

Murakami, N., and Konishi, T. (1988) Functional comparison of DCCD-sensitive Na+/H+ antiporter in Halobacterium halobium with monensin. *Biochimie.* **70**:819-26.

Müller, JA., and DasSarma, S. (2005) Genomic analysis of anaerobic respiration in the archaeon Halobacterium sp. strain NRC-1: dimethyl sulfoxide and trimethylamine N-oxide as terminal electron acceptors. *J Bacteriol*. **187**:1659-67.

Nakamura, T., Yamamuro, N, Stumpe, S., and Bakker, E.P. (1998) Cloning of the *trkAH* gene cluster and characterization of the Trk K^+-uptake system of *Vibrio alginolyticus*. *Microbiology* **144**:2281-2289.

Ng, W.V., Ciufo, S.A., Smith, T.M., Bumgarner, R.E., Baskin, D., Faust, J., Hall, B., Loretz, C., Seto, J., Slagel, J., Hood, L., and DasSarma S. (1998) Snapshot of a large dynamic replicon in a halophilic archaeon: megaplasmid or minichromosome? *Genome Res.* **8**:1131-41.

Ng, W.V., Kennedy, S.P., Mahairas, G.G., Berquist, B., Pan, M., Shukla, H.D., *et al.* (2000) Genome sequence of *Halobacterium* species NRC-1. *Proc Natl Acad Sci USA* **97**:12176-12181.

Norais, C., Hawkins, M., Hartman, A.L., Eisen, J.A., Myllykallio, H., and Allers, T. (2007) Genetic and physical mapping of DNA replication origins in Haloferax volcanii. *PLoS Genet*. **3**:e77.

Nutsch, T., Oesterhelt, D., Gilles, E.D., and Marwan, W.(2005) The Switch Cycle of an Archaeal Flagellar Motor and its Sensory Control. *Biophys. J.* **89**:2307-2323.

Oren, A. (1995) Comment on "Convergent evolution of amino acid usage in archaebacterial and eubacterial lineages adapted to high salt", by M. Gandbhir *et al.* (*Res. Microbiol*., 1995, **146**:113-120) *Res Microbiol.* **146**:805-6.

Oren, A. (1999) Bioenergetic aspects of halophilism. *Microbiol Mol Biol Rev* **63**: 334-348.

Oren, A. (2005) „A hundret years of *Dunaliella* research: 1905 – 2005. *Saline Systems.* **1**:2.

Ouhammouch, M., Dewhurst, R., Hausner, W., Thomm, M. and Geiduschek, E. P. (2003). Activation of archaeal transcription by recruitment of the TATA-binding protein. *Proc Natl Acad Sci U S A* **100**:5097–5102.

Özyamak, E. (2005). Charakterisierung des kdpFABCcat3-Promotors aus Halobacterium salinarum R1, Diploma Thesis, University of Osnabrück.

Palmgren, M.G., and Axelsen, K.B. (1998) Evolution of P-type ATPases. *Biochim Biophys Acta* **1365**:37-45.

Palmer, J.R., and Daniels, C.J. (1995) In vivo definition of an archaeal promoter. *J Bacteriol* **177**:1844-1849.

Pareja, E., Pareja-Tobes. P., Manrique, M., Pareja-Tobes, E., Bonal, J., and Tobes, R. (2006) ExtraTrain: a database of Extragenic regions and Transcriptional information in prokaryotic organisms. *BMC Microbiology* **6:**29.

Pérez-Fillol, M., and Rodríguez-Valera, F. (1986) Potassium ion accumulation in cells of different halobacteria. *Microbiologia.* **2**:73-80.

Pérez-Martín J, de Lorenzo V. (1997) Clues and consequences of DNA bending in transcription. *Annu Rev Microbiol*. **51**:593-628.

Pfeifer, F., Offner, S., Krüger, K., Ghahraman, P., and Englert C. (1994) Transformation of halophilic archaea and investigation of gas-vesicle synthesis. *Syst Appl Microbiol*. **16**:569-577.

Pflüger, K., Müller, V. (2004) Transport of compatible solutes in extremophiles. *J. Bioenerg. Biomembr.* **36**:17-24.

Qureshi, S.A., and Jackson, S.P. (1998) Sequence-specific DNA binding by the *S. shibatae* TFIIB homolog, TFB, and its effect on promoter strength. *Mol Cell* **1**:389-400.

Reeve, J.N. (2003) Archaeal chromatin and trancription. *Mol Microbiol*. **48**:587-598.

Reiter, W.D., Hüdepohl, U., and Zillig, W. (1990) Mutational analysis of an archaebacterial promoter: essential role of a TATA box for transcription efficiency and start-site selection in vitro. *Proc Natl Acad Sci USA* **87**: 9509-9513.

Rhoads, D. B., Waters, F. B., and Epstein, W. (1976) Cation transport in *Escherichia coli*. VIII. Potassium transport mutants, *J. Gen. Physiol.* ***67***:325-341.

Roberts, M.F. (2005) Organic compatible solutes of halotolerant and halophilic microorganisms. *Saline Systems* **1**:5.

Ruepp, A., and Soppa, J. (1996) Fermentative arginine degradation in Halobacterium salinarium (formerly Halobacterium halobium): genes, gene products, and transcripts of the arcRACB gene cluster. *J Bacteriol*. **178**:4942-7.

Ruepp, A., Graml, W., Santoz-Martinez, M.-L., Koretke, K.K., Volker, C., Mewes, H.-W., *et al.,* (2000) The genome sequence of the thermoacidophilic scavenger *Thermoplasma acidophilum*. *Nature* **407**:508-513.

Roesser, M., and Muller, V. (2001) Osmoadaptation in bacteria and archaea: common principles and differences. *Environ. Microbiol*. **3**:743-754.

Saitou, N. and Nei., M. (1987). The neighbor-joining method: a new method for reconstructing phylogenetic trees. *Mol Evol Biol* **4**:406-425.

Sambrook, J., Fritsch, E.F., and Maniatis, T. (2001). Molecular cloning: a laboratory manual, 3rd ed. Cold Spring Harbor, NY: Cold Spring Harbor Laboratory Press.

Sartorius-Neef, S. & Pfeifer, F. (2004) In vivo studies on putative Shine–Dalgarno sequences of the halophilic archaeon Halobacterium salinarum. *Mol Microbiol*. **51**:579-588.

Schleussinger, E., Schmid, R., and Bakker, E.P. (2006) New type of kdp region with a split sensor-kinase kdpD gene located within two divergent kdp operons from the thermoacidophilic bacterium Alicyclobacillus acidocaldarius. *Biochim Biophys Acta*. **1759**:437-41.

Schlösser, A., Hamann, A., Bossemeyer, D., Schneider, E. and Bakker, E. P. (1993). NAD+ binding to the Escherichia coli K+-uptake protein TrkA and sequence similarity between TrkA and domains of a family of dehydrogenases suggest a role for NAD in bacterial transport. *Mol Microbiol* **9**:533-543.

Shioda, M., Sugimori, K., Shiroya, T,. And Takayanagi, S. (1989) Nucleosomelike structures associated with chromosomes of the archaebacterium Halobacterium salinarium. *J Bacteriol*. **171**:4514-7.

Siebers, A., and Altendorf, K. (1993) K^+-translocating Kdp-ATPases and other bacterial P-type ATPases In Alkali cation transport systems in prokaryotes. Bakker, E.P. (ed.). Boca Raton, Fla: CRC Press, Inc., pp. 225-252.

Simon, P. (2003) Q-Gene: processing quantitative real-time RT-PCR data. *Bioinformatics*. **22:**1439-40.

Soppa, J. (1999) Transcription initiation in Archaea: facts, factors and future aspects. *Mol Microbiol* **31**:1295-1305.

Stoeckenius, W., and Kunau, W. H. (1968) Further characterization of particulate fractions from lysed cell envelopes of *Halobacterium halobium* and isolation of gas vacuole membranes. *J Cell Biol* **38**:337-357.

Stumpe, S., Schlösser, A., Schleyer, M., and Bakker, E.P. (1996) K^+ circulation across prokaryotic cell membrane: K^+ uptake systems. In Handbook of biological physics Vol. 2. Konings, W.N., Kaback, H.R., and Lolkema, J.S. (eds.). Amsterdam: Elsevier Science, pp. 473-499.

Takayanagi, S., Morimura, S., Kusaoke, H., Yokoyama, Y., Kano, K., and Shioda, M. (1992) Chromosomal structure of the halophilic archaebacterium Halobacterium salinarium. *J Bacteriol*. **174**:7207-16.

Tehei, M., Franzetti, B., Wood, K., Gabel, F., Fabiani, E., Jasnin, M., Zamponi, M., Oesterhelt, D., Zaccai, G., Ginzburg, M., and Ginzburg, B.Z. (2007) Neutron scattering reveals extremely slow cell water in a Dead Sea organism. *Proc Natl Acad Sci U S A*. **104**:766-71.

Thiele, S. (2007) Untersuchungen zur Einfluss variierender externer Salzkonzentrationen auf das Ionengleichgewicht über der Zellmembran von Halobacterium salinarum. Bachelor Thesis, University of Osnabrück.

Thompson, J.D., Higgins, D.G., and Gibson, T.J. (1994) CLUSTAL W: improving the sensitivity of progressive multiple sequence alignment through sequence weighting, position-specific gap penalties and weight matrix choice. *Nucleic Acids Res* **22**:4673-4680.

Tolstrup, N., Sensen, C.W., Garrett, R., and Clausen, I.G. (2000) Two different and highly organized mechanisms of translation initiation in the archaeon Sulfolobus solfataricus. Extremophiles **4**:175–179.

Tower, J. (2004) Developmental gene amplification and origin regulation. *Annu Rev Genet*. **38**:273-304.

Twellmeyer, J. (2007) Etablierung der DNA-Mikroarray-Transkriptom-Analyse für Halobacterium salinarum R1. Dissertation, LMU München.

Ventosa, A., Nieto, J. J., und Oren, A.(1998) Biology of moderately halophilic aerobic bacteria. *Microbiol Mol Biol Rev.* **62:**504-44.

Wagner, G., Hartmann, R., and Oesterhelt, D. (1978) Potassium uniport and ATP synthesis in *Halobacterium halobium*. *Eur J Biochem* **89**:169-179.

Walsby, A. E. (1994). Gas vesicles. *Microbiol. Rev*. **58**:94-144.

Woese, C.R., Kandler, O., and Wheelis, M.L. (1990) Towards a natural system of organisms: proposal for the domains Archaea, Bacteria, and Eucarya. *Proc Natl Acad Sci USA* **87**:4576-4579.

Yancey, P.H. (2005) Organic osmolytes as compatible, metabolic and counteracting cryoprotectants in high osmolarity and other stresses. *J Exp Biol* **208**:2819–2830.

Zarembinski,T.I., Hung,L.W., Mueller-Dieckmann,H.J., Kim,K.K., Yokota,H., Kim,R., and Kim, S.H. (1998) Structure-based assignment of the biochemical function of a hypothetical protein: a test case of structural genomics. *Proc Natl Acad Sci USA* **43**:15189-15193.

Zhang, R., and Zhang, C.T. (2003) Multiple replication origins of the archaeon Halobacterium species NRC-1. *Biochem Biophys Res Commun*. **302**:728-34.

Zimmann, P., Steinbrugge, A., Schniederberend, M., Jung, K., and Altendorf, K. (2007) The extension of the fourth transmembrane helix of the sensor kinase KdpD of Escherichia coli is involved in sensing. *J Bacteriol*. **189**:7326-34.

I want to express my sincere thanks to all the people who supported my over the time.

First I want to thank my supervisor Prof. Dr. Karlheinz Altendorf who supported my over the whole time with advice and the possibility to work as autonomously as possible. I want to express my gratitude for the high degree of trust in providing me the opportunity to work on and establish this project from the very beginning on.

I am grateful to Prof. Dr. Felicitas Pfeifer for the evaluation of the thesis.

I am deeply thankful to Dr. Jörg-Christian Greie for the great supervision and support during these five years. Your willingness and openness to support me in following all those different ideas and nuances of this work made, above all, this project to interesting for me. Especially, I want to thank you for your friendship and open ear for all the non scientific problems of everyday life.

Furthermore, I am thankful to Prof. Dr. Evert Bakker who was always a great support and help in questions regarding all those “other” transporters.

I want to acknowledge Dr. Andy Wende as well as Prof. Dr. Dieter Oesterhelt for their cooperation and valuable discussions supporting my work.

In particular, I want to acknowledge Ertan Özyamak, Dorthe Kixmüller, Sabrina Hockemeyer and Stefan “Zwiebel” Thiele for their friedship and for their exellent support and cooperation in halobusiness.

I am deeply thankful to Ursula Krehe in a very warm and special way. She was a brilliant and uncomplaining help in the last half of this thesis.

Special thanks go to all my colleagues in the lab 119, Jessica, Rene, Thomas “der grieche”, Thomas “Heidi”, and Doris as well as in the whole microbiology group. Everyone was always willing to help in scientific and everyday problems.

Last but not least, I want to thank Boehringer Ingelheim Fonds, Dr. Hermann Fröhlich, Dr. Claudia Walther, Monika Beutelspacher, and the whole B.I.F family, not only for the financial support but also for the great time spend together in Blaubeuren and Hirschegg.

Curriculum Vitae

Personal Information:

Name	Henrik Strahl
Date of Birth	10.08.1978
Place of Birth	Seinäjoki, Finland
Citizenship	Finnish, German
Marital Status	Single

Education:

Ongoing Dissertation:	Division of Microbiology, University of Osnabrück, Germany Title: Kdp-dependent K^+ homeostasis of the halophilic archaeon *Halobacterium salinarum*
Diploma	Division of Microbiology, University of Osnabrück, Germany, 2003 Title: Klonierung und Charakterisierung des *kdp*-Operons aus *Halobacterium salinarum*
Intermediate Diploma	University of Osnabrück, Germany, 1999
University Entrance Qualification	Seinäjoen Lukio, Seinäjoki, Finland, 1997

Erklärung über die Eigenständigkeit der erbrachten wissenschaftlichen Leistung

Ich erkläre hiermit, dass ich die vorliegende Arbeit ohne unzulässige Hilfe Dritter und ohne Benutzung anderer als der angegebenen Hilfsmittel angefertigt habe. Die aus anderen Quellen direkt oder indirekt übernommenen Daten und Konzepte sind unter Angabe der Quelle gekennzeichnet.

Bei der Auswahl und Auswertung folgenden Materials haben mir die nachstehend aufgeführten Personen in der jeweils beschriebenen Weise entgeltlich/unentgeltlich geholfen.

Die DNA-microarray Analysen wurden in Kooperation mit der Arbeitsgruppe von Prof. Dr. Dieter Oesterhelt, Max-Planck-Institut für Biochemie, Martinsried und insbesondere in Zusammenarbeit mit Dr. Andy Wende durchgeführt.

Weitere Personen waren an der inhaltlichen materiellen Erstellung der vorliegenden Arbeit nicht beteiligt. Insbesondere habe ich hierfür nicht die entgeltliche Hilfe von Vermittlungs- bzw. Beratungsdiensten (Promotionsberater oder andere Personen) in Anspruch genommen. Niemand hat von mir unmittelbar geldwerte Leistungen für Arbeiten erhalten, die im Zusammenhang mit dem Inhalt der vorgelegten Dissertation stehen.

Die Arbeit wurde bisher weder im In- noch im Ausland in gleicher oder ähnlicher Form einer anderen Prüfungsbehörde vorgelegt.

Osnabrück, 22.10.2007
(Ort, Datum)

(Henrik Strahl)